

**Low Emissions  
Aftertreatment and Diesel  
Emissions Reduction**

**DE-FC26-99EE50575**

**FINAL REPORT**

Prepared for:

**Department of Energy**

**February 2005**

**DETROIT DIESEL**  
CORPORATION



**A DaimlerChrysler Company**

## TABLE OF CONTENTS

LIST OF FIGURES .....	iii
LIST OF TABLES .....	viii
ACRONYMS .....	ix
I. EXECUTIVE SUMMARY .....	1
II. PROGRAM OVERVIEW .....	3
III. TECHNICAL DETAILS .....	14
Task 1 Modeling and System Development .....	14
Task 1.1 Modeling Development and Integration .....	14
Task 1.2 Aftertreatment Systems Characterization .....	34
Task 1.2.1 SCR Characterization .....	36
1.2.1.1 SCR Characterization in Steady State Modes .....	38
1.2.1.2 Characterization of SCR Aging Effects Using the DELTA Engine .....	43
1.2.1.3 SCR Storage Characterization .....	46
1.2.1.4 Characterization of Urea Injection Mixing .....	50
Task 1.2.2 CSF Characterization .....	55
1.2.2.1 CSF Regeneration Characterization .....	55
1.2.2.2 CSF Regeneration Strategy Development .....	61
1.2.2.3 Other CSF Projects .....	63
Task 1.2.3 Characterization of LNT+CSF System .....	63
Task 1.2.4 DOC Characterization .....	70
Task 2 Engine-Based Development .....	74
Task 2.1 Advanced Combustion Development .....	74
Task 2.2 Air Management Development .....	78
Task 3 Aftertreatment System Development and Integration for a Neon Passenger Car .....	80
Task 3.1 Test Preparation .....	80
Task 3.2 Vehicle Test Results .....	81
Task 3.3 Data Repeatability .....	88
Task 4 Scalability Confirmation .....	90
Task 4.1 Simulated Vehicle Tests in a Transient Engine Testing Cell .....	91
Task 4.2 Vehicle Tests .....	92
IV. DEVELOPMENT CHALLENGES .....	96
V. REFERENCES .....	102
APPENDIX 1: WET CHEMISTRY SET-UP .....	103

APPENDIX 2: AMA TEST CYCLE .....	104
1. Driving Instructions.....	104
2. Circuit Instructions.....	105
APPENDIX 3: PNGV MULE VEHICLE DESCRIPTION.....	106
APPENDIX 4: FTP75 AND HIGHWAY FUEL ECONOMY TEST CYCLES .....	107
APPENDIX 5: TEST SET-UP .....	108
1. Schematic of the Test Set-Up .....	108
2. Dynamometer Coefficients.....	108
3. Vehicle Instrumentation.....	109
APPENDIX 6: TIER 2 EMISSIONS REGULATIONS .....	110
ACKNOWLEDGEMENTS .....	111

## LIST OF FIGURES

Figure 0.1 "Dieselization" of Light Trucks Offers Significant Reduction to U.S. Transportation Energy Use .....	4
Figure 0.2 Program Development Plan .....	4
Figure 0.3 Original Program Goal .....	5
Figure 0.4 Program Goal Adjusted to Aggressive Emissions Targets .....	6
Figure 0.5 Demonstrated Tier 2 Bin 3 Emissions for Passenger Car .....	6
Figure 0.6 Demonstrated Tier 2 Bin 3 Emissions for Light Duty Truck .....	7
Figure 0.7 Integrated Experimental and Analytical Approach to System Development .....	9
Figure 0.8 Simultaneous Reduction in NO <sub>x</sub> and PM Achieved via CLEAN Combustion® on the DELTA Engine .....	10
Figure 0.9 Exhaust Temperature Increase with CLEAN Combustion® Over FTP75 Test .....	11
Figure 0.10 Increase in NO <sub>2</sub> /NO <sub>x</sub> Ratio Attributed to CLEAN Combustion® .....	11
Figure 0.11 Integrated Engine and Aftertreatment System for Tier 2 Emissions .....	12
Figure 0.12 Urea Control Strategy Development over a Transient Cycle Using 1D SCR Model .....	12
Figure 0.13 Experimental Validation of Urea Injection Control Strategy Development .....	13
Figure 1.1.1 DDC's Three-Layer Virtual Lab Development Strategy .....	14
Figure 1.1.2 Concurrent Virtual Lab Integration for Entire Vehicle / Engine / AT System .....	16
Figure 1.1.3 CSF Model Validation against Transient Test Data .....	17
Figure 1.1.4 Vanadium-Based SCR Model Validation against Transient Vehicle Test Data .....	17
Figure 1.1.5 LNT Model Validation During Lean and Rich Regeneration .....	18
Figure 1.1.6 DOC Model Validation against Transient Vehicle Test Data .....	18
Figure 1.1.7 Comparison of Measured and CSF Model Simulated Pressure Drop across a Clean CSF with Temperature Between 260° - 360°C and NO <sub>x</sub> /PM Ratio 34 - 48 .....	19
Figure 1.1.8 Comparison of Measured and CSF Model Simulated HC Conversion for the Three CSF Loading Cases Corresponding to Figure 1.1.7 .....	20
Figure 1.1.9 Comparison of Measured and CSF Model Simulated CO Conversion for the Three CSF Loading Cases Corresponding to Figure 1.1.7 .....	21
Figure 1.1.10 Comparison of Measured and CSF Model Simulated NO <sub>2</sub> Emission from the Three CSF Loading Cases Corresponding to Figure 1.1.7 .....	21
Figure 1.1.11 Comparison of Measured and CSF Model Simulated NO Oxidation for the Three CSF Loading Cases Corresponding to Figure 1.1.7 .....	22
Figure 1.1.12 Comparison of Measured and CSF Model Simulated Trapped (Unburned) Soot at the end of the Three CSF Loading Cases Corresponding to Figure 1.1.7 .....	22

Figure 1.1.13 Comparison of Measured and CSF Model Simulated Soot Mass Balance for the CSF Loading Case 3 (358°C) from Figure 1.1.7 .....	23
Figure 1.1.14 Comparison of Measured and CSF Model Simulated Soot Mass Balance for the CSF Loading Case 2 (277°C) from Figure 1.1.7 .....	23
Figure 1.1.15 Integration of AT Models with Ricardo's Engine Cycle Simulation Tool - WAVE .....	24
Figure 1.1.16 Integration of AT Models with Gamma Technologies' Engine Cycle Simulation Tool – GT-Power .....	25
Figure 1.1.17 Coupling Methodology with Representative Channels for Catalyst Modeling .....	26
Figure 1.1.18 Representative Channel Transport to/from Large Scale .....	26
Figure 1.1.19 Conjugate Heat Transfer Schematic .....	27
Figure 1.1.20 Lateral Cross-Section Filter Geometry Schematic .....	27
Figure 1.1.21 Axial Cross-Section Filter Geometry Schematic .....	28
Figure 1.1.22 Spherical Unit Collector .....	28
Figure 1.1.23 Representative Channel (Axial Scale Greatly Foreshortened) .....	29
Figure 1.1.24 Representative Channel Cross-Sectional Grid (1/8th Symmetry) .....	30
Figure 1.1.25 Axial Velocity and Pressure Contours on Centerline Channel .....	30
Figure 1.1.26 Axisymmetric Large-Scale Grid .....	31
Figure 1.1.27 Regeneration with Heat Losses and Non-Uniform Inlet Temperature (t=1 hr) .....	32
Figure 1.1.28 Channel NH <sub>3</sub> and NO Contours (T=262°C) .....	33
Figure 1.2.1 Multiple-Leg Aging System .....	34
Figure 1.2.2 Engelhard Experimental Set Up in Engine Testing Cell .....	35
Figure 1.2.3 Experimental Set-Up for SCR/CSF System Characterization at DDC .....	36
Figure 1.2.4 Engelhard Urea Injection System .....	37
Figure 1.2.5 Prototype Urea Injection System Capable of Vehicle Installation .....	37
Figure 1.2.6 Mode Characterization Speed and Load Points .....	39
Figure 1.2.7 Initial Results Summary: Gas Phase Emissions and Particulate Reduction .....	40
Figure 1.2.8 200-Hour Results Summary: Gas Phase Emissions and Particulate Reduction .....	41
Figure 1.2.9 Effect of AMA Aging on PM Removal Efficiency .....	41
Figure 1.2.10 Effect of AMA Aging on NO <sub>x</sub> Conversion Efficiency .....	42
Figure 1.2.11 Effect of AMA Aging on NH <sub>3</sub> Slip .....	42
Figure 1.2.12 Emissions Reduction Strategy over Modal Conditions .....	43
Figure 1.2.13 SCR NO <sub>x</sub> Conversion at Various Aging Stages (2000 rpm and 260 N·m) .....	44
Figure 1.2.14 SCR NO <sub>x</sub> Conversion at Various Aging Stages (1650 rpm and 180 N·m) .....	44
Figure 1.2.15 SCR NO <sub>x</sub> Conversion at Various Aging Stages (1500 rpm and 140 N·m) .....	45
Figure 1.2.16 SCR NO <sub>x</sub> Conversion at Various Aging Stages (1350 rpm and 120 N·m) .....	45

Figure 1.2.17 Ammonia Storage and Release Effect .....	46
Figure 1.2.18 Ammonia Storage Capacity as Function of Temperature and Space Velocity .....	47
Figure 1.2.19 NO <sub>x</sub> Prediction During Storage and Release @ 2000 rpm and 308°C .....	48
Figure 1.2.20 NH <sub>3</sub> Balance During Storage and Release @ 2000 rpm and 308°C .....	48
Figure 1.2.21 Urea Injection Control Logic Diagram .....	49
Figure 1.2.22 Optimization Region of Interest Identified via the Analytical Tool .....	49
Figure 1.2.23 Urea Injection Control Issue - Hole-to-Hole Flow Rate Variation .....	50
Figure 1.2.24 SCR Piping System and Computational Grid .....	51
Figure 1.2.25 Two Urea Injection Distributions Obtained from CFD Simulations .....	52
Figure 1.2.26 Ammonia Distribution for a Straight Pipe Configuration .....	52
Figure 1.2.27 Mal-Distribution Index for a Straight Pipe Configuration .....	53
Figure 1.2.28 Ammonia Distribution for the 90° Elbow Configuration .....	54
Figure 1.2.29 Mal-Distribution Index for Straight Pipe and Elbow Configurations .....	54
Figure 1.2.30 Effect of Additional Mixing on NO <sub>x</sub> Reduction for the 90° Elbow Configuration .....	55
Figure 1.2.31 Impact of CSF Regeneration on Fuel Economy .....	56
Figure 1.2.32 CSF Failure as a Result of Uncontrolled Regeneration .....	57
Figure 1.2.33 Apparent Lack of Correlation between Accumulated Soot and Pressure Drop .....	57
Figure 1.2.34 Baseline Mass Shift after Multiple Regenerations .....	58
Figure 1.2.35 Passive Regeneration for the 1.5L HEV Engine .....	58
Figure 1.2.36 Balance Point Determination at 2200 rpm for a 1.5L HEV Engine Application .....	59
Figure 1.2.37 Balance Point Determination at 2700 rpm for a 1.5L HEV Engine Application .....	59
Figure 1.2.38 CSF Soot Balance Analysis Using DDC Developed CSF Model .....	60
Figure 1.2.39 General Regeneration Strategy for Stop and Start Triggering .....	61
Figure 1.2.40 Simplification of a 2D CSF Model to a Real-Time 0D Model .....	61
Figure 1.2.41 Regeneration Control Algorithm .....	62
Figure 1.2.42 Regeneration Behavior Simulated in Real Time .....	62
Figure 1.2.43 Effect of Soot Loading on Regeneration .....	63
Figure 1.2.44 Two LNT Configurations Considered under the LEADER Program .....	64
Figure 1.2.45 Dual Parallel-Leg LNT/CSF System Using Exhaust Fuel Injection .....	65
Figure 1.2.46 Exhaust Fuel Injector .....	65
Figure 1.2.47 Example Results from a Dual Leg LNT System with 60s Lean / 2s Rich Operation Resulting in over 90% NO <sub>x</sub> Conversion .....	66
Figure 1.2.48 Example Results of NO <sub>x</sub> Conversion with Lean/Rich Operation Optimization at 1500 rpm / 140 N·m .....	67
Figure 1.2.49 Example of Trade-off of Hydrocarbon Slip and NO <sub>x</sub> Conversion at 1500 rpm / 140 N·m .....	67

Figure 1.2.50 Sensitivity of NOx Conversion to Rich Operation Time and Injector Duty Cycle for Six Steady State Modes .....	68
Figure 1.2.51 NOx Conversion Recovery after Desulfation at 700°C .....	68
Figure 1.2.52 Summary of Fuel Economy Penalty versus NOx Conversion Efficiency .....	69
Figure 1.2.53 Experimental Setup Used for DOC Characterization.....	70
Figure 1.2.54a NOx Concentration versus Inlet Temperature of DOC for Mix 1.....	71
Figure 1.2.54b NOx Concentration versus Inlet Temperature of DOC for Mix 3.....	72
Figure 1.2.54c NOx Concentration versus Inlet Temperature of DOC for Mix 4.....	72
Figure 1.2.54d NOx Concentration versus Inlet Temperature of DOC for Mix 5.....	73
Figure 1.2.54e NOx Concentration versus Inlet Temperature of DOC for Mix 6.....	73
Figure 2.1 Personal Transportation LEADER Engines .....	74
Figure 2.2 DDC's CLEAN Combustion® Development .....	75
Figure 2.3 CLEAN Combustion® Concept.....	75
Figure 2.4 Controllable CO Emissions Produced by CLEAN Combustion® .....	76
Figure 2.5 Controllable HC Emissions Produced by CLEAN Combustion® .....	77
Figure 2.6 High Engine Out NO <sub>2</sub> /NOx Ratios Due to CLEAN Combustion® .....	77
Figure 2.7 Seven Selected Modes for Air Management Strategy Development.....	78
Figure 2.8 Air Fuel Ratio Comparisons Using Different Air Management Strategies.....	79
Figure 2.9 Turbine-Out Exhaust Temperature Comparisons with Different Air Management Strategies.....	79
Figure 3.1 Dodge Neon CSF-SCR Exhaust Aftertreatment System .....	80
Figure 3.2 Schematic of the Vehicle Test Set-Up .....	81
Figure 3.3 FTP75 Emissions Milestones for the PNGV Mule Vehicle.....	82
Figure 3.4 Combined Fuel Economy for Tier 2 Emissions Milestones.....	83
Figure 3.5 FTP75 Vehicle Out NOx versus Engine Out NOx .....	84
Figure 3.6 Aftertreatment Effectiveness During FTP75 .....	84
Figure 3.7 Average SCR Inlet Temperature During FTP75 .....	85
Figure 3.8 NOx, PM, MPG for Highway Fuel Economy Test Cycle .....	85
Figure 3.9 Urea Control Strategy Development over Hot 505 Transient Cycle Using 1D SCR Model .....	86
Figure 3.10 NOx Reduction and NH <sub>3</sub> Slip Trade-Off Identified via the Analytical Tool .....	87
Figure 3.11 Experimental Validation of the Urea Injection Control Strategy Development.....	87
Figure 3.12 PM Loading Standard Deviation Over Mean Value, Hot 505 .....	88
Figure 3.13 Mean Filter Mass Loading, Hot 505 .....	89
Figure 3.14 Simulated CSF Filtration Efficiency During Particulate Loading .....	89

Figure 3.15 Simulation Model-Predicted CSF Filtration Efficiency, C-505 and S867 Portions of FTP75 .....	90
Figure 4.1 Simulated Hot 505 Cycle for Optimization of Different Calibration Packages.....	91
Figure 4.2 Calibration Strategy Development Path in a Transient Engine Testing Cell.....	92
Figure 4.3 2001 Dakota Quad Cap Sport 4x2 Vehicle .....	92
Figure 4.4 CSF and SCR System Layout in the Dakota Vehicle .....	93
Figure 4.5 Light Truck Chassis Dynamometer Results (Bin 6).....	94
Figure 4.6 Light Truck Chassis Dynamometer Results (Near Tier 2 Bin 9 without Active AT) ..	94
Figure 4.7 Light Truck Chassis Dynamometer Results (Tier 2 Bin 3).....	95
Figure 5.1 Impact of CSF Regeneration Frequency on Fuel Economy .....	96
Figure 5.2 Temperature Profiles for LT/SUV and Passenger Car Applications over FTP75 ....	97
Figure 5.3 Soot Oxidation and Trapped Soot inside a Filter over a FTP75 Cycle .....	98
Figure 5.4 Packaging Challenging for Passenger Car Applications with Complicated NOx Aftertreatment and CSF System.....	98
Figure 5.5 Ash Loading in Sintered Metal Filter (Left Side) and Cordierite Filter (Right Side)...	99
Figure 5.6 Pressure Loss Comparisons for a Filter with Ash Filling from 0% to 50%.....	100
Figure A1 Wet Chemistry Test Set-Up.....	103
Figure A2 Vehicle Speed During AMA Driving Cycle.....	104
Figure A3 FTP75 Test Cycle.....	107
Figure A4 Highway Fuel Economy (HWYFE) Test Cycle .....	107
Figure A5 Schematic of the Vehicle Test Set-Up.....	108

## LIST OF TABLES

Table 1.1.1 Three-Layer CSF Models.....	15
Table 1.1.2 Three-Layer SCR Models .....	15
Table 1.1.3 Comparison of Measured and CSF Model Simulated Data Corresponding to Figure 1.1.7 Cases.....	20
Table 1.2.1 Initial SCR Performance over Five Modes.....	40
Table 1.2.2 Steady State Modes for Characterization of Aged SCR .....	43
Table 1.2.3 NO <sub>2</sub> Conversion Efficiency for Aged Catalyzed Soot Filters .....	60
Table 1.2.4 Steady State Modes for Characterization of LNT/CSF System .....	66
Table 1.2.5 Reactor Bench Text Matrix .....	70
Table 3.1 Low Sulfur Fuel Properties.....	81
Table A1 Comparison of the DDC PNGV Mule Vehicle with the Production VW Lupo .....	106
Table A2 Vehicle Instrumentation .....	109
Table A3 Tier 2 Emissions Regulations, FTP75 at 120,000 km .....	110

## ACRONYMS

AMA	Approved Mileage Accumulation
AT	Aftertreatment
BMEP	Brake Mean Effective Pressure
CFD	Computational Fluid Dynamics
CIDI	Compression Ignition Direct Injection
CLEAN Combustion®	Controlled Low Emission Aftertreatment Nurturing Combustion®
CSF	Catalyzed Soot Filter
DDC	Detroit Diesel Corporation
DEER	Diesel Engine Emissions Reduction
DELTA	Diesel Engine Light Truck Application
DOC	Diesel Oxidation Catalyst
DOE	Department of Energy
DPF	Diesel Particulate Filter
EC	Engelhard Corporation
EERE	Energy Efficiency and Renewable Energy
EGR	Exhaust Gas Recirculation
FTIR	Fourier Transform InfraRed
FTP	Federal Test Procedure
Gen	Generation
HC	Hydrocarbon
HEV	Hybrid Electric Vehicle
HSDI	High Speed Direct Injection
HWYFE	Highway Fuel Economy
LEADER	Low Emissions Aftertreatment and Diesel Emissions Reduction
LDT	Light-duty Truck
LNT	Lean NOx Trap
MPG	Miles Per Gallon
NOx	Nitrous Oxides
NSR	Normalized Stoichiometric Ratio

OD	Outer Diameter
OEM	Original Equipment Manufacturer
PM	Particulate Matter
PNGV	Partnership for Next Generation Vehicle
ROI	Return on Investment
SAE	Society of Automotive Engineers
SCR	Selective Catalytic Reduction
SFTP	Supplemental Federal Test Procedure
SOF	Soluble Organic Fraction
SUV	Sports Utility Vehicle
VGT	Variable Geometry Turbo
WOT	Wide Open Throttle

**LEADER**  
**Low Emissions Aftertreatment Diesel Emissions Reduction**  
**Final Report**  
**DE-FC26-99EE50575**

## **I. EXECUTIVE SUMMARY**

Detroit Diesel Corporation (DDC) has successfully completed a five-year Low Emissions Aftertreatment and Diesel Emissions Reduction (LEADER) program under a DOE project entitled: "Research and Development for Compression-Ignition Direct-Injection Engines (CIDI) and Aftertreatment Sub-Systems."

The objectives of the LEADER Program were to:

- Demonstrate technologies that will achieve future federal Tier 2 emissions targets.
- Demonstrate production-viable technical targets for engine out emissions, efficiency, power density, noise, durability, production cost, aftertreatment volume and weight.

These objectives were successfully met during the course of the LEADER program. The most noteworthy achievements in this program are listed below:

- Demonstrated Tier 2 Bin 3 emissions target over the FTP75 cycle on a PNGV-mule Neon passenger car, utilizing a CSF + SCR system. These aggressive emissions were obtained with no ammonia ( $\text{NH}_3$ ) slip and a combined fuel economy of 63 miles per gallon, integrating FTP75 and highway fuel economy transient cycle test results. Demonstrated feasibility to achieve Tier 2 Bin 8 emissions levels without active NOx aftertreatment.
- Demonstrated Tier 2 Bin 3 emissions target over the FTP75 cycle on a light-duty truck utilizing a CSF + SCR system, synergizing efforts with the DOE-DDC DELTA program. This aggressive reduction in tailpipe out emissions was achieved with no ammonia slip and a 41% fuel economy improvement, compared to the equivalent gasoline engine-equipped vehicle.
- Demonstrated Tier 2 near-Bin 9 emissions compliance on a light-duty truck, without active NOx aftertreatment devices, in synergy with the DOE-DDC DELTA program.
- Developed and applied advanced combustion technologies such as "CLEAN Combustion<sup>®</sup>", which yields simultaneous reduction in engine out NOx and PM emissions while also improving engine and aftertreatment integration by providing favorable exhaust species and temperature characteristics. These favorable emissions characteristics were obtained while maintaining performance and fuel economy.

These aggressive emissions and performance results were achieved by applying a robust systems technology development methodology. This systems approach benefits substantially from an integrated experimental and analytical approach to technology development, which is one of DDC's core competencies. Also, DDC is uniquely positioned to undertake such a

systems technology development approach, given its vertically integrated commercial structure within the DaimlerChrysler organization.

State-of-the-art analytical tools were developed targeting specific LEADER program objectives and were applied to guide system enhancements and to provide testing directions, resulting in a shortened and efficient development cycle. Application examples include ammonia/NO<sub>x</sub> distribution improvement and urea injection controls development, and were key contributors to significantly reduce engine out as well as tailpipe out emissions.

Successful cooperation between DDC and Engelhard Corporation, the major subcontractor for the LEADER program and provider of state-of-the-art technologies on various catalysts, was another contributing factor to ensure that both passenger car and LD truck applications achieved Tier 2 Bin 3 emissions levels.

Significant technical challenges, which highlight barriers of commercialization of diesel technology for passenger cars and LD truck applications, are presented at the end of this report.

## II. PROGRAM OVERVIEW

DDC has successfully completed the five-year LEADER program and demonstrated the technical viability of achieving Tier 2 Bin 3 emissions levels on the light passenger car platform as well as the light-duty truck/SUV platform. These aggressive emissions levels were obtained while simultaneously achieving state-of-the-art fuel economy and performance metrics. The successful completion of the LEADER program is in support of the broader EERE and DOE goal of dramatically reducing or even ending U.S. dependence on foreign oil.

The oil consumption by the U.S. transportation sector is the dominant contributor to the overall U.S. oil consumption. In order to meet the current demand of oil, nearly 12.4 million barrels of oil are imported into the U.S. per day and account for 63% of the total oil consumption. Recent studies on the future energy outlook show the U.S. transportation oil consumption to increase substantially over the next two decades. In these studies, energy use among automobiles was shown to be fairly steady from 2000 to 2020, while that for Class 3 through Class 8 trucks (heavy-duty type vehicles) was predicted to increase marginally over that same twenty-year time frame. However, a significant increase was seen in the energy use of Class 1 and Class 2 trucks (pickups, vans and SUVs). In some cases, these types of vehicles are used commercially, but the primary source of increase was seen as part of the growing personal transportation market. This major projected increase in the energy use of these vehicles is expected to increase on-highway transportation energy use from approximately 10.5 million barrels of petroleum per day in the late 1990s up towards 16 million barrels in 2020<sup>1,2</sup>. (See Figure 0.1.)

Such studies also forecast that dieselization of the vehicle fleet, primarily these Class 1 and Class 2 light trucks, would result in a significant reduction in the U. S. transportation energy use. In the late 1990s, however, there were several questions regarding the diesel engine's potential to achieve future Tier 2 emissions and the resulting fuel economy improvement.

As a response to this challenge, a series of collaborative projects between the Department of Energy and DDC were initiated. Examples include the DELTA and LEADER programs. The key objectives of these programs were to demonstrate the technical viability of meeting Tier 2 emissions and to evaluate the resulting fuel economy impact. This report will only focus on the LEADER program. This five-year program featured four major technical tasks as shown in Figure 0.2.

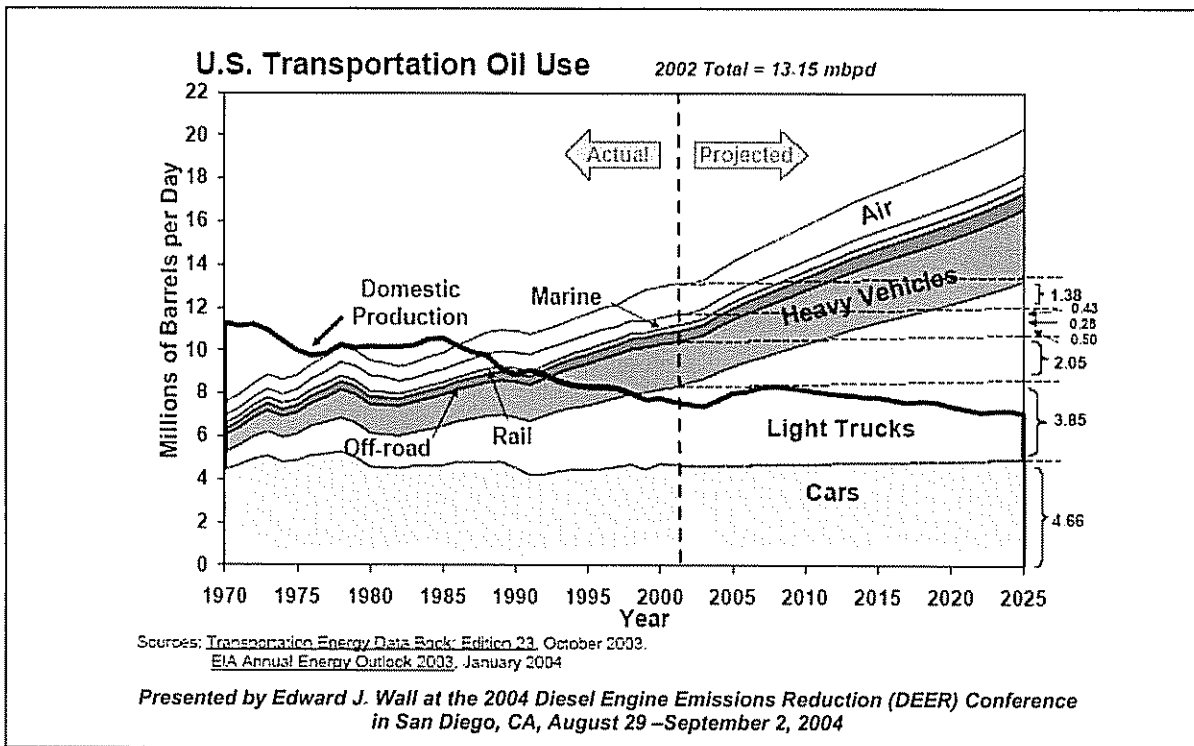


Figure 0.1 “Dieselization” of Light Trucks Offers Significant Reduction to U.S. Transportation Energy Use

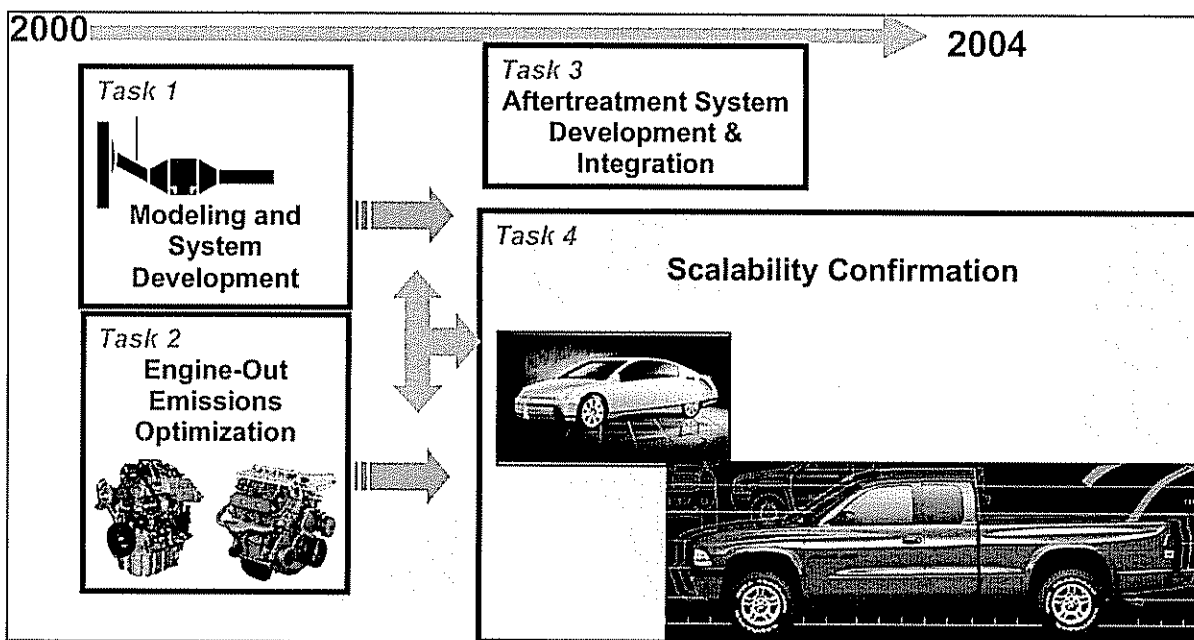


Figure 0.2 Program Development Plan

Detroit Diesel utilized an integrated analytical and experimental approach for technology development. This approach utilized DDC's state-of-the-art analytical tools in the early stages of the program to develop the concepts required for engine design as well as strategy development, followed by experimental verification of the down-selected strategies and technical approaches.

Task 1 focused on aftertreatment modeling and characterization of different catalysts including CSF, SCR, LNT and DOC. Task 2 covered all engine-related development including advanced combustion technologies development, such as CLEAN Combustion®, on both the 1.5L and the 4.0L engine platforms. Task 3 included the integration of the 1.5L engine and aftertreatment in a PNGV-type mule Neon vehicle. Task 4 was a scalability confirmation, applying the technologies developed under Tasks 2 and 3 to scale up to the 4.0L DELTA engine and its integration with aftertreatment and vehicle. A LD Dakota pick-up truck was used for Task 4. Detailed information regarding the DELTA engine can be viewed in Reference (3).

The LEADER program objectives were continuously enhanced as the program progressed. Figure 0.3 shows the original program objectives which targeted achieving the Tier 2 Bin 7 emissions level. With successful integration of the first generation of aftertreatment system (SCR + CSF), the program goals were adjusted to much more aggressive emissions targets at Tier 2 Bin 5 for both the passenger car and LD truck applications as shown in Figure 0.4.

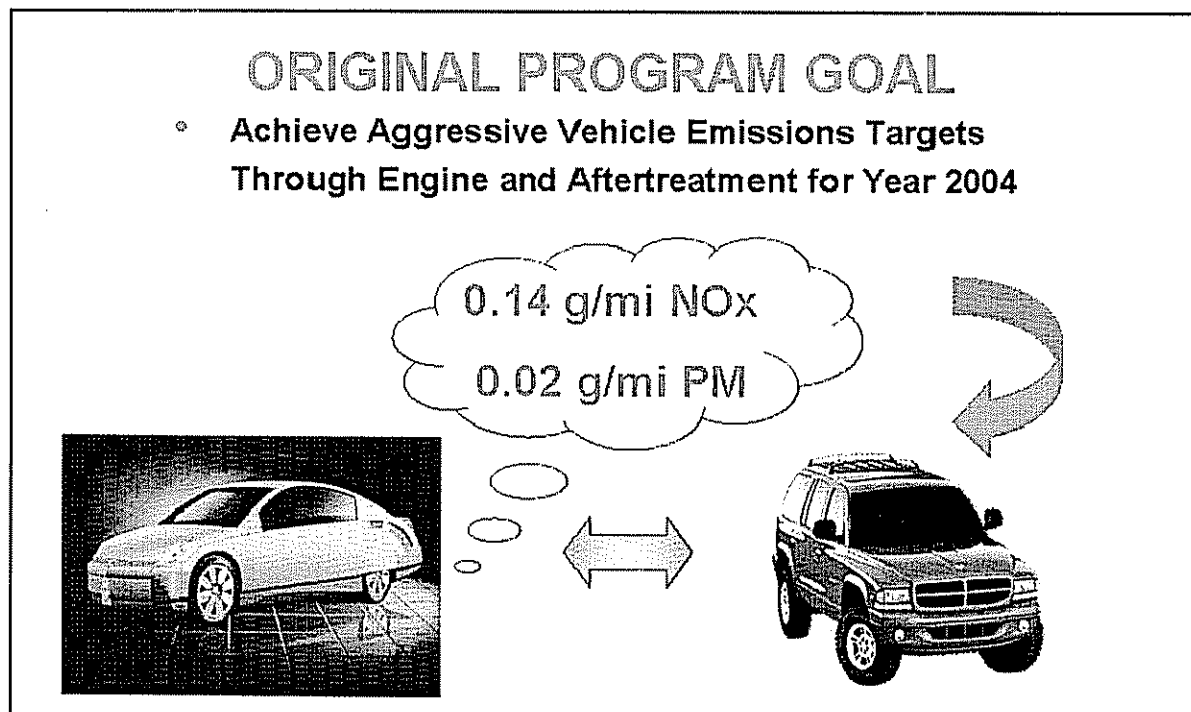


Figure 0.3 Original Program Goal

- Achieve Aggressive Vehicle Emissions Targets for 2007+

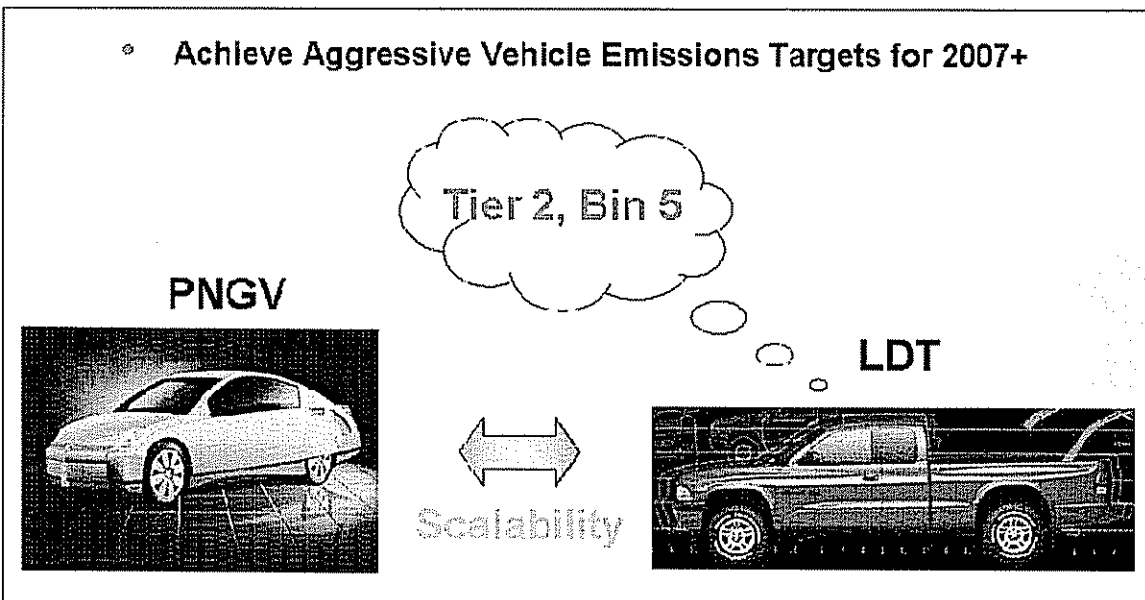


Figure 0.4 Program Goal Adjusted to Aggressive Emissions Targets

The LEADER program not only achieved the adjusted program goals of Tier 2 Bin 5 emissions levels, but also demonstrated even more aggressive emissions levels down to Tier 2 Bin 3 for both passenger car and LD truck application platforms. (Figures 0.5 and 0.6)

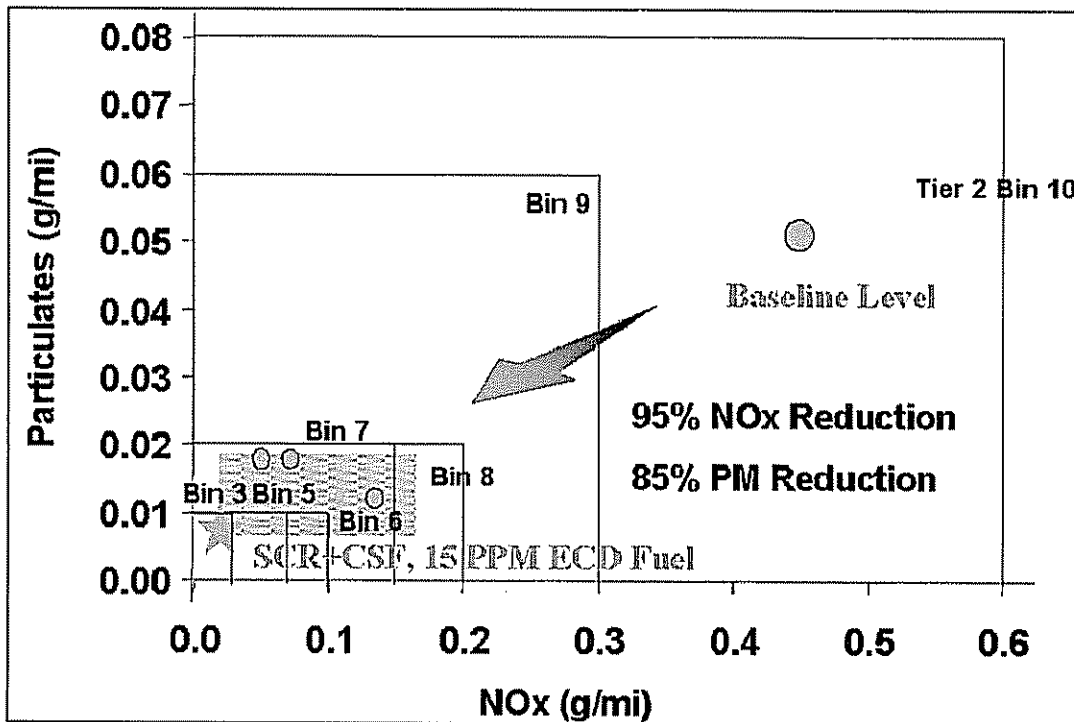


Figure 0.5 Demonstrated Tier 2 Bin 3 Emissions for Passenger Car

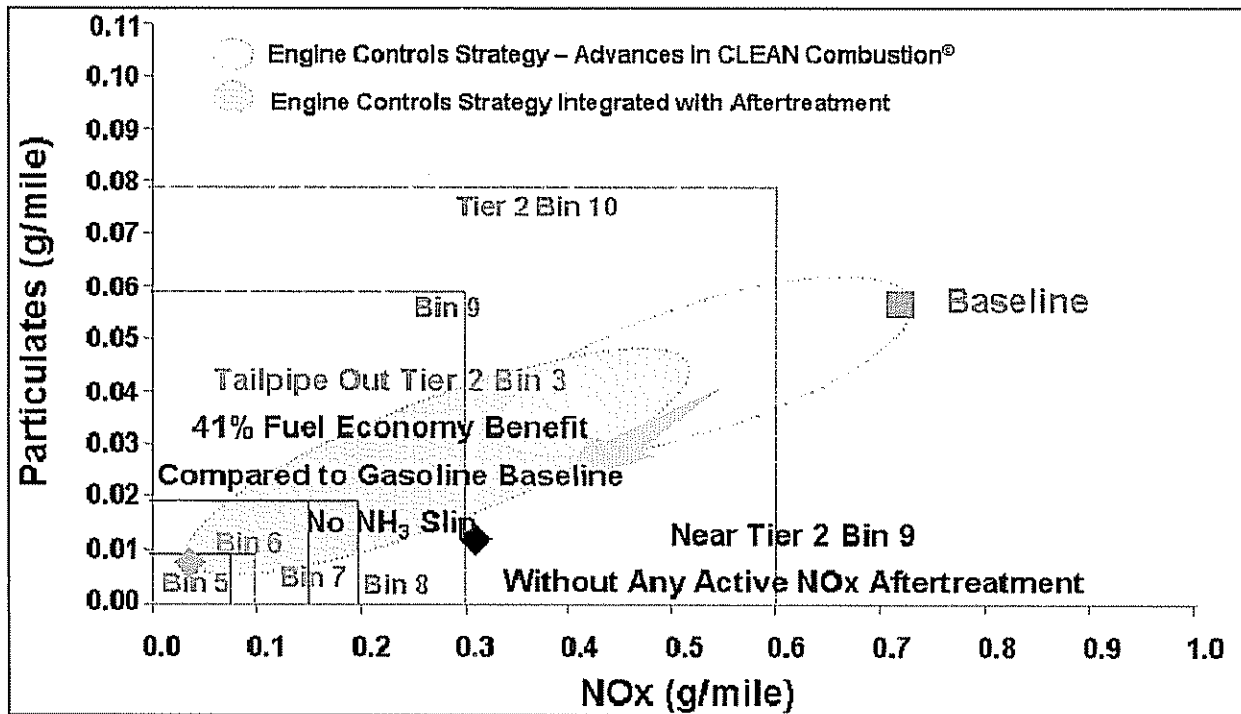


Figure 0.6 Demonstrated Tier 2 Bin 3 Emissions for Light Duty Truck

It should be pointed out that synergy with the DOE-funded DELTA program<sup>3</sup> played an important role in the success of the LD truck application achieving Bin 3 emissions.

The key accomplishments during the course of the program can be summarized as follows:

- Developed an integrated CIDI engine and emissions-control system (CSF + SCR) for passenger car and light-duty truck applications.
- Demonstrated Tier 2 Bin 3 emissions target over the FTP75 cycle on a PNGV-mule Neon car, utilizing a CSF + SCR system. These aggressive emissions were obtained with no NH<sub>3</sub> slip and a combined fuel economy of 63 miles per gallon, integrating FTP75 and highway fuel economy transient cycle test results. Demonstrated feasibility to achieve Tier 2 Bin 8 emissions levels without active NO<sub>x</sub> aftertreatment.
- Demonstrated Tier 2 Bin 3 emissions target over the FTP75 cycle on a light-duty truck utilizing a CSF + SCR system, synergizing efforts with the DOE-DDC DELTA program. This aggressive reduction in tailpipe emissions was obtained with no NH<sub>3</sub> slip and a 41% fuel economy improvement, compared to the equivalent gasoline engine-equipped vehicle.
- Demonstrated Tier 2 near-Bin 9 emissions compliance without active NO<sub>x</sub> aftertreatment devices on a light-duty truck, in synergy with the DOE-DDC DELTA program.
- Developed advanced combustion strategies such as "CLEAN Combustion<sup>®</sup>" which yields simultaneous reduction in engine out NO<sub>x</sub> and PM emissions while also improving engine and aftertreatment integration by providing favorable species and temperature

characteristics of the exhaust gases. These favorable emissions characteristics were obtained while maintaining performance and fuel economy.

- Conducted systematic investigation of characteristics of different air management approaches for CSF regeneration, including air by-pass, in-cylinder post injection and their combination.
- Developed a multiple exhaust leg aging system to simultaneously age up to four catalyst systems, resulting in accelerated test evaluations. An aging protocol for integrated CSF and LNT systems was also developed.
- Systematically characterized SCR + CSF aging behavior. Performance quantification of an SCR + CSF system aged up to 1000 hours did not reveal any noticeable SCR performance deterioration.
- Developed an LNT + CSF system that was applied to the 4.0L DELTA engine. Demonstrated greater than 90% NO<sub>x</sub> reduction over several critical FTP75 relevant modal steady state operating conditions.
- Developed and validated multiple aftertreatment (AT) simulation models and integrated them with existing engine and vehicle simulation tools.
- Applied the integrated simulation tool, featuring engine, AT and vehicle models to provide design and testing directions. New strategies for urea injection control of SCR applications and CSF regeneration control were developed.

The significant emissions reduction achieved in this program can be attributed to three key factors. These include the technology development methodology, sub-system optimization and integrated system optimization and are briefly summarized below:

### **1. Integrated Analytical and Experimental Approach to Technology Development**

The increasing complexity of diesel engine and aftertreatment sub-systems required to meet the future emissions regulations while meeting customer expectations for performance, fuel economy and reliability inherently demands a systems approach for technology development. This systems approach benefits substantially from an integrated experimental and analytical approach, which is one of DDC's core competencies (Figure 0.7). This integrated approach results in a shortened and efficient development cycle. An important element of this approach is DDC's state-of-the-art analytical toolbox, including 3D analysis for component optimization, 1D for system integration and 0D for real-time controls. This three-layer analysis approach will be described in detail under the description of Task 1.1. These models were regularly utilized during the program to enhance understanding of experimental results and to formulate strategies for the next cycle of development.

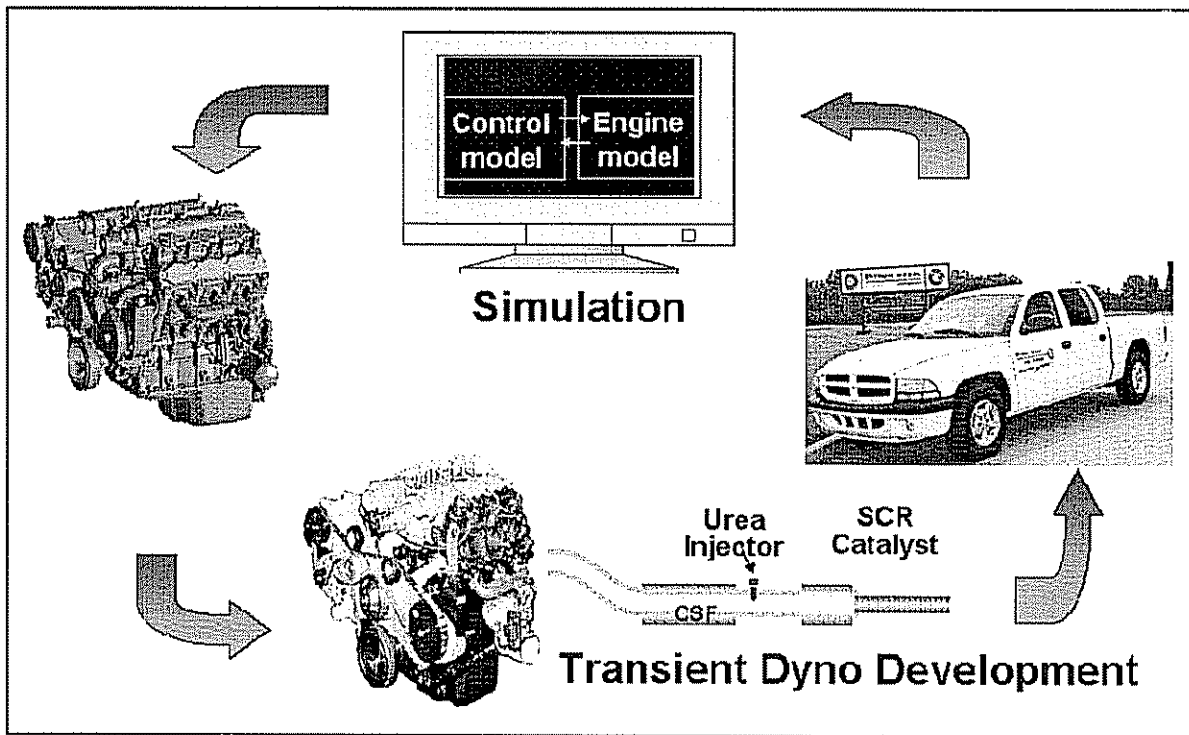


Figure 0.7 Integrated Experimental and Analytical Approach to System Development

## 2. Sub-System Optimization

Utilizing the technology development methodology described above, all of the major engine and aftertreatment sub-systems were optimized. The major sub-systems include the combustion, fuel, air/EGR, CSF, SCR and controls. As an example, the combustion system optimization resulted in the development of novel combustion strategies such as DDC's CLEAN Combustion®.

CLEAN Combustion® is characterized by a low temperature and low equivalence ratio combustion process, which results in simultaneous reduction of NOx and PM while controlling carbon monoxide (CO) and hydrocarbon (HC) to desired levels for aftertreatment integration. Figure 0.8 shows an example of simultaneous NOx and PM reduction obtained with CLEAN Combustion® for the DELTA engine compared to the classical NOx-PM trade-off curve associated with conventional diesel combustion characteristics. Enabling technologies such as a fully flexible fuel injection system and optimizing EGR flow over accelerations allow CLEAN Combustion® to be implemented over transient operation. These strategies have been successfully integrated on multiple vehicle platforms (with and without aftertreatment) and have demonstrated beyond state-of-the-art emissions levels that comply with transient emissions regulations over a chassis dynamometer for 2007 and beyond.

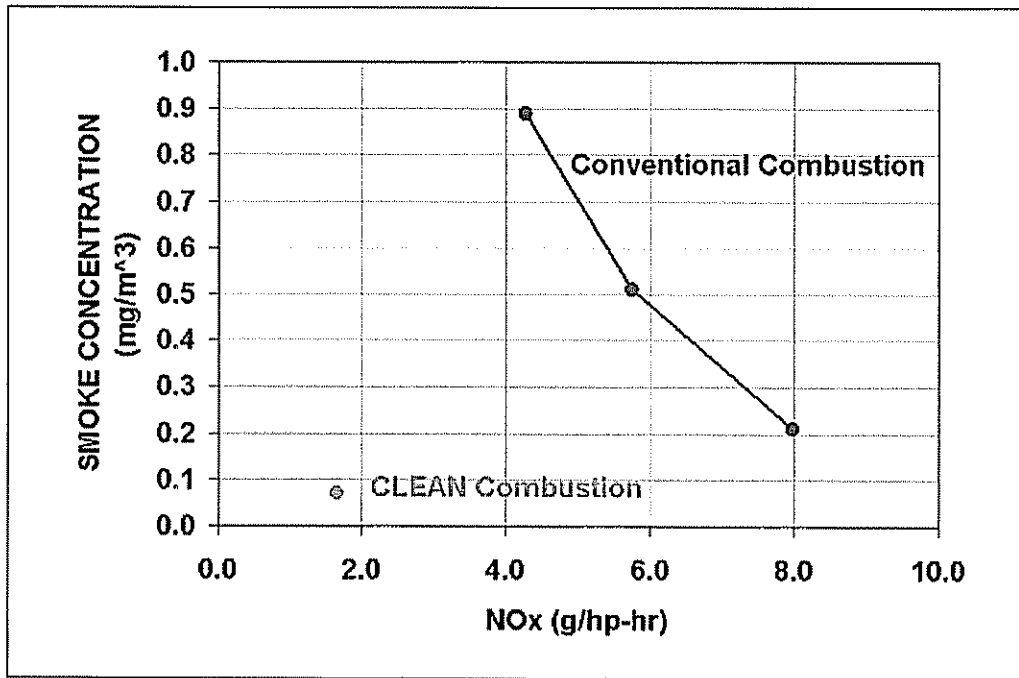


Figure 0.8 Simultaneous Reduction in NOx and PM Achieved via CLEAN Combustion® on the DELTA Engine

### 3. Integrated System Optimization

In addition to engine and aftertreatment sub-system optimization as briefly described above via the combustion system example, integrated system (engine, aftertreatment and vehicle) optimization was a focus area of the LEADER program. For example, combustion system strategies were developed to yield extremely low engine out emissions while simultaneously rendering favorable exhaust species and temperature characteristics for aftertreatment integration.

Figure 0.9 shows an example where the use of DDC's unique CLEAN Combustion® is made to increase exhaust temperature, while Figure 0.10 shows the favorable NO<sub>2</sub>/NOx ratio obtained via this combustion technology. The latter results in enhanced SCR and CSF performance, since NO<sub>2</sub> is a more reactive agent than NO. Optimization of the integrated system, comprised of advancements in sub-system technologies, allowed an overall 90% aftertreatment NOx reduction to be achieved as shown in Figure 0.11.

Another system optimization focus area was to fully utilize advanced analytical tool sets developed under the LEADER program to provide system integration and optimization directions. Figure 0.12 shows the application of DDC's 1D SCR model to a transient HOT 505 cycle in order to develop optimized urea control strategies. As seen from this figure, in addition to the baseline control strategy represented by the baseline "NOx Out" trace, additional urea injection control strategies were developed and applied. The "X" and "Y" traces represent examples of two such control strategies and show significant reduction in NOx compared to the baseline. Figure 0.13 shows the cumulative engine out and tailpipe out NOx traces obtained via experimental vehicle testing on a chassis dynamometer. The two control strategies shown by the traces X' and Y' were developed based on the directions

provided by the 1D SCR tool as explained above. These results are yet another validation example of the utilization of analytical tools, demonstrating the integrated experimental and analytical technology development methodology. Additional details on the vehicle testing results are presented in the description of Task 3.2.

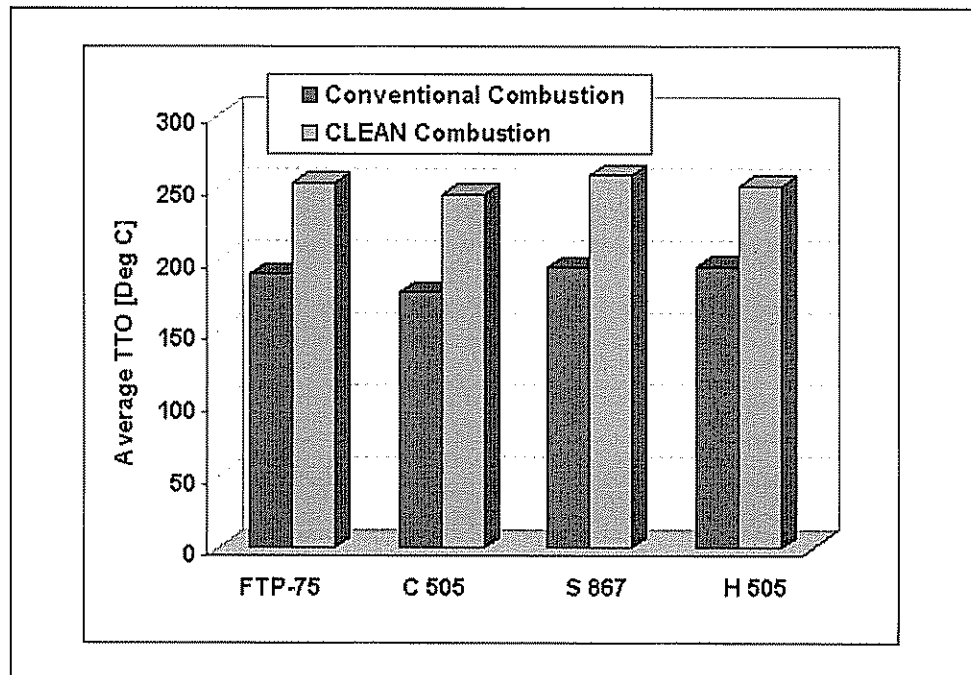


Figure 0.9 Exhaust Temperature Increase with CLEAN Combustion<sup>®</sup> Over FTP75 Test

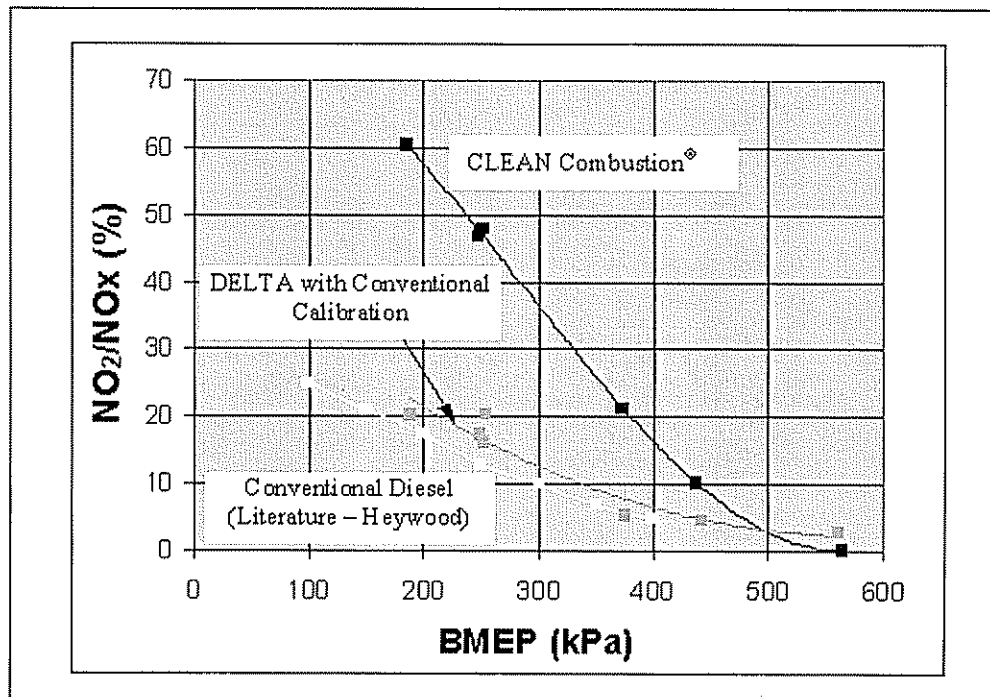


Figure 0.10 Increase in NO<sub>2</sub>/NOx Ratio Attributed to CLEAN Combustion<sup>®</sup>

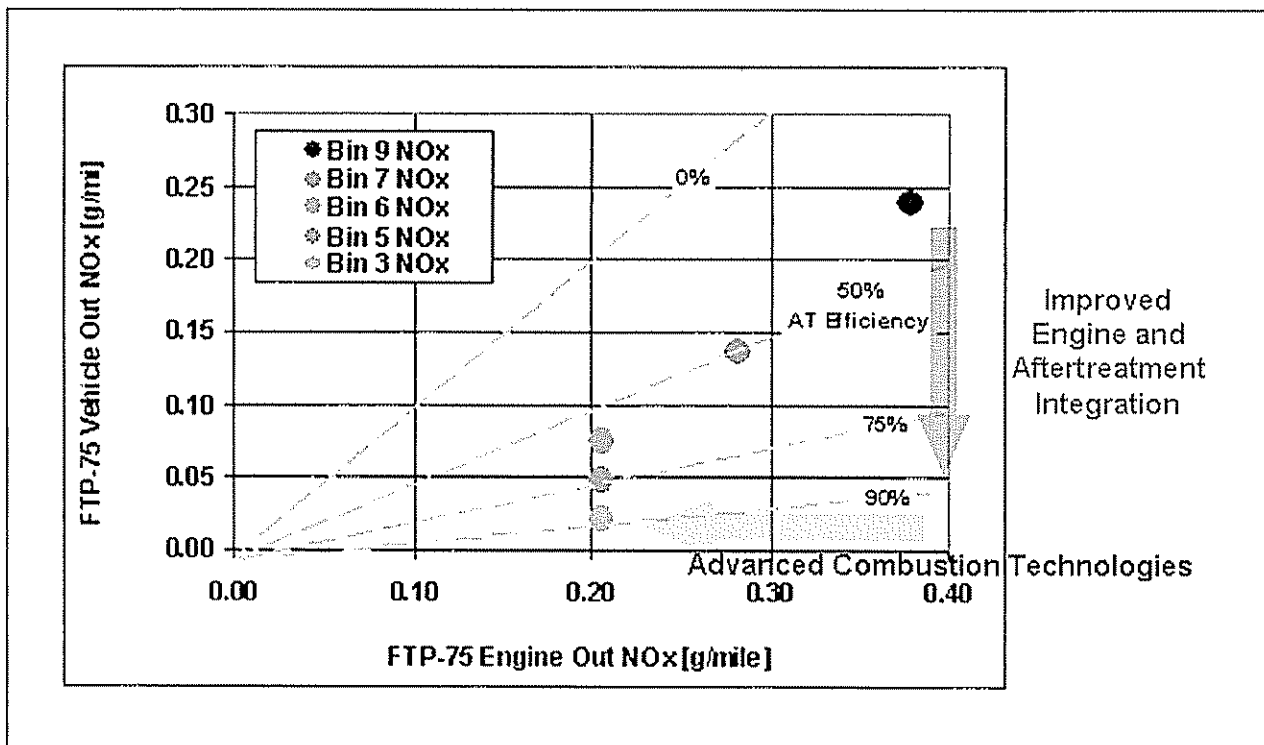


Figure 0.11 Integrated Engine and Aftertreatment System for Tier 2 Emissions

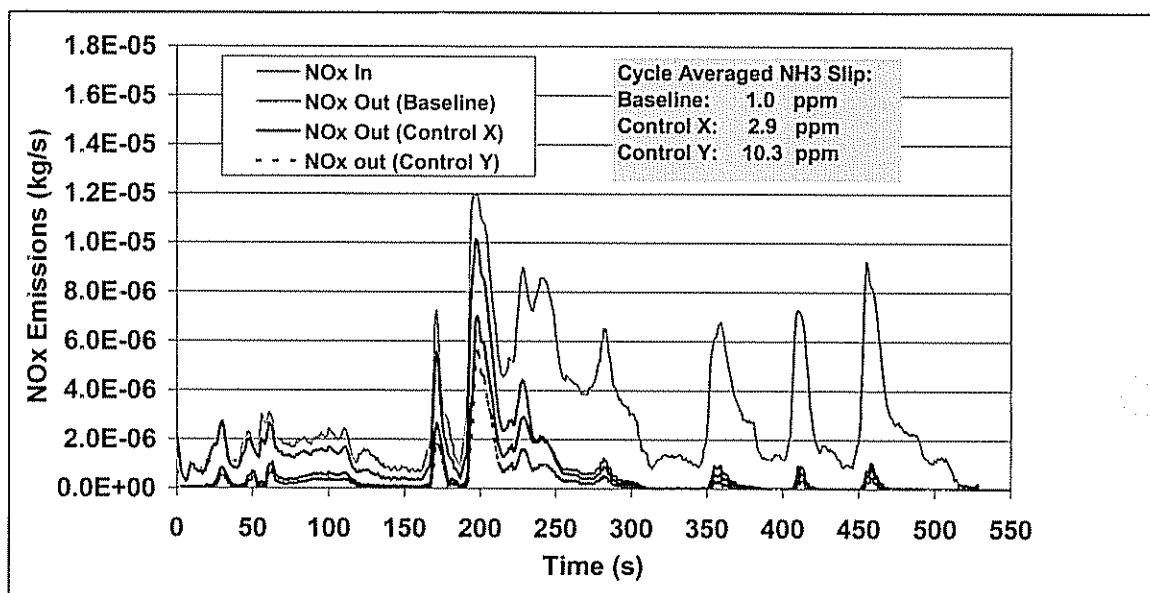
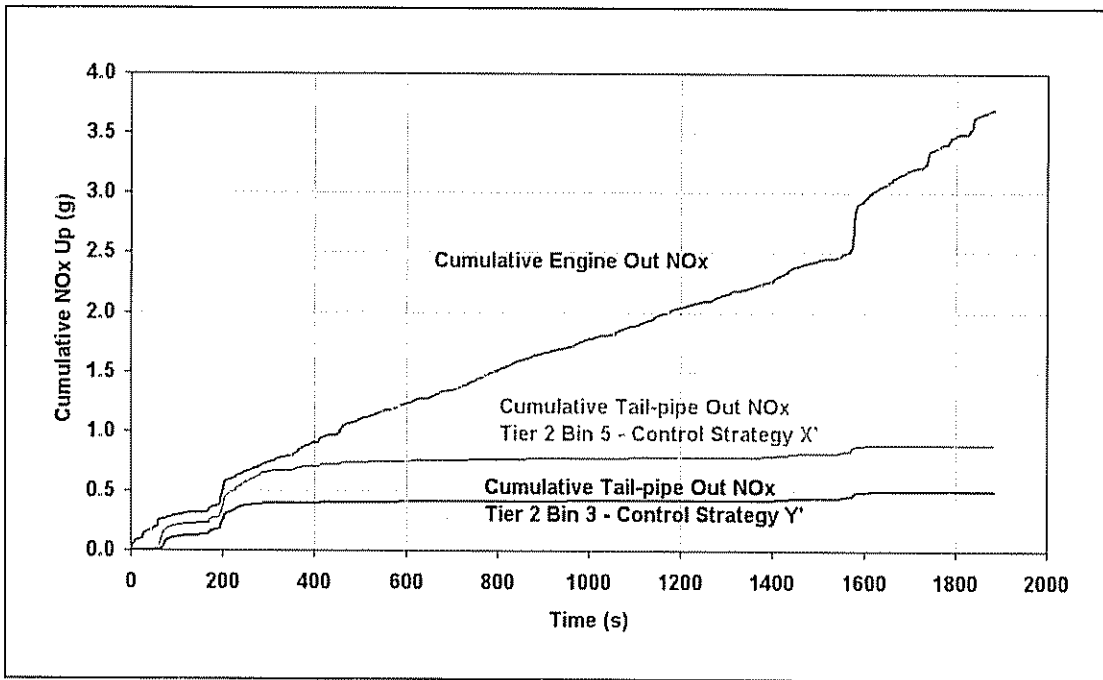


Figure 0.12 Urea Control Strategy Development over a Transient Cycle Using 1D SCR Model



**Figure 0.13 Experimental Validation of Urea Injection Control Strategy Development**

In the next section, technical details pertaining to the various program accomplishments are described. The technical reporting structure will follow the task order given in the earlier part of this section.

### III. TECHNICAL DETAILS

#### Task 1 Modeling and System Development

Two major subtasks are involved in this Modeling and System Development focus area. The first one is aftertreatment modeling development and its integration with total engine system tool box; and the second one is the characterization of different aftertreatment catalysts including DOC, CSF, SCR and LNT.

##### Task 1.1 Modeling Development and Integration

Utilizing advanced physics and computational fluid dynamics, a validated virtual lab comprised of 0D, 1D, 2D and 3D analytical tools provides developers and modelers the opportunity to carry out virtual experimental tests. These analytical tools, if used properly, provide abundant data that are either impossible or too expensive to obtain via conventional experimental techniques. Through parametric studies sensitive to the AT performance and emissions, these tools provide design directions of how the system can be optimized before expensive and time-consuming hardware tests are carried out.

DDC has developed a three-layer virtual lab strategy through the LEADER program as indicated in Figure 1.1.1. This strategy features a top layer for detailed physical understanding and design using 3D models, a middle layer for overall system integration using 1D models and a bottom layer for real time control using 0D models. Substantial progress has been made towards the three-layer virtual lab development and its integration during the course of this program<sup>4,5,6,7,8,9</sup>. Tables 1.1.1 and 1.1.2 show examples of different levels of CSF and SCR models, detailing resolution for various physical processes as handled by the various sub-models. The final goal of DDC's virtual lab is to comprehensively model the entire vehicle/engine/AT system as shown in Figure 1.1.2, for system integration and optimization.

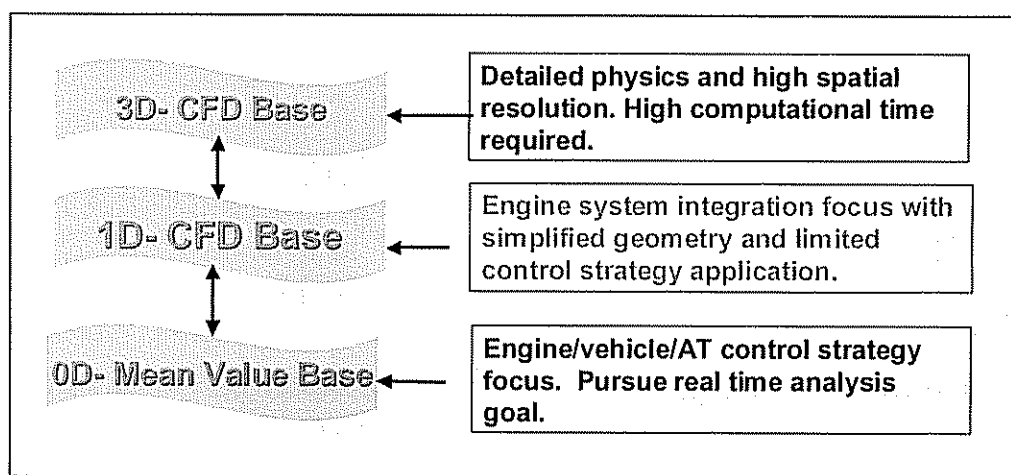


Figure 1.1.1 DDC's Three-Layer Virtual Lab Development Strategy

Table 1.1.1 Three-Layer CSF Models

	Flow Channel	Flow Wall	Thermal Channel	Thermal Wall	Filtration	DP
Lumped 0D Model	0D	0D	0D	0D	0D	0D
1D Model	1D	Quasi 1D	1D	Quasi 1D	Quasi 1D	Quasi 1D
2D Model	2D	Quasi 1D	2D	2D	1D	1D
3D Model	3D	3D	3D	3D	2D	2D

Table 1.1.2 Three-Layer SCR Models

	Urea Mixing	Flow	Thermal Channel	Kinetics	Time Scale
Lumped 0D Model	N/A	N/A	N/A	Macro-kinetics	Real time
1D Model	0D	1D	1D	Macro-kinetics	Minutes
2D Model	3D	3D	3D	Micro-kinetics	Hours

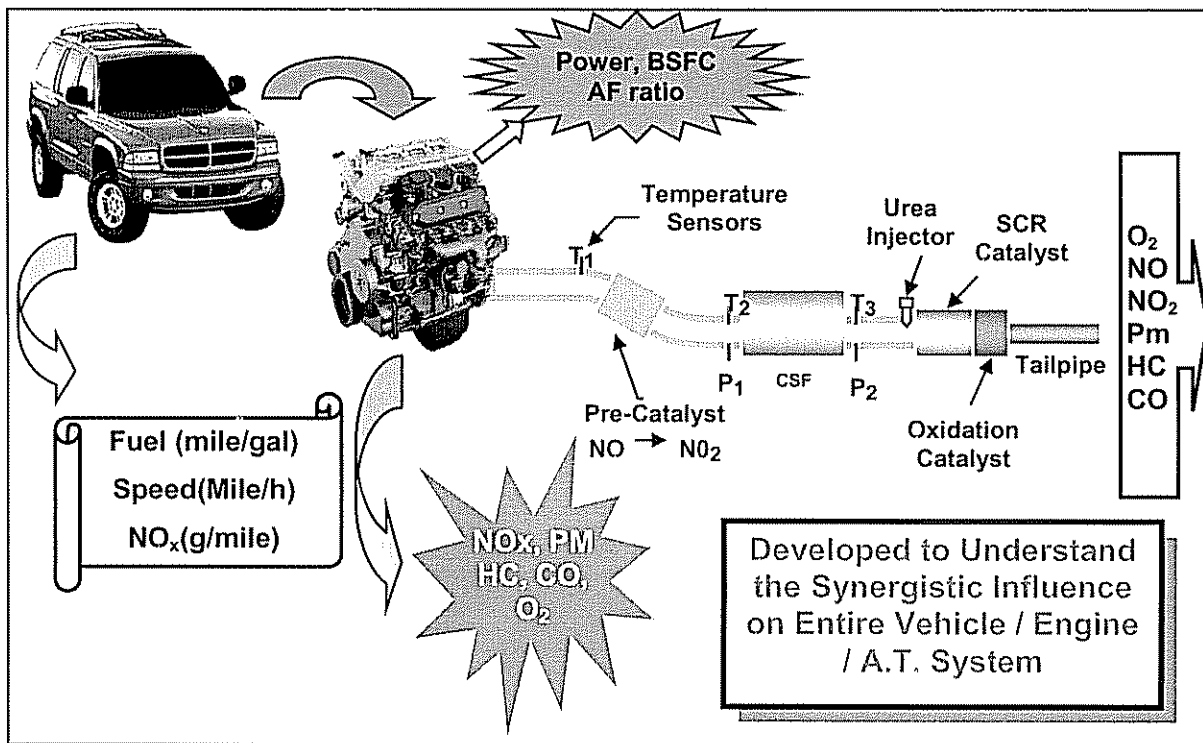


Figure 1.1.2 Concurrent Virtual Lab Integration for Entire Vehicle / Engine / AT System

All individual AT models have been validated against testing data obtained on steady state as well as transient cycles. Figures 1.1.3 - 1.1.6 show selective samples of model validation carried out against transient testing data.

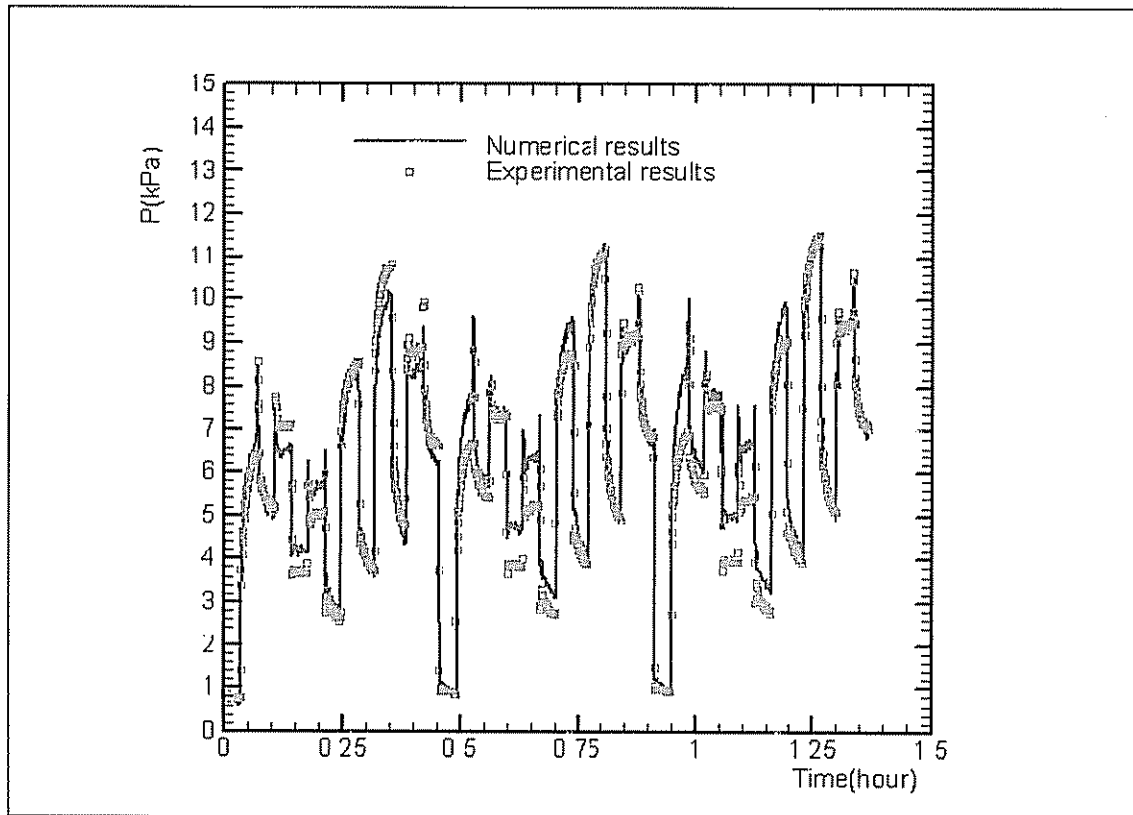


Figure 1.1.3 CSF Model Validation against Transient Test Data

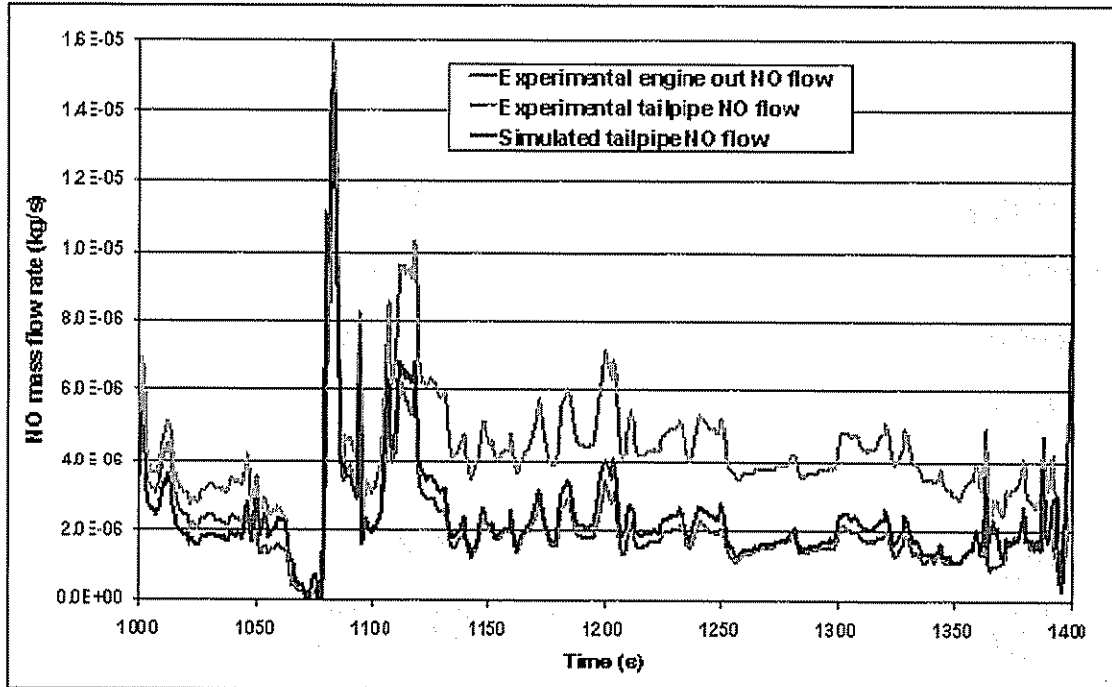


Figure 1.1.4 Vanadium-Based SCR Model Validation against Transient Vehicle Test Data

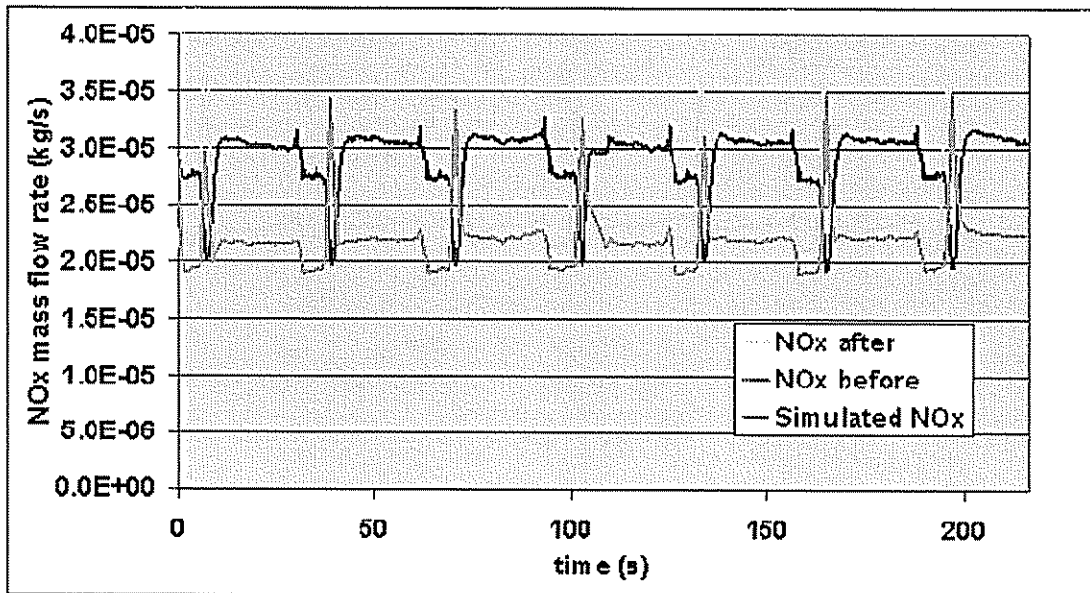


Figure 1.1.5 LNT Model Validation During Lean and Rich Regeneration

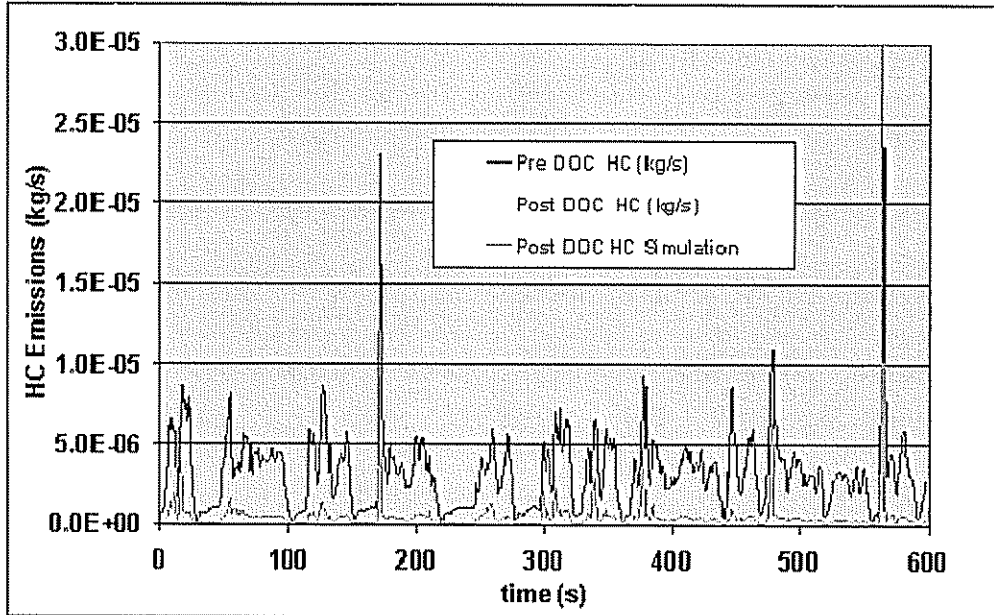
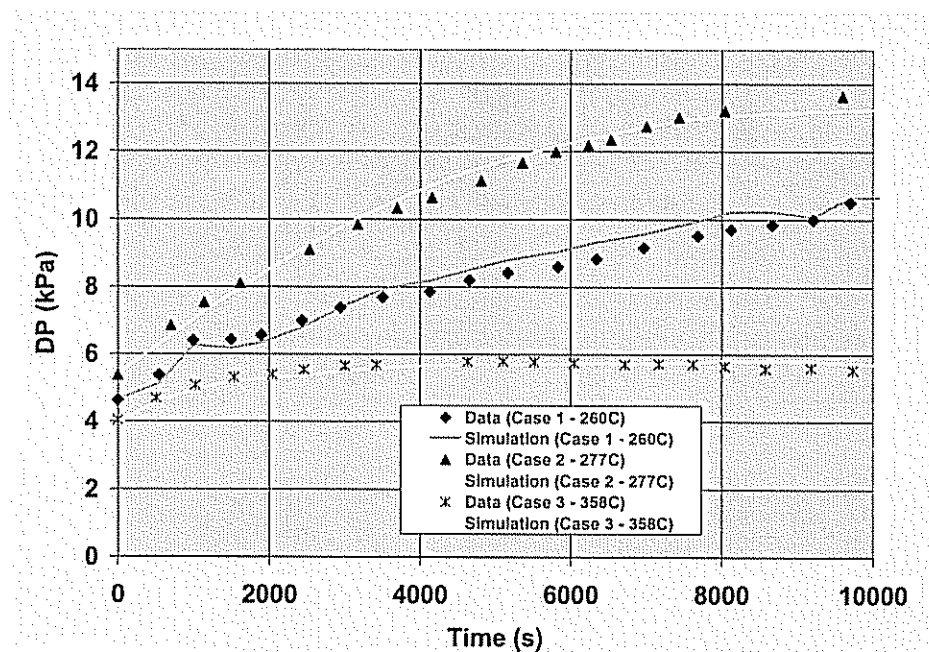


Figure 1.1.6 DOC Model Validation against Transient Vehicle Test Data

The CSF model was utilized to conduct additional validation against soot loading data. The data discussed below compares model predictions against CSF loading studies that included passive regeneration. The temperature range considered for these tests and analyses was 260°C - 360°C while the NOx/PM ratio varies between 34:1-48:1. In all of these cases, the same kinetic model constants are used. Pressure drop across the CSF as a function of time, and thus trapped soot level, is compared for the CSF simulation model and test data for three

cases from the LEADER program in Figure 1.1.7. Comparison of measured and computed data with regard to a few selective performance parameters such as gaseous emissions oxidation (CO, HC, NO) and soot loading are presented in Table 1.1.3. Excellent agreement is obtained between computed and experimental results for all the three cases.



**Figure 1.1.7 Comparison of Measured and CSF Model Simulated Pressure Drop across a Clean CSF with Temperature Between 260° - 360°C and NOx/PM Ratio 34 - 48**

Figures 1.1.8 - 1.1.11 show the comparison of measured and computed data with regard to gaseous emissions oxidation characteristics. Again, very good agreement is shown between the simulation model result and the experimental data. Of particular interest are the soot loading data and the soot mass conservation balances shown in Figures 1.1.12 - 1.1.14. Soot mass conservation data requires rigorous experimental methodology and demonstrates the fidelity of the CSF model. Engine out PM as well as tailpipe out PM were measured experimentally using conventional mini-dilution tunnel filter measurements. Measuring tailpipe out PM is challenging due to the very low tailpipe out soot over the 3-hour loading experiment. Trapped soot mass in the CSF after the 3-hour loading test was also measured experimentally. "Measured" filtered out PM by the CSF shown in Figures 1.1.13 and 1.1.14 is the difference between the engine out and tailpipe out PM. The CSF simulation model directly calculates all of these values and the model-predicted results show excellent agreement with this tedious experimental CSF technique.

**Table 1.1.3 Comparison of Measured and CSF Model Simulated Data Corresponding to Figure 1.1.7 Cases**

**Measurement**

Speed (rpm)	Torq (N·m)	CSF in T (°C)	CSF HC%	CSF CO%	CSF NO%	CSF OUT NO <sub>2</sub> (ppm)	Trapped Mass (g)
3500	45	260	89	99	39	124	5.6
3500	57	277	89	99	46	163	7.5
2800	102	358	92	99	49	278	2.8

**Simulation**

Speed (rpm)	Torq (N·m)	CSF in T (°C)	CSF HC%	CSF CO%	CSF NO%	CSF OUT NO <sub>2</sub> (ppm)	Trapped Mass (g)
3500	45	260	89	98	36	127	6.9
3500	57	277	88	99	36	131	7.1
2800	102	358	88	99	53	307	0.6

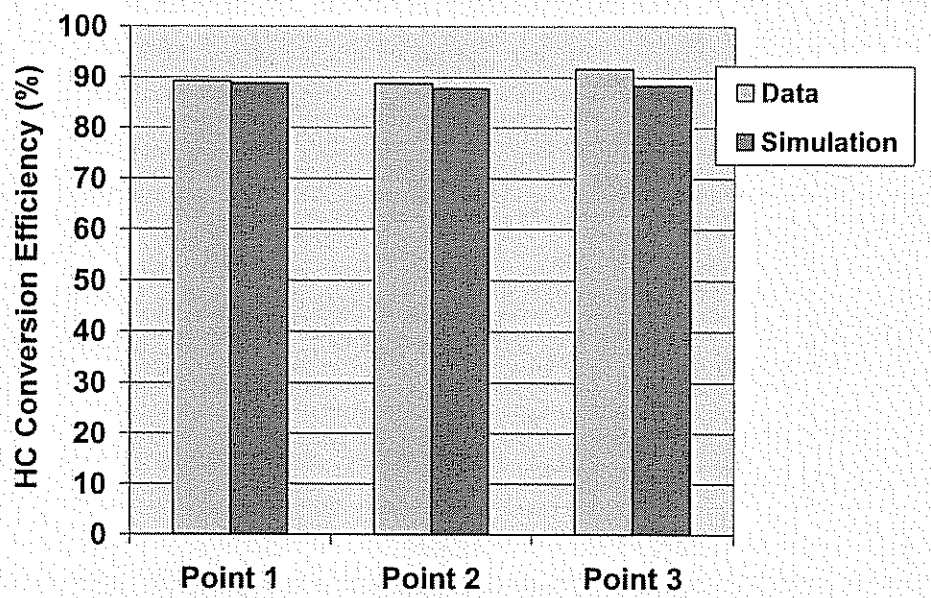


**Figure 1.1.8 Comparison of Measured and CSF Model Simulated HC Conversion for the Three CSF Loading Cases Corresponding to Figure 1.1.7**

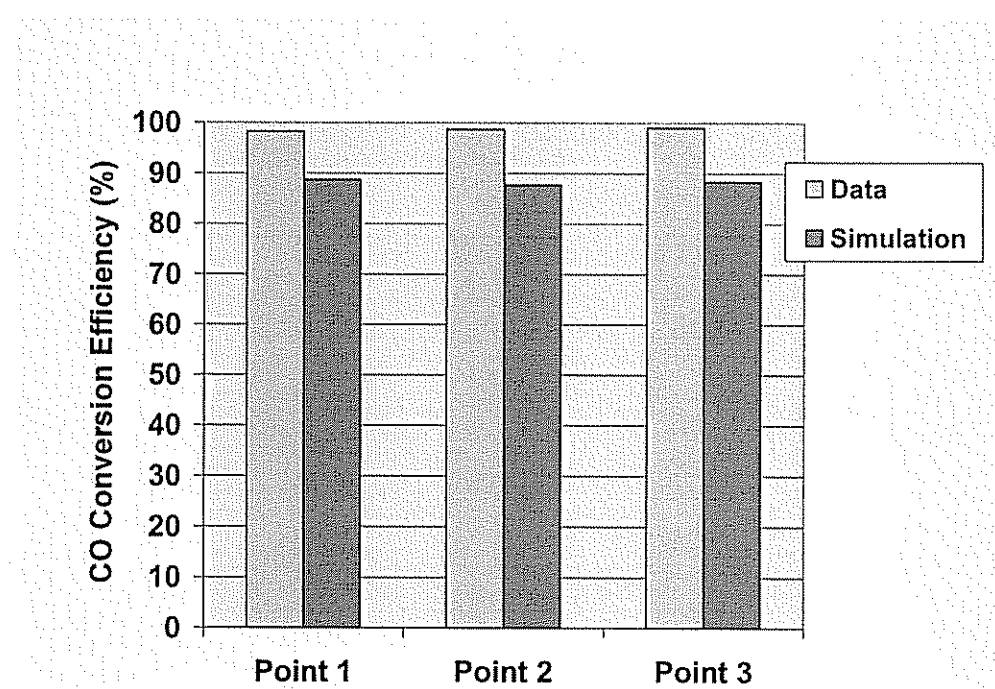


**Figure 1.1.9 Comparison of Measured and CSF Model Simulated CO Conversion for the Three CSF Loading Cases Corresponding to Figure 1.1.7**

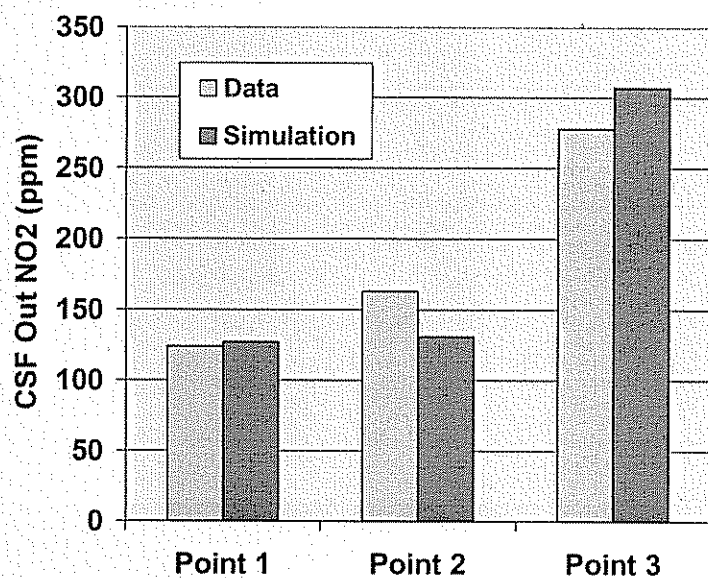


**Figure 1.1.10 Comparison of Measured and CSF Model Simulated NO<sub>2</sub> Emission from the Three CSF Loading Cases Corresponding to Figure 1.1.7**

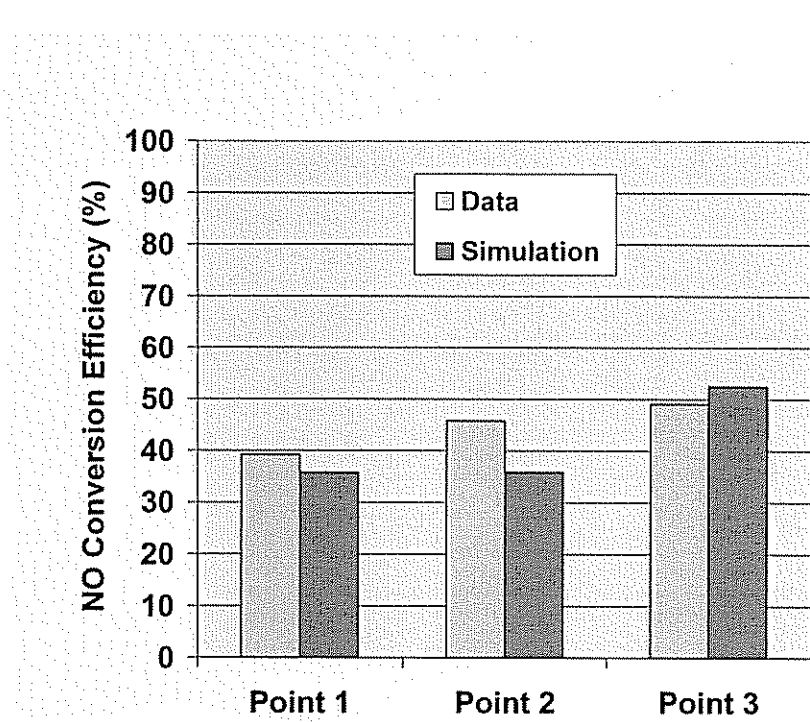


**Figure 1.1.11 Comparison of Measured and CSF Model Simulated NO Oxidation for the Three CSF Loading Cases Corresponding to Figure 1.1.7**

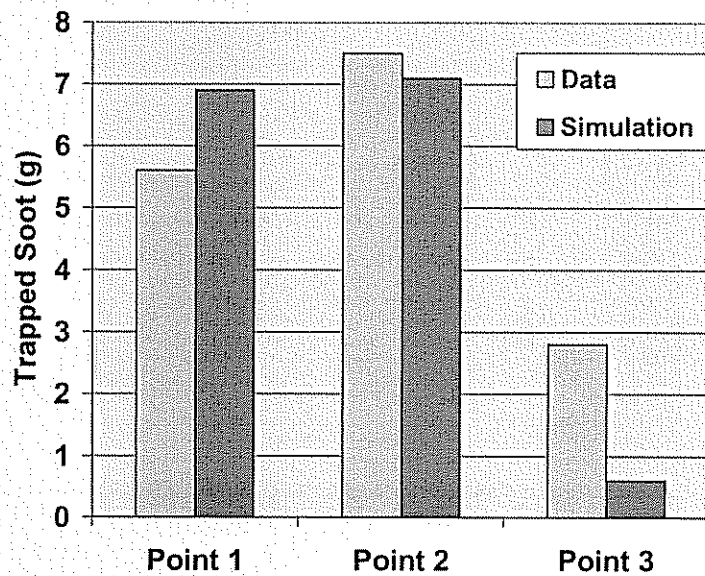


**Figure 1.1.12 Comparison of Measured and CSF Model Simulated Trapped (Unburned) Soot at the end of the Three CSF Loading Cases Corresponding to Figure 1.1.7**

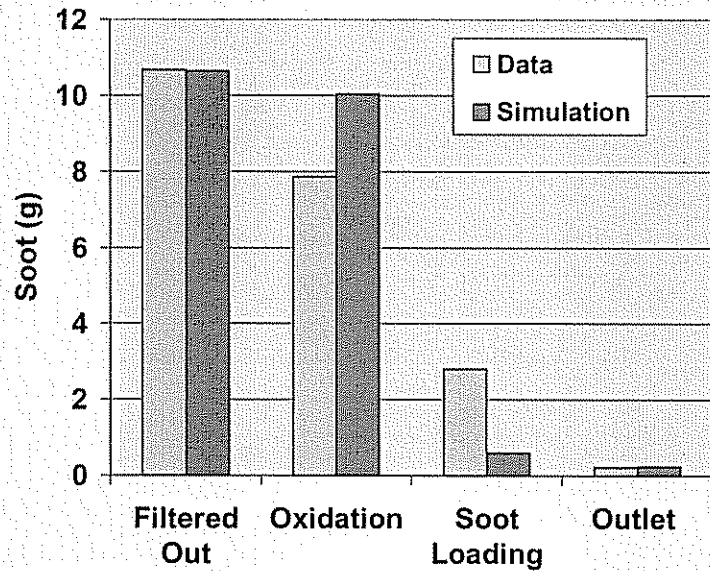


Figure 1.1.13 Comparison of Measured and CSF Model Simulated Soot Mass Balance for the CSF Loading Case 3 (358°C) from Figure 1.1.7

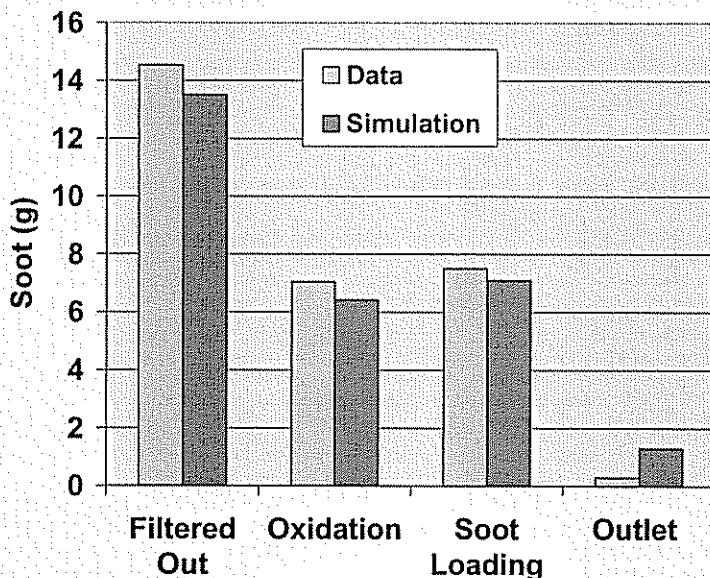
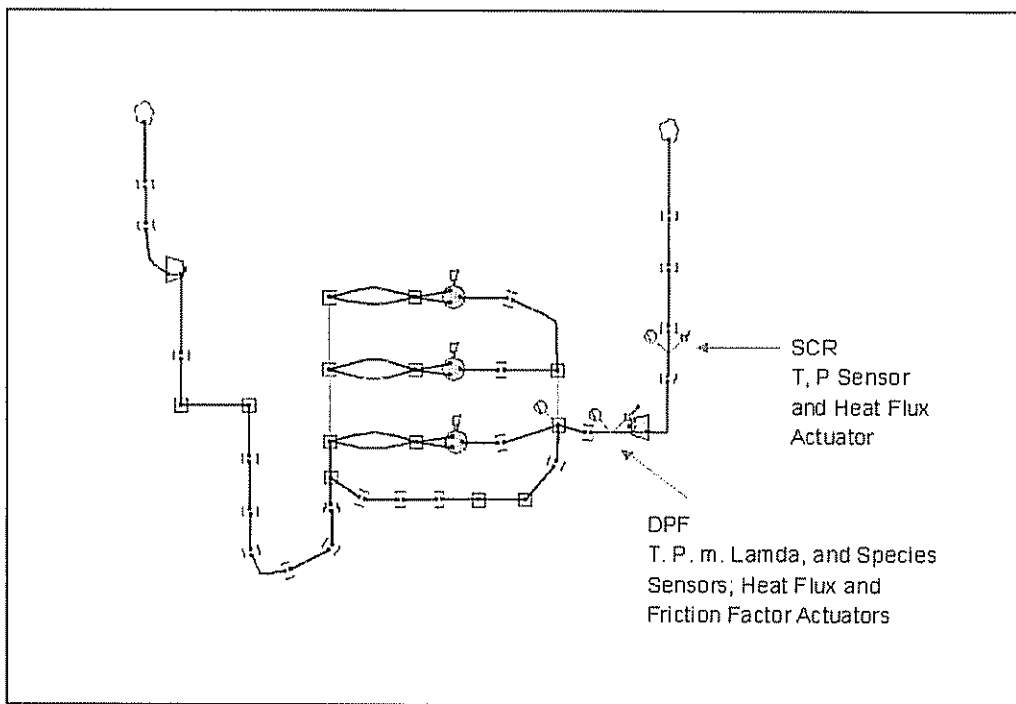
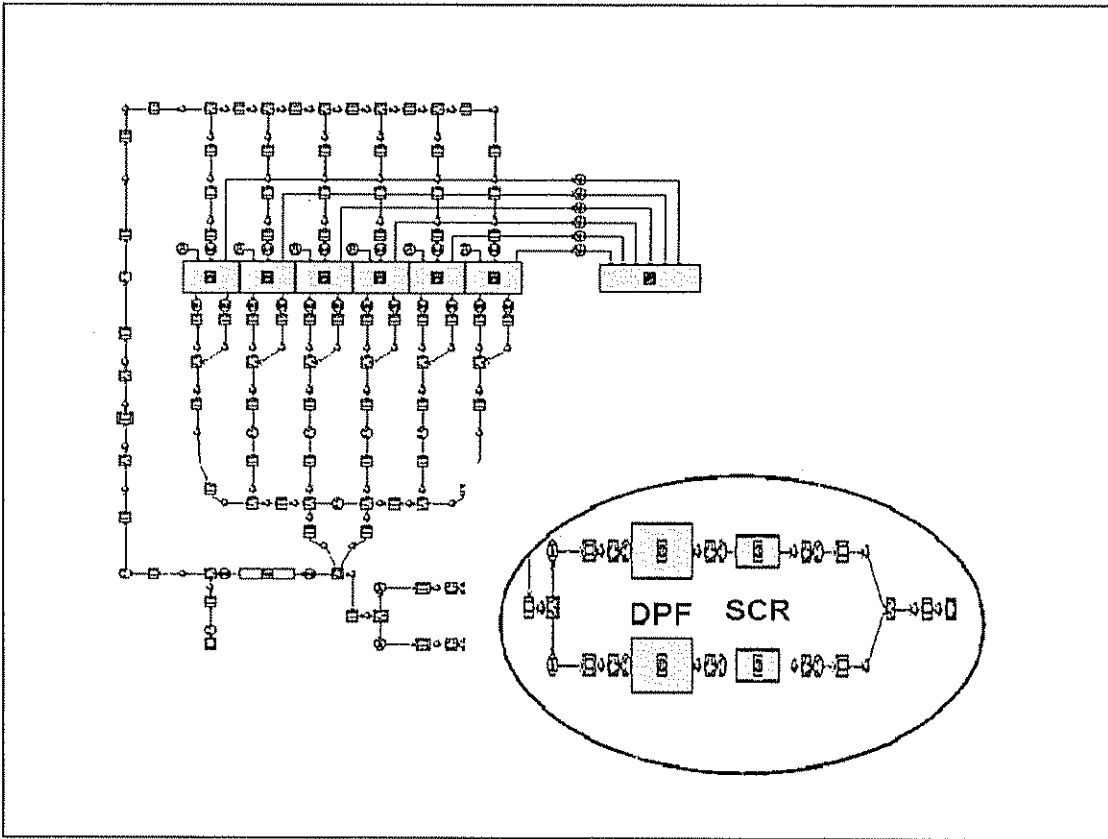


Figure 1.1.14 Comparison of Measured and CSF Model Simulated Soot Mass Balance for the CSF Loading Case 2 (277°C) from Figure 1.1.7

As part of the LEADER program, these validated AT models were also integrated with other engine system analytical tools. Figures 1.1.15 and 1.1.16 are schematics of integrated models, comprised of conventional engine cycle simulation models and the LEADER aftertreatment models. This integrated system level modeling allows users to run complete engine system analysis and AT analysis in a concurrent manner, thus allowing an opportunity for total system optimization. Example issues that were addressed via this approach include fuel economy impact due to the AT sub-system backpressure contribution and synergizing the AT sub-systems with the combustion, air and EGR sub-systems. This engine and AT system model could be further integrated with powertrain and vehicle modeling tools, thus including additional system dimensions in the analysis.



**Figure 1.1.15 Integration of AT Models with Ricardo's Engine Cycle Simulation Tool - WAVE**



**Figure 1.1.16 Integration of AT Models with Gamma Technologies' Engine Cycle Simulation Tool – GT-Power**

In addition to the emphasis on 1D analytical tools for system level optimization, significant focus was also placed on multi-dimensional 3D modeling for component optimization, consistent with the three-layer virtual lab development strategy shown in Figure 1.1.1. New techniques and methodologies for utilizing 3D CFD for aftertreatment development were established as part of the LEADER program. Figures 1.1.17 and 1.1.18 show the representative channel methodology for modeling a typical catalyst, which allows the relevant physics to be resolved without significant penalty in computational cost.

- The coupled approach allows for all physical details of the problem to be considered***
- STAR-CD+CHEMKIN is used to compute fluid/chemistry interaction within each channel***
- User sets up associations between each flow domain which allows for continuity among all solution variables***

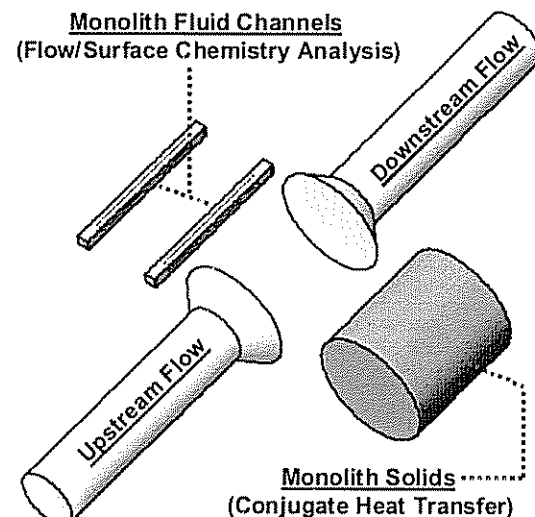


Figure 1.1.17 Coupling Methodology with Representative Channels for Catalyst Modeling

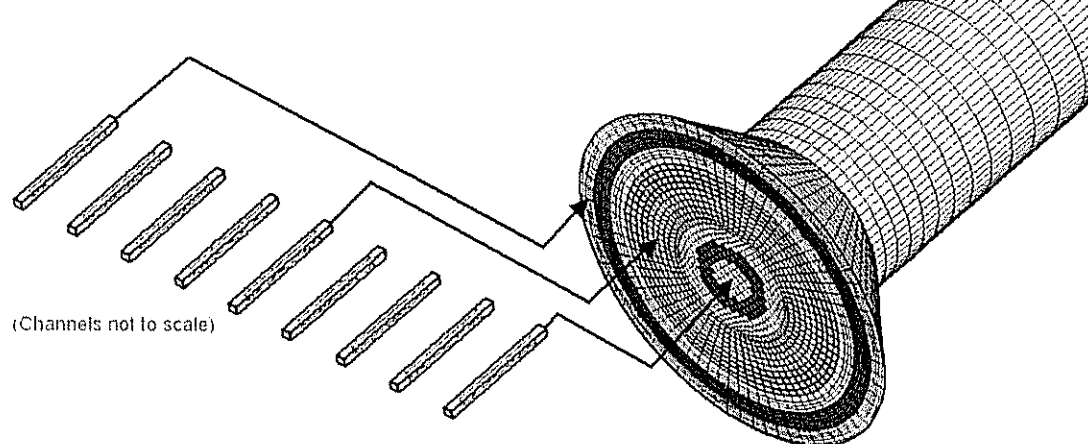
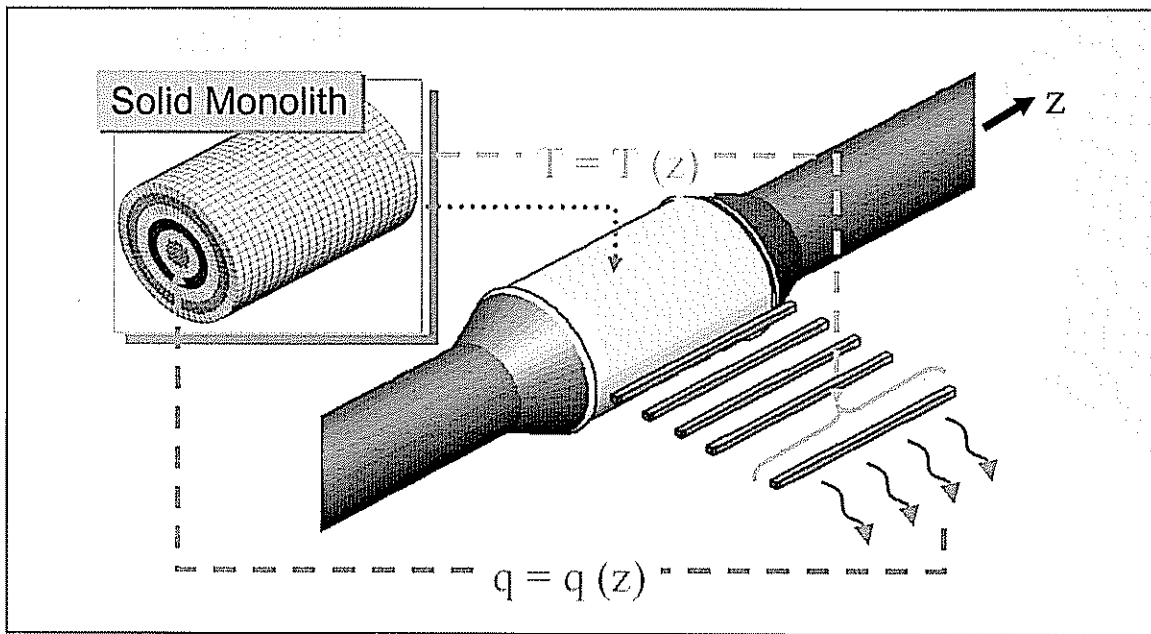


Figure 1.1.18 Representative Channel Transport to/from Large Scale

For heat transfer, the treatment of large-scale transport of heat from the gas to the solid portions of the brick monolith is shown in Figure 1.1.19 and is modeled via user routines.



**Figure 1.1.19 Conjugate Heat Transfer Schematic**

In the following pages, CSF modeling will be described first, followed by SCR modeling. Figures 1.1.20 and 1.1.21 show the lateral and axial cross-sections of a CSF geometry schematic, respectively. Figure 1.1.20 also shows the computational unit geometry including all the relevant physical domains of the CSF.

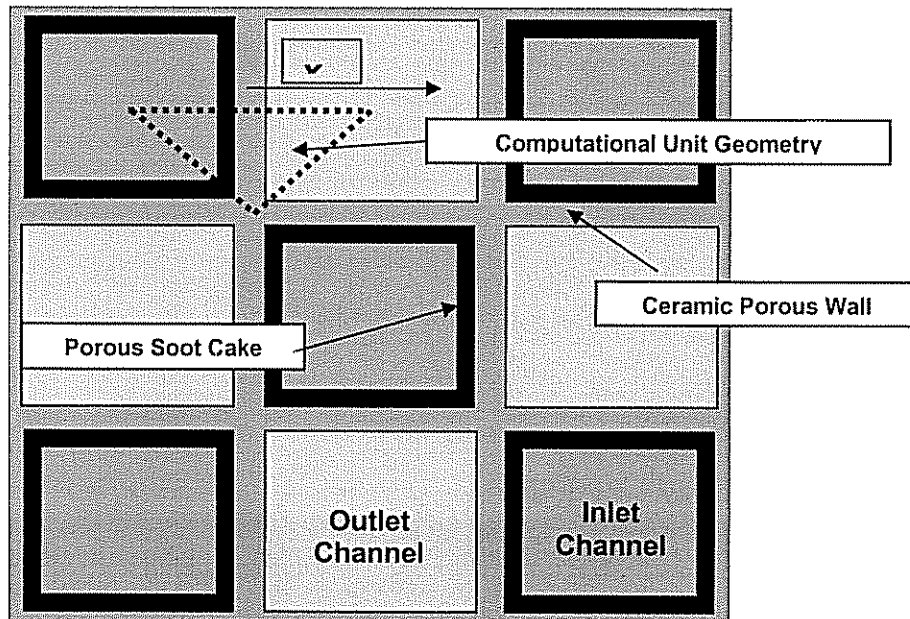


**Figure 1.1.20 Lateral Cross-Section Filter Geometry Schematic**

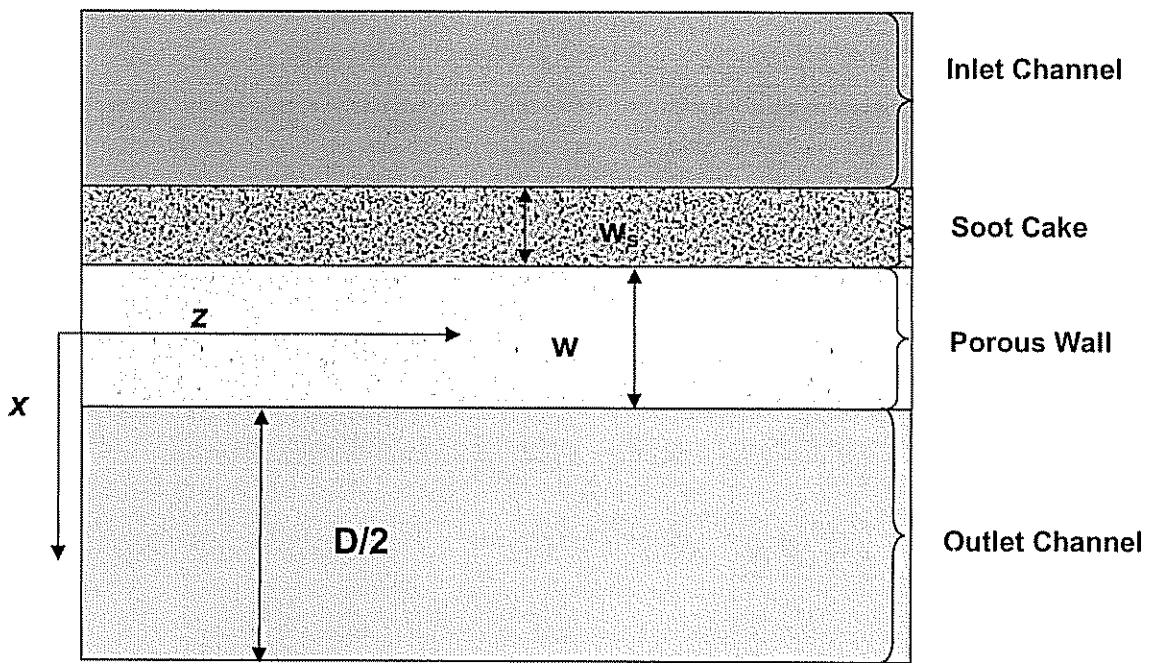


Figure 1.1.21 Axial Cross-Section Filter Geometry Schematic

The porous media filter model is built in based on a unit cell model of Konstandopoulos and Johnson<sup>10</sup> and is shown schematically in Figure 1.2.22. The basic concept is to express the spherical collection efficiency based on the local Peclet number.

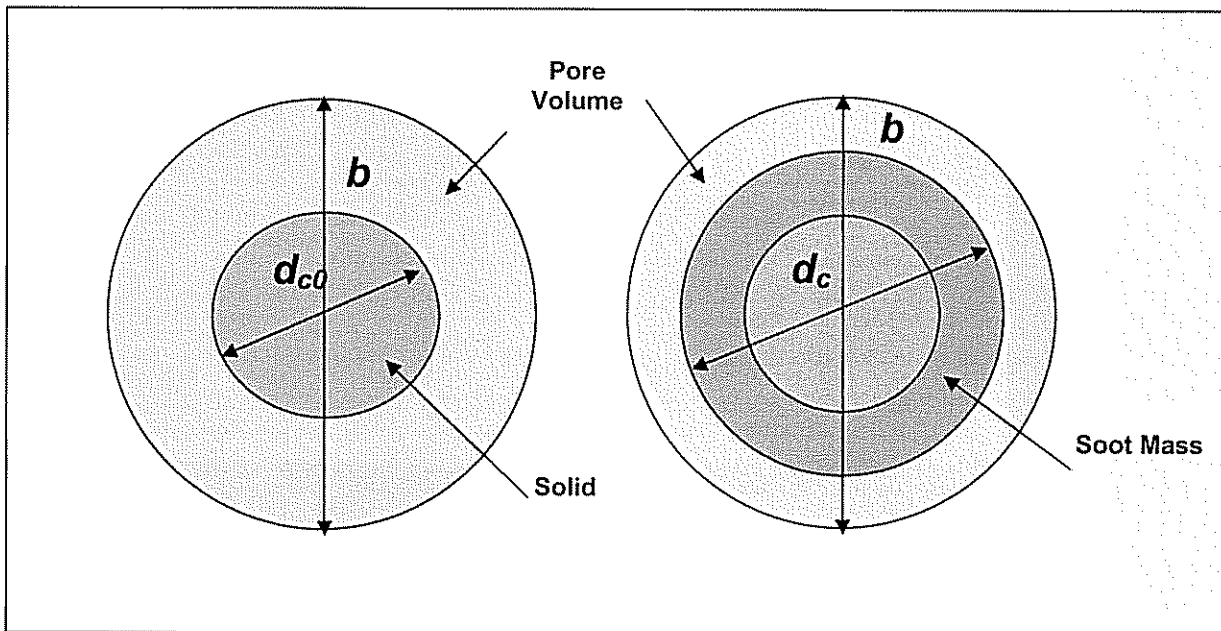


Figure 1.1.22 Spherical Unit Collector

"Deep-bed" filtering of the porous wall was used, which allows the soot in the porous wall to transition to soot-cake filtering mode where most of the mass is deposited on top of the porous wall on the inlet channel side. A "partition coefficient" models the clogging of the pores and defines the portion of gas phase soot flux, which actually enters the pores of the wall. The duration of this transition is set by an adjustable percolation factor. Eventually, the partition coefficient reaches unity where no soot enters the porous wall, and 100% of the soot is filtered by the soot cake.

Figures 1.1.23 and 1.1.24 respectively show the representative channel and grid used in this computational study.

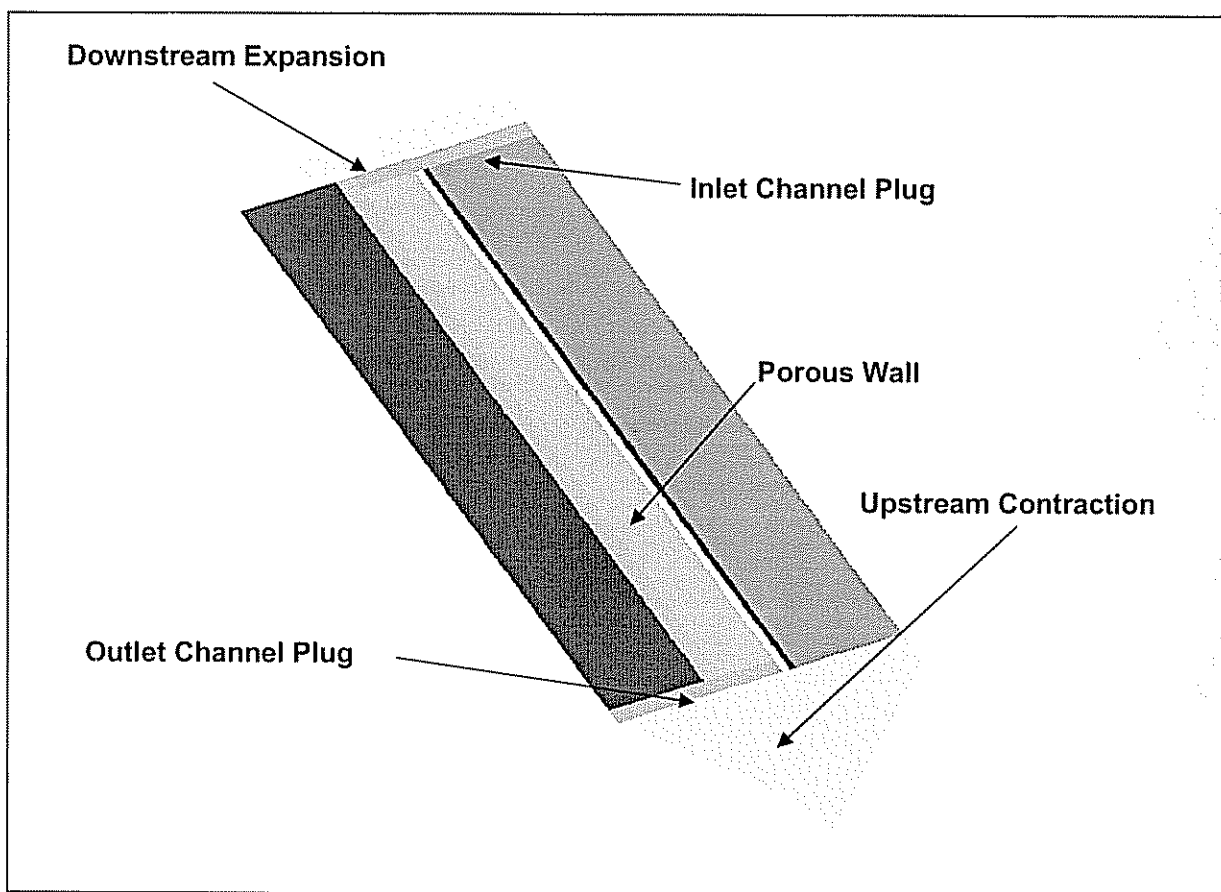


Figure 1.1.23 Representative Channel (Axial Scale Greatly Foreshortened)

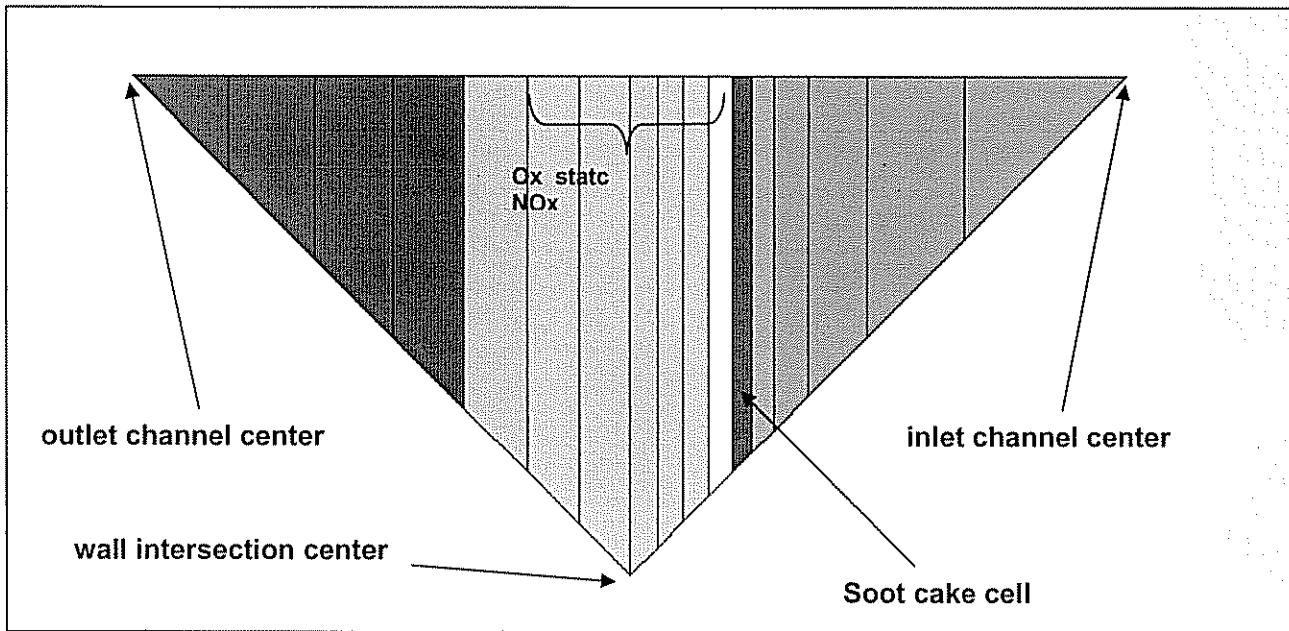


Figure 1.1.24 Representative Channel Cross-Sectional Grid (1/8th Symmetry)

Figure 1.1.25 shows examples of axial velocity and pressure contours computed for a typical loading case. As indicated in the contour plot, the axial velocity in the inlet channel is high at the filter inlet and gradually approaches zero at the end of the channel. The axial velocity in the outlet channel, on the other hand, is low at the filter entrance and reaches its maximum value at the outlet of the filter.

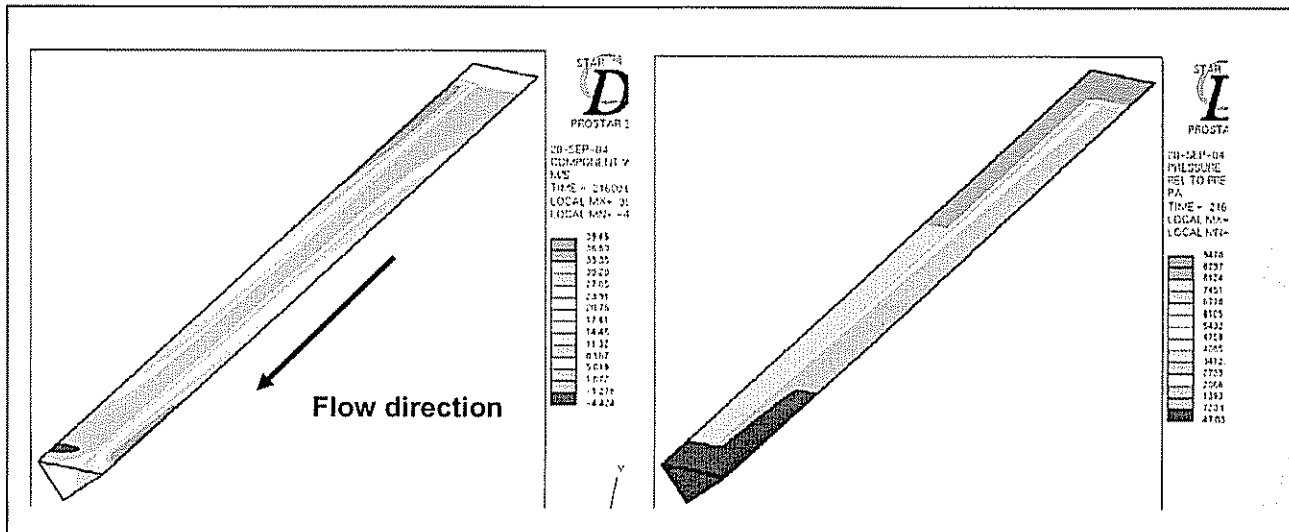


Figure 1.1.25 Axial Velocity and Pressure Contours on Centerline Channel

In many cases, if there is no indication of mal-distribution of flow into the CSF, the simulation can be further simplified, by assuming axisymmetric flow (3D flow on a 2° wedge). Such a model includes the inlet expansion and outlet expansions cones, the brick monolith and the insulation as shown in Figure 1.1.26. In initial studies, five representative channels (with the computational grid as shown in Figures 1.1.23 and 1.1.24) were generated and associated with the solid cells in the brick. This is a fairly coarse number of channels but was sufficient for preliminary studies. If the inlet conditions are uniform into the CSF and there is no heat loss from the CSF, then only one representative channel is required.

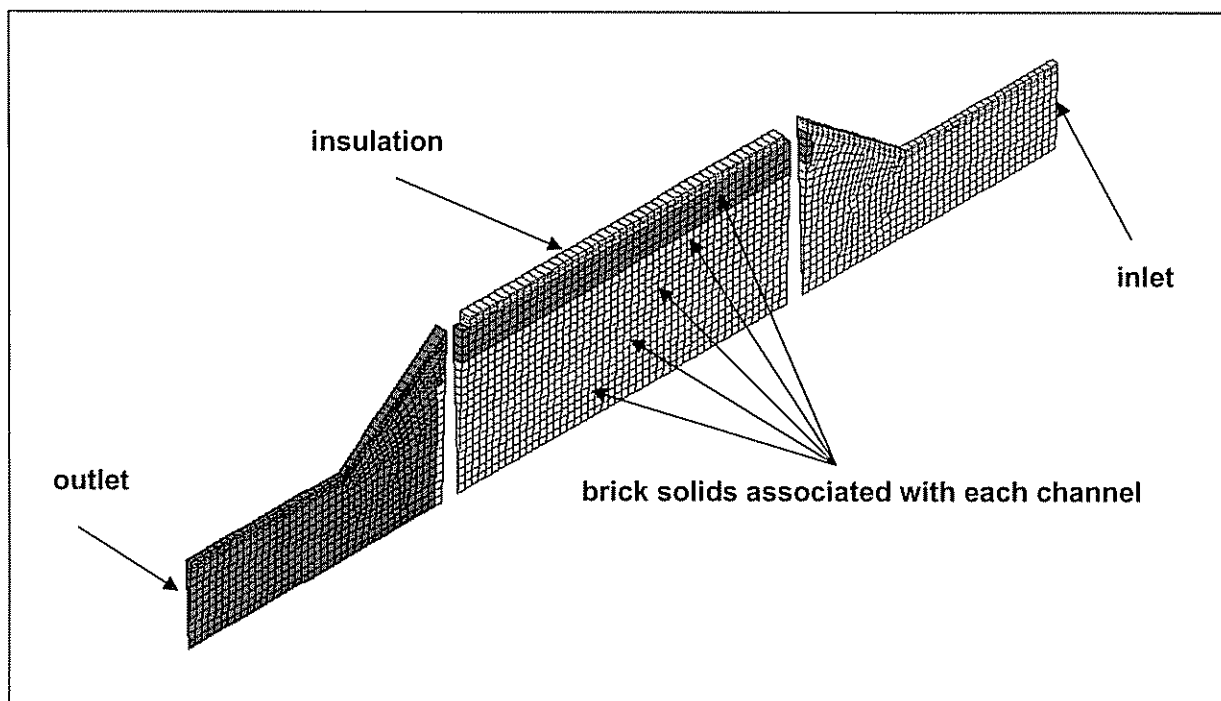


Figure 1.1.26 Axisymmetric Large-Scale Grid

A soot regeneration case was also studied with assumptions of heat losses and non-uniform inlet temperature. Figure 1.1.27 shows the volume averaged soot density and velocity mapped to the monolith grid. Because of the cooler outer diameter (OD) temperatures, the retained soot density at the end of the regeneration event is about 1.5 times larger on the OD than on the centerline. The velocity also shows some slight differences of about 10% with the OD gas moving slower, relative to that in the center of the filter. This prediction is certainly in agreement with observations with regard to incomplete regeneration near the OD.

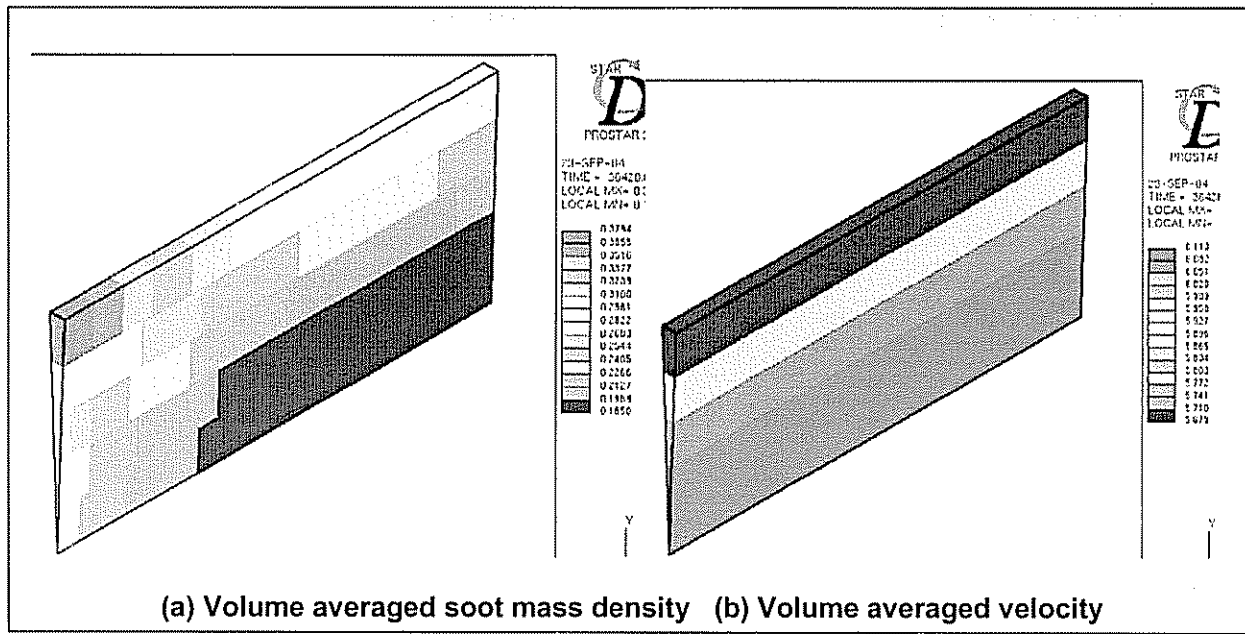
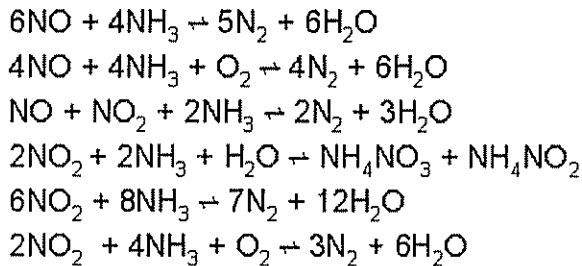


Figure 1.1.27 Regeneration with Heat Losses and Non-Uniform Inlet Temperature (t=1 hr)

In addition to CSF model development, significant effort was also invested in 3D SCR modeling including urea mixing characteristics as well as species characteristics inside the SCR. Urea mixing simulations will be presented in the description of Task 1.2.1.4, which includes conclusions inferred from the experimental data as well. The description below only focuses on modeling the species characteristics inside the SCR. The following global reactions were considered as part of this modeling effort.



Reaction rates were modeled using the usual Arrhenius expression

$$k = AT^b e^{-E/RT}$$

and coefficients are reported in standard units (A in [mole-K/m<sup>2</sup>-s] and E in kcal/mol). CHEMKIN is used to model chemical reactions. To demonstrate that the results with CHEMKIN can be transferred to STAR-CD + CHEMKIN, a test case was setup and run. As an example of the detailed information that can be obtained via such analysis, the NO and NH<sub>3</sub> contour plots are shown in Figure 1.1.28.

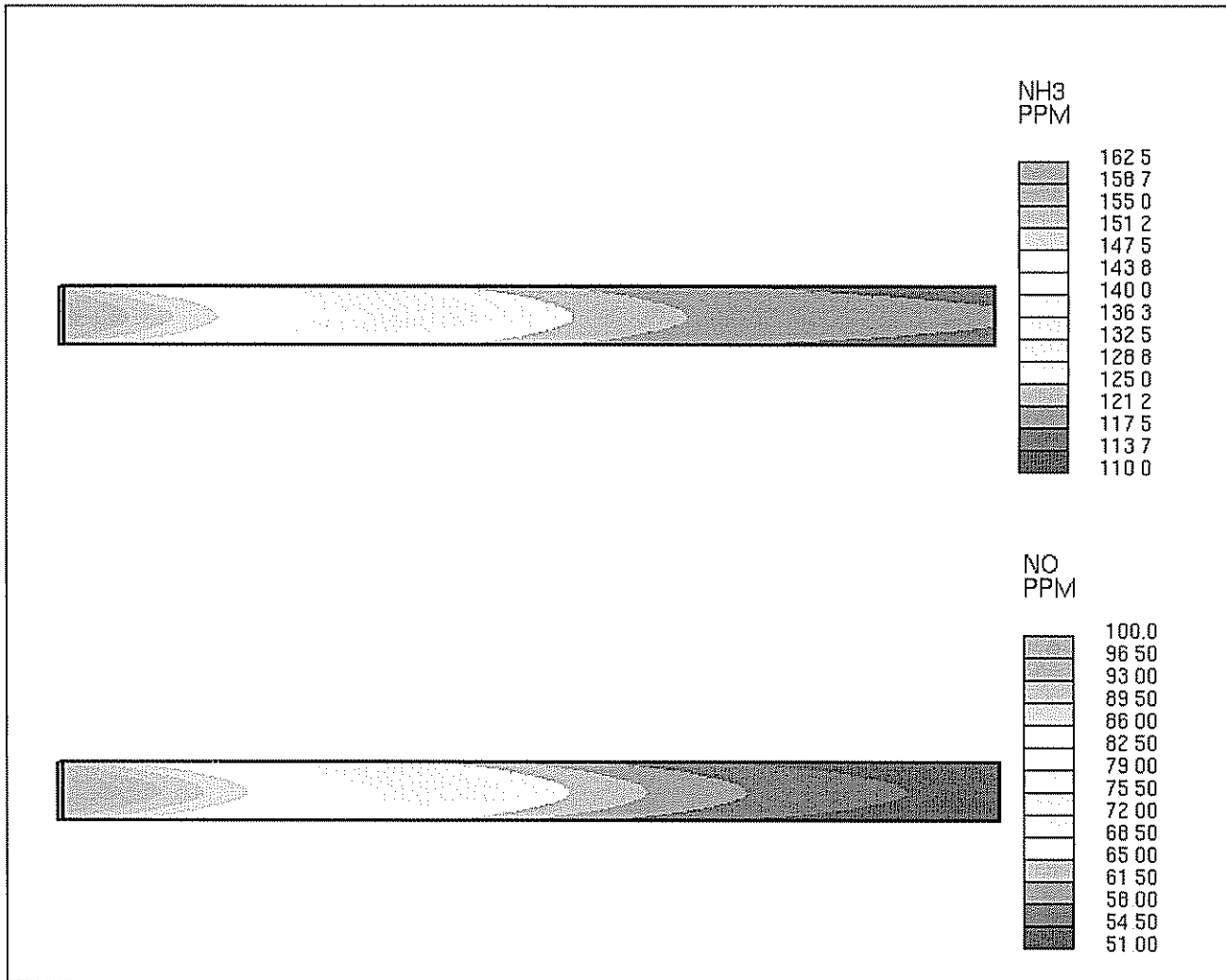


**Figure 1.1.28 Channel  $\text{NH}_3$  and  $\text{NO}$  Contours ( $T=262^{\circ}\text{C}$ )**

One of the major accomplishments of the LEADER program was to apply these state-of-the-art analytical models to solve real life problems. Successful application of these models resulted in design and testing recommendations as well as increased understanding of the physical performance characteristics of the individual AT sub-systems and the integrated engine and AT system. Additional technical details of virtual lab application combined with testing results will be presented in the next few sections, thus showing the utility of the analytical toolbox.

## Task 1.2 Aftertreatment Systems Characterization

In this subtask, performance characterization of various aftertreatment systems, including CSF, SCR, LNT and DOC was conducted. In addition, integrated systems such as a CSF with a SCR device downstream and a CSF with a LNT downstream were also characterized. This characterization was conducted at the DDC Engineering Laboratory and contractual facilities and at the Engelhard Technical Facility in New Jersey. A low sulfur fuel, with a maximum sulfur content of 15 ppm, was utilized in this program.

Several test-beds were utilized for the performance characterization of these aftertreatment systems and will be briefly described next. Figure 1.2.1 shows one of the test-beds, consisting of a four parallel leg exhaust system which enabled four aftertreatment systems to be simultaneously tested. This allowed accelerated aging testing, resulting in an efficient and shortened development cycle. This system was used during the entire program to age different catalyst systems (CSF, SCR and LNT) up to 2000 hours. This system was also used for degreening the catalysts. Once the catalyst systems were degreened or aged, they were used for performance characterization in conjunction with a passenger-car or LD truck engine.

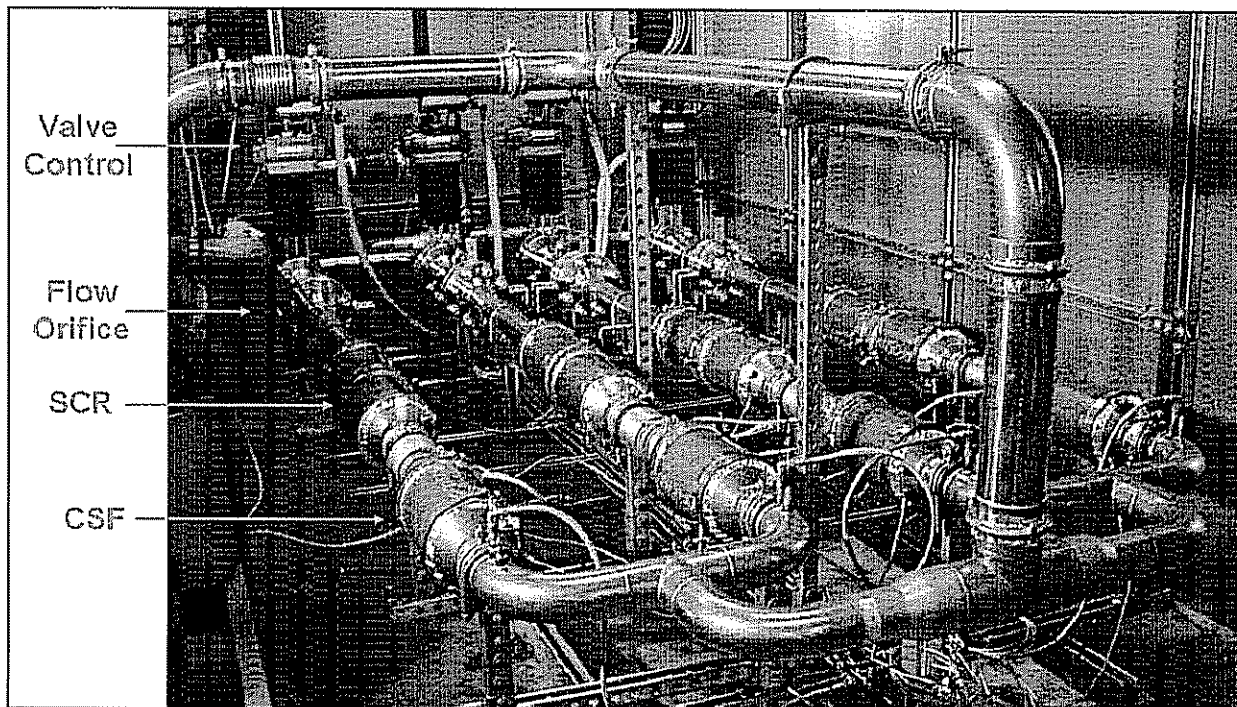


Figure 1.2.1 Multiple-Leg Aging System

Other test-beds used for aftertreatment system characterization focused on system integration and used a passenger car engine or a LD truck engine. The passenger car engine is a 1.5 liter, 3 cylinder in line, with a rated power of 55 kW (denoted as the HEV engine), while the LD truck engine is a 4.0 liter, 6 cylinder Vee (denoted as the DELTA engine). This characterization testing of catalyst systems was conducted at both Engelhard and DDC testing facilities.

Figure 1.2.2 shows the experimental set up at the Engelhard test site. Hot sampling valves were utilized to direct the exhaust gas sample from a desired location to the emissions analyzers and/or an FTIR spectrometer system, thus allowing detailed gaseous emissions characterization throughout the exhaust system, including engine out, CSF out, SCR in and SCR out. With a single dilution mini-tunnel, total particulate matter (PM) including soluble organic fraction (SOF) and sulfates was sampled as well.

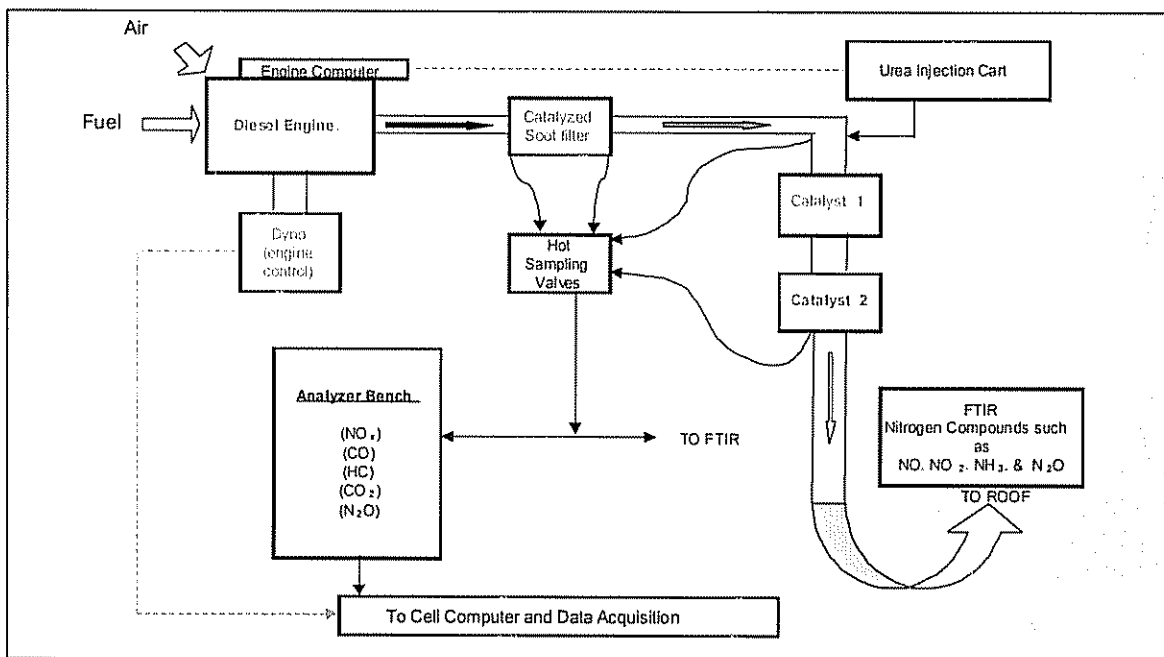
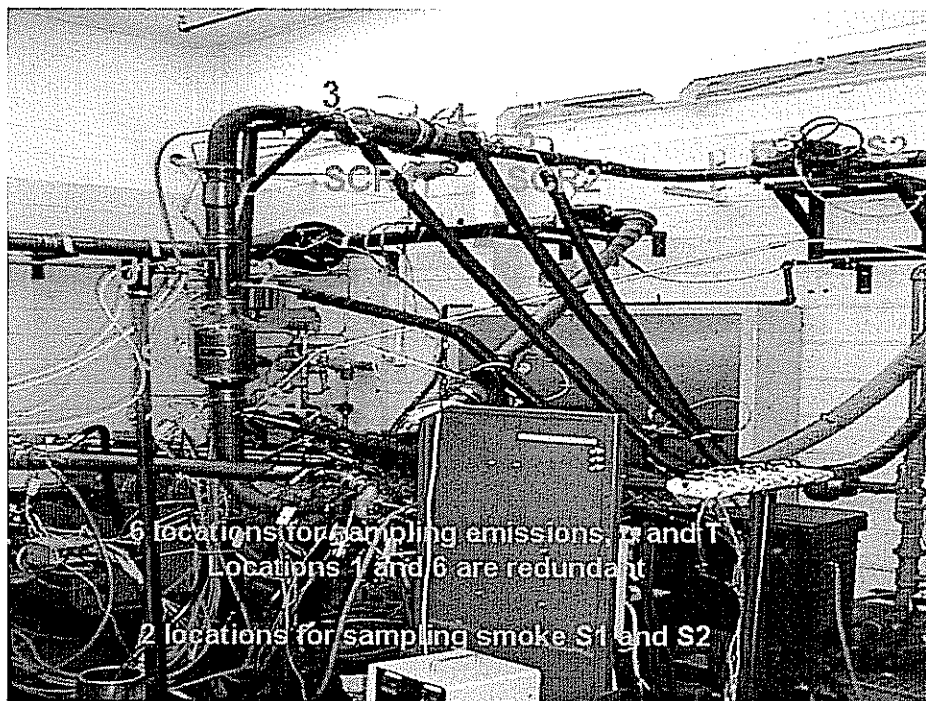


Figure 1.2.2 Engelhard Experimental Set Up in Engine Testing Cell

Figure 1.2.3 shows the experimental setup for one of the LEADER test-beds at DDC. Six sampling locations were selected to provide a detailed characterization of exhaust system pressures, temperatures and gaseous emissions. These included engine out, CSF out, SCR in, SCR mid and SCR out. In addition, a smoke meter was used to measure smoke at two locations (engine out and CSF out).



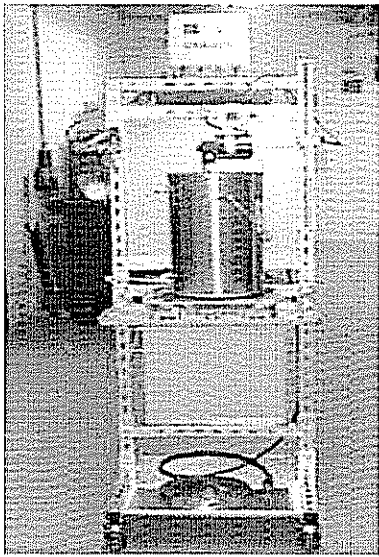
**Figure 1.2.3 Experimental Set-Up for SCR/CSF System Characterization at DDC**

These state-of-the-art facilities were used to conduct a systematic and comprehensive characterization of the engine and aftertreatment system. This included performance characterization using fresh catalysts and aging characterization with different aging cycles and duration. During the course of the program, the integrated SCR and CSF system was thoroughly characterized. This characterization laid a solid foundation for the engine and aftertreatment to be integrated and tested in vehicles and was a key contributing factor in achieving the aggressive Tier 2 Bin 3 emissions goals. The results of vehicle tests will be presented in the description of Tasks 3 and 4. The integrated CSF and LNT system was also characterized at steady state operating conditions. In the following sections, the characterization results of the SCR/CSF system are first presented, followed by those of the LNT/CSF system and DOC.

#### **Task 1.2.1 SCR Characterization**

A zeolite-type SCR, based on state-of-the-art technology available at Engelhard, was used for the LEADER program. The catalyst volume was 5L for the 1.5L HEV engine and 10L for the 4.0L DELTA engine. Base metal components were coated on a ceramic flow-through substrate targeting a NOx conversion > 50% over the US FTP75 cycle.

Two urea injection systems were used during various stages of the program. A pre-prototype urea injection system was developed by Engelhard to allow the characterization and integration of the urea SCR system fairly early in the program. Figure 1.2.4 shows this system and lists its major components and required software characteristics. This system was used at Engelhard as well as at DDC for preliminary test cell and vehicle chassis dynamometer testing.



- **Hardware**
  - Pumps, injectors, air mixing and urea mixing are packaged on a movable cart
- **Software**
  - communication with the engine is via the CAN (SAE J1939)
  - Injection models are modularized to allow rapid changes in injector calibration, engine out emissions and catalyst NSR maps.

Figure 1.2.4 Engelhard Urea Injection System

Another prototype urea injection system, with emphasis on vehicle installation and packaging and improved performance characteristics was also procured and tested and is shown in Figure 1.2.5. This system was extensively used for transient engine and aftertreatment development both on a dynamometer test-bed as well as a vehicle chassis dynamometer test-bed.

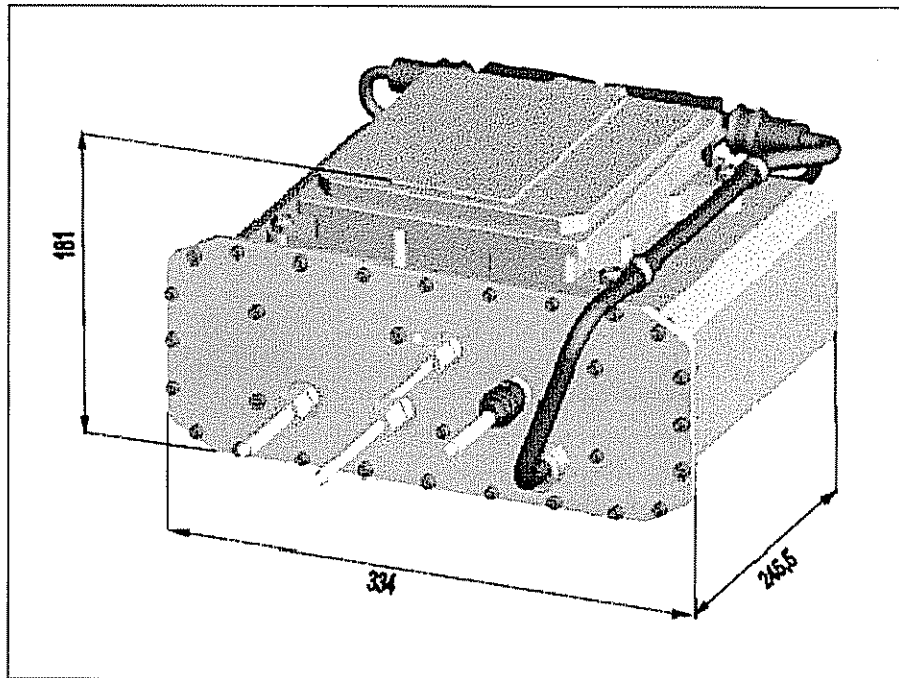


Figure 1.2.5 Prototype Urea Injection System Capable of Vehicle Installation

While focused on achieving the aggressive Tier 2 emissions levels, the development effort also placed a strong emphasis on measuring and controlling unregulated species such as ammonia ( $\text{NH}_3$ ) and dinitrogen oxide ( $\text{N}_2\text{O}$ ). Multiple techniques and instruments were utilized to capture detailed speciation characteristics of the exhaust emissions, both regulated as well as unregulated. These methods include:

- (1) Wet Chemistry
- (2) FTIR Spectrometer
- (3) Laser Diode

Wet chemistry was used to measure ammonia emissions by using non-spectroscopic traditional solution analysis. The system set up can be seen in Appendix 1. The technique is economical, relatively easy to apply and provides sufficient accuracy for time-averaged integrated ammonia slip data over a transient test cycle or a period of time at steady state conditions in situations where instantaneous measurements are not required. This method is particularly useful in vehicle chassis dynamometer testing where other more accurate but more expensive methods, such as FTIR and laser diode, cannot be easily set up.

An FTIR spectrometer was mainly used at the EC testing site for detailed speciation of the exhaust gas, including ammonia slip measurement. With its high accuracy and capability to measure species instantaneously, this instrument was used throughout the entire program.

A laser diode-based  $\text{NH}_3$  measurement device was also utilized in the LEADER program. Due to its fast transient response and accurate measurement, it was used at the DDC facility to quantify SCR storage capacity and ammonia mass balance transient characteristics including storage, consumption and release in addition to slip.

#### **1.2.1.1 SCR Characterization in Steady State Modes**

The engine used in this steady-state characterization was the 1.5L HEV engine. Five steady state modes based on the AMA cycle, which is commonly used for gasoline engine aging, were selected for SCR characterization as shown in Figure 1.2.6. Additional detailed information on the AMA cycle is given in Appendix 2. It should be pointed out that the characterization system included a CSF with a downstream SCR system. Both SCR and CSF performance data will be reported in this section for the sake of completeness. In this study, an Engelhard customized urea dosing system was used.

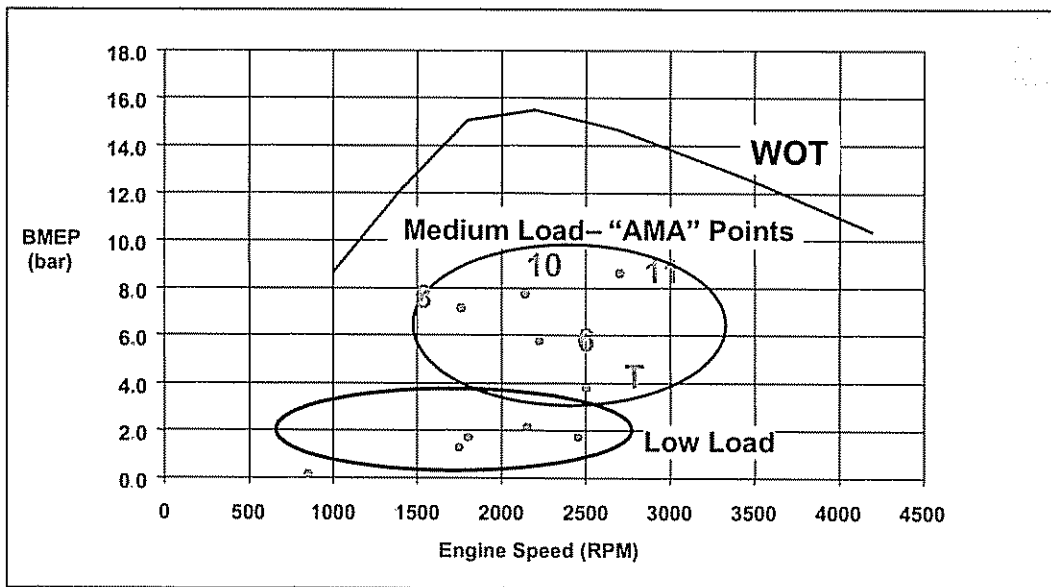


Figure 1.2.6 Mode Characterization Speed and Load Points

Table 1.2.1 shows the summarized results for key performance parameters, and Figure 1.2.7 shows the gaseous emissions conversion efficiency and the particulate reduction for the five modes. It is seen that rather high conversion efficiencies of over 90% were obtained for NOx and CO reduction. N<sub>2</sub>O formation was observed in all modes. This can be attributed to high NO<sub>2</sub> formation as evidenced by the high NO<sub>2</sub>/NOx ratios from Table 1.2.1. This also shows that the coating formulation on the catalyzed soot filter requires more refinement to reduce NO<sub>2</sub> formation. Figure 1.2.8 shows the 200-hour results summary. As can be seen, the 200-hour aged SCR actually performs better than the fresh SCR. This is probably due to the "degreening" effect. Figures 1.2.9 and 1.2.10 show additional data-sets summarizing the impact of 100 hours and 200 hours aging on PM and NOx reduction. Figure 1.2.11 shows the aging effect on ammonia slip. Interestingly, ammonia slip was significantly reduced after 200-hour aging compared to the fresh SCR results.

Table 1.2.1 Initial SCR Performance over Five Modes

	Mode 6	Mode 8	Mode 10	Mode 11	Mode T
Speed/Load, RPM/N-m	2275/75	1759/90	2143/100	2700/110	2500/44
Filter Inlet, °C	310	323	355	370	270/280
SCR Inlet, °C	280	280	312	335	244/255
CO Engine Out, ppm	95	55	90	165	255/275
CO SCR Out	5	4	2	4	4
NOx SCR Inlet, ppm	438	960	900	780	160/260
NO <sub>2</sub> / NOx	0.8	0.75	0.69		0.86/0.80
Max. NOx Conversion %	100	94	100	100	100
NH @ Max. NOx Conversion, ppm	0	0	0	25	13
NO <sub>2</sub> @ Max. NOx Conversion, ppm	50	90	70	40	25

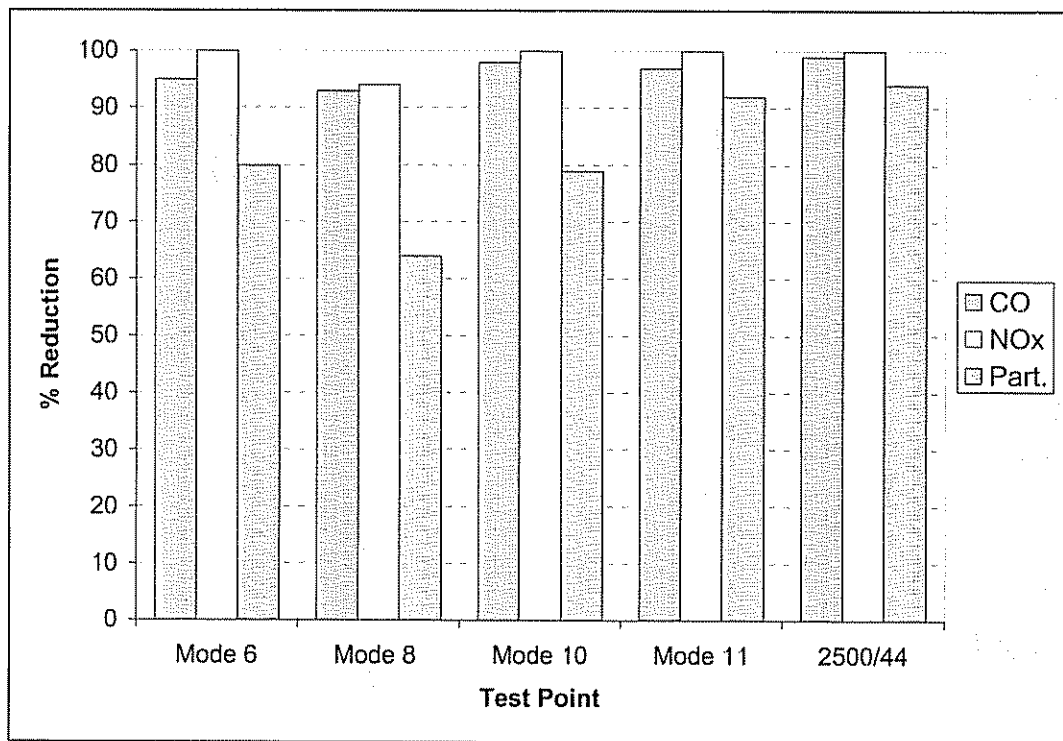
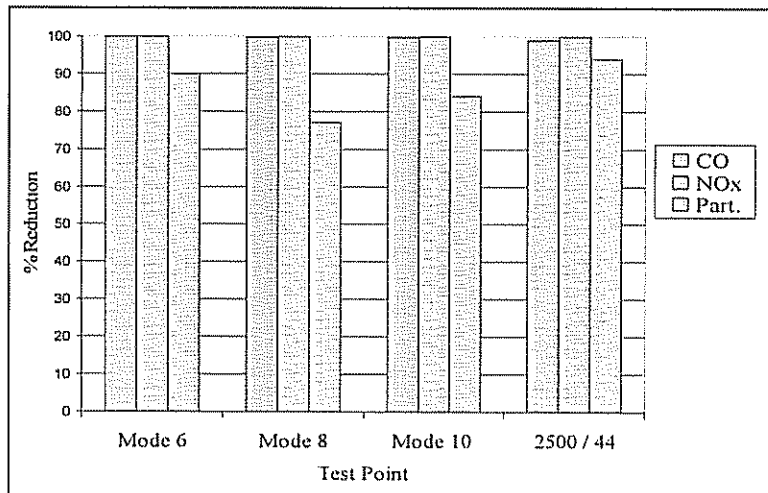
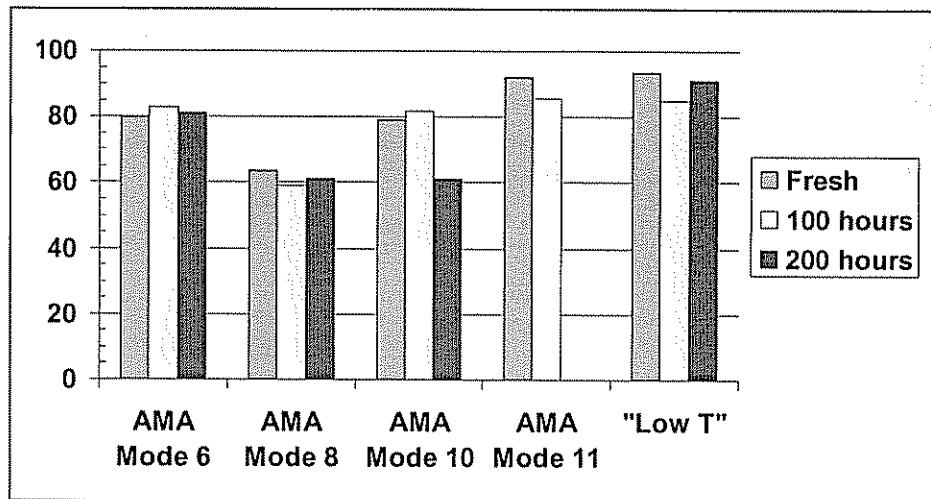


Figure 1.2.7 Initial Results Summary: Gas Phase Emissions and Particulate Reduction



**Figure 1.2.8 200-Hour Results Summary: Gas Phase Emissions and Particulate Reduction**



**Figure 1.2.9 Effect of AMA Aging on PM Removal Efficiency**

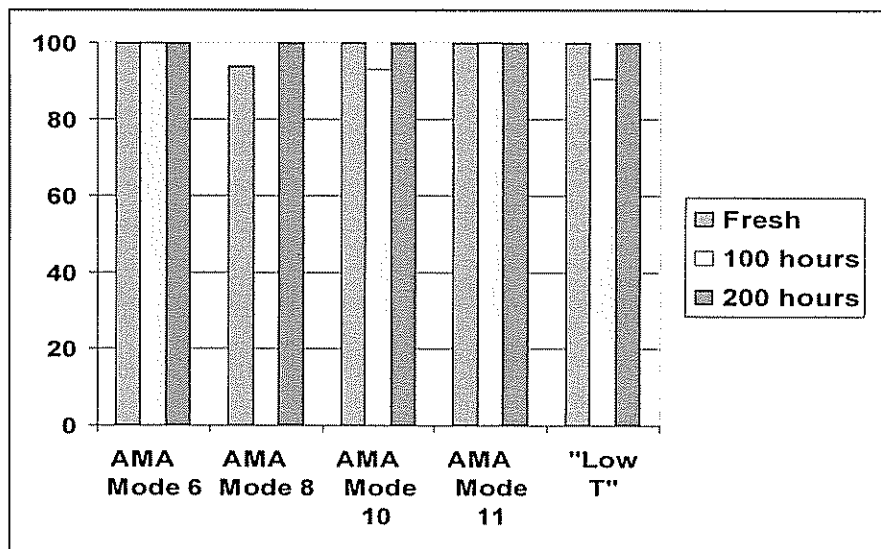


Figure 1.2.10 Effect of AMA Aging on NOx Conversion Efficiency

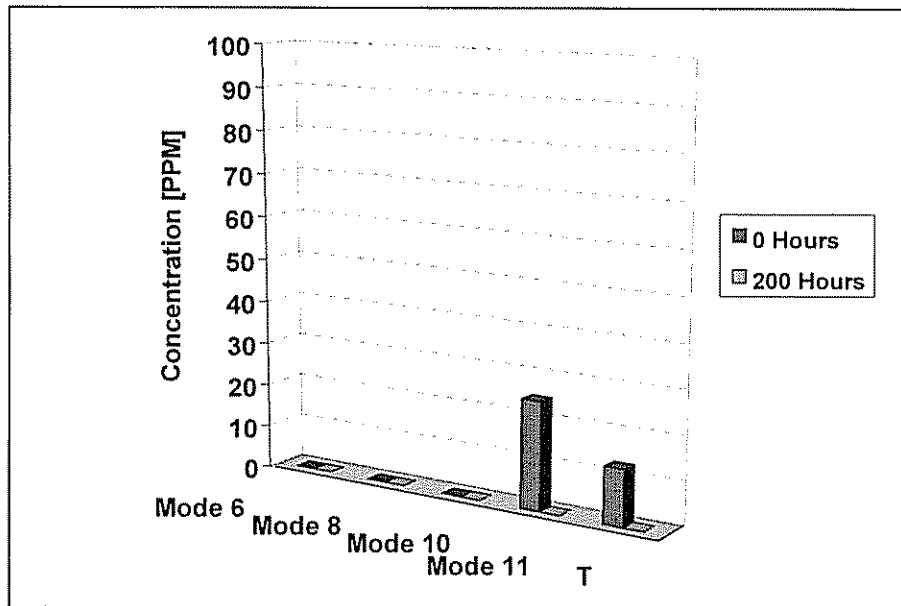


Figure 1.2.11 Effect of AMA Aging on NH<sub>3</sub> Slip

While SCR and CSF system characterization focused on medium load was being carried out at the EC facility, parallel testing with a similar SCR and CSF system was also conducted at DDC's engine testing facility. However, the testing at DDC focused on integration of the SCR/CSF system with advanced engine management. The emphasis was to develop strategies for transient emissions reduction utilizing representative steady-state conditions. These modal conditions included several low load conditions less than 2 bar BMEP, typical of transient vehicle operation. Figure 1.2.12 summarizes the emissions reduction strategy that evolved for these

representative conditions. Utilizing advanced engine management and aftertreatment systems strategies, near zero NOx and PM emissions were obtained for the range of speeds and loads tested. This testing laid a strong foundation for subsequent vehicle testing, enabling Tier 2 Bin 3 emissions to be achieved. The vehicle testing results will be presented in the description of Task 3.

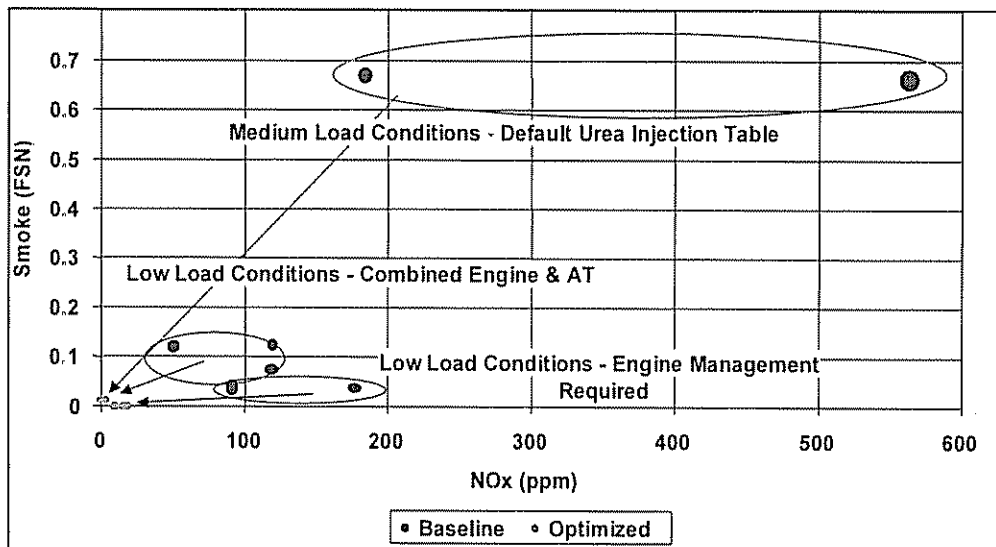


Figure 1.2.12 Emissions Reduction Strategy over Modal Conditions

### 1.2.1.2 Characterization of SCR Aging Effects Using the DELTA Engine

The previous section focused on the SCR/CSF system characterization with the 1.5L HEV engine. In order to accomplish the scalability objective of this program, characterization of the SCR/CSF system was also conducted on the 4.0L DELTA engines, mainly at the EC facility.

The testing procedure included aging the designated SCR in the parallel leg exhaust system using a gen-set engine. No urea injection was used during the aging cycle. The gen-set engine ran through a simulated AMA cycle for 50, 300, 600 and 1000 hours. After aging in this parallel leg aging system, the SCR was then put into an engine test-bed to characterize its performance under specified steady-state modes. A 4.0L DELTA engine was used for this purpose, and four modes were tested as shown in Table 1.2.2.

Table 1.2.2 Steady State Modes for Characterization of Aged SCR

Speed (RPM)	Load (N·m)	SCR Inlet Temp (°C)
2000	260	370
1650	180	275
1500	140	235
1350	120	189

Figures 1.2.13 - 1.2.16 summarize the aging results. While some variation in NOx conversion efficiency can be observed, especially after 600 hours aging, in general, the SCR device shows no performance degradation after 1000 hours aging.

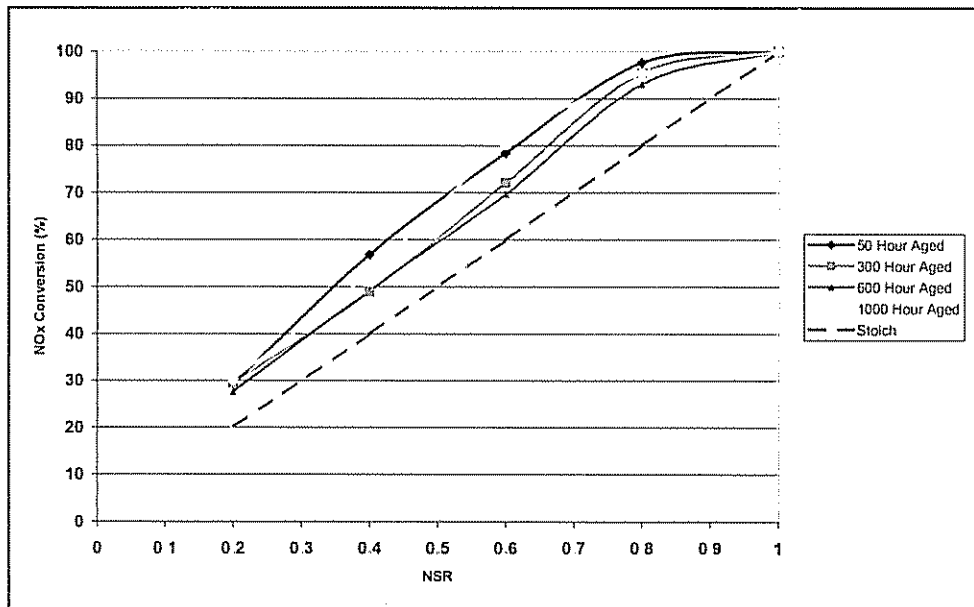


Figure 1.2.13 SCR NOx Conversion at Various Aging Stages (2000 rpm and 260 N·m)

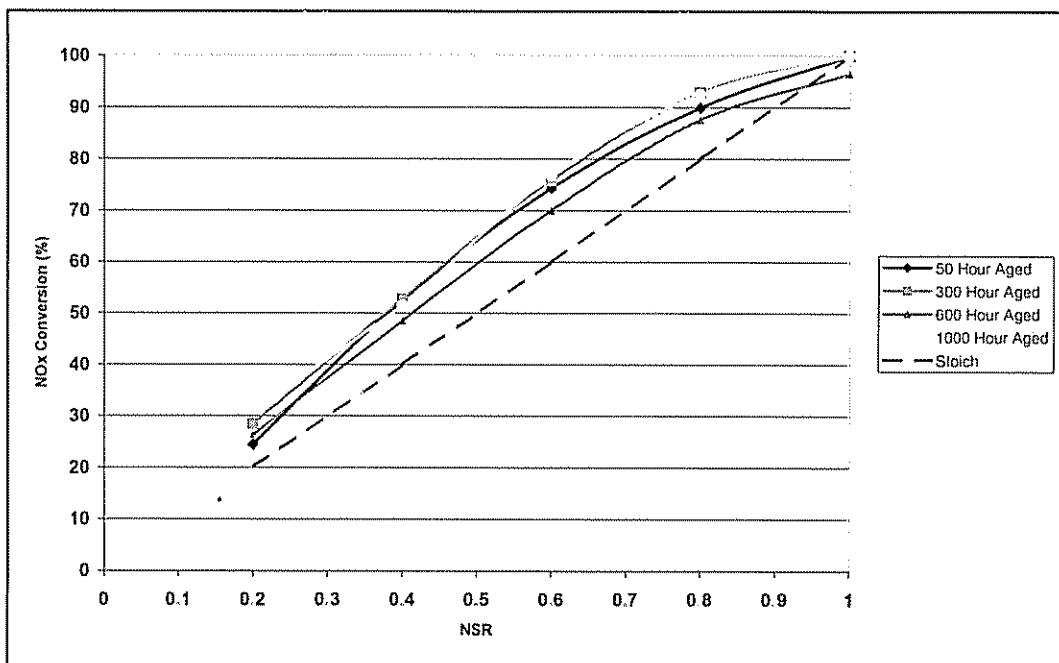


Figure 1.2.14 SCR NOx Conversion at Various Aging Stages (1650 rpm and 180 N·m)

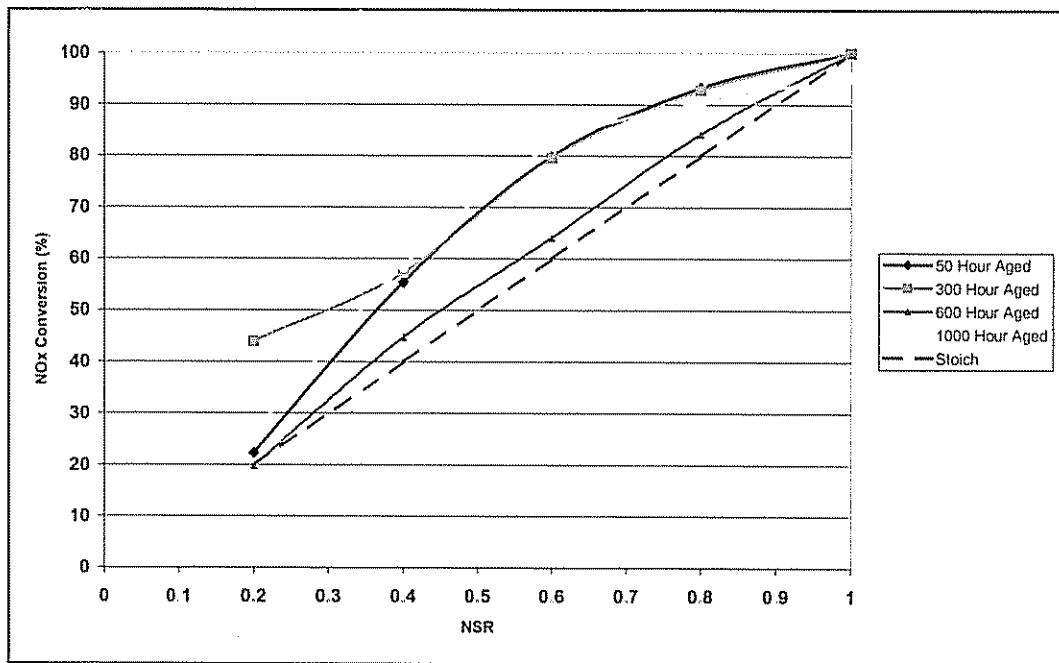


Figure 1.2.15 SCR NOx Conversion at Various Aging Stages (1500 rpm and 140 N·m)

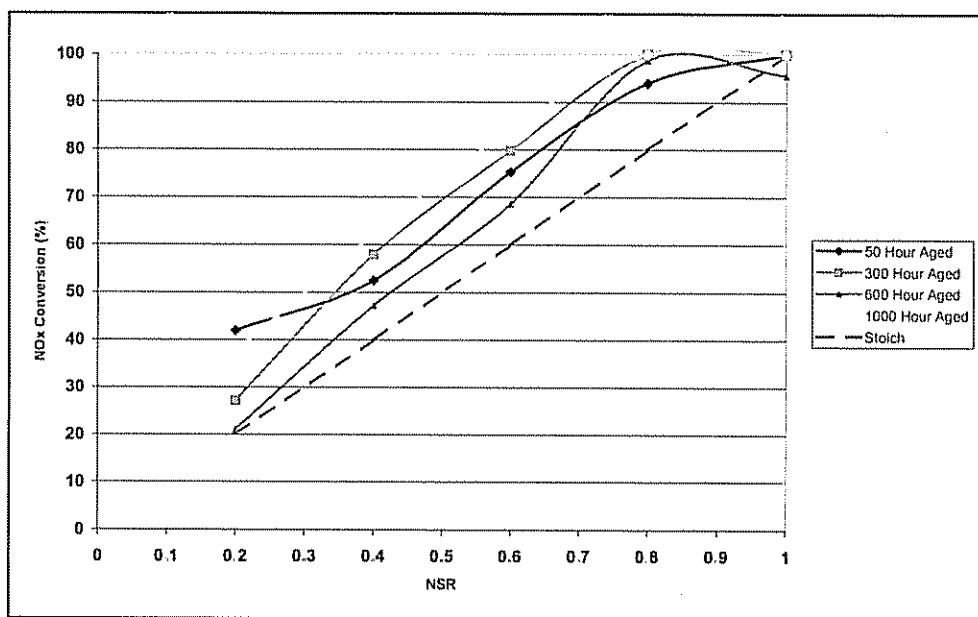


Figure 1.2.16 SCR NOx Conversion at Various Aging Stages (1350 rpm and 120 N·m)

### 1.2.1.3 SCR Storage Characterization

The SCR device used in the program was a zeolite-based catalyst, featuring a strong species storage capability. While this storage characteristic presents opportunities for emissions control, there are several challenges associated with it. Without a sophisticated controls strategy to manage the amount of species storage on the catalyst, undesirable "slip" can take place, especially during transient operation which can involve abrupt changes in exhaust space velocity and temperature. Figures 1.2.17 shows the ammonia storage effect as a function of time over a typical operating condition.

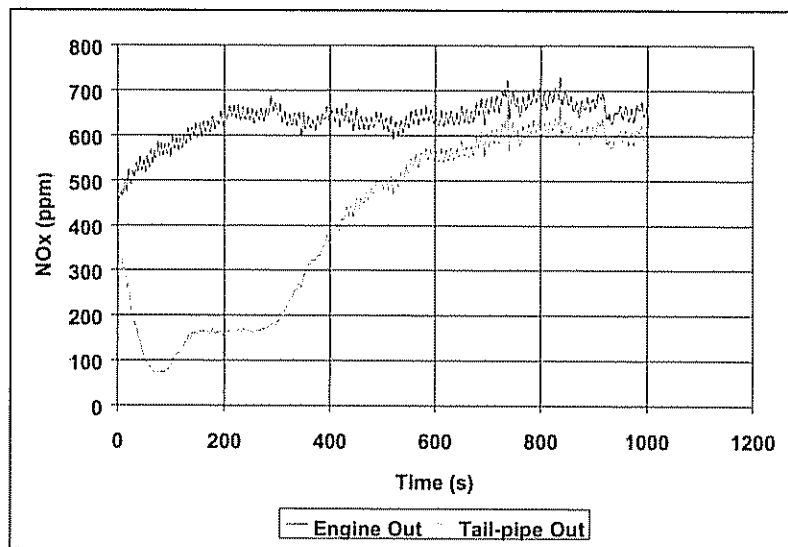


Figure 1.2.17 Ammonia Storage and Release Effect

In this test, urea injection was shut down at  $t=0$  s after a relatively prolonged period of injection. As can be seen, the NOx emissions continue to reduce for about 500 s even though no urea is being injected. In order to understand the nature of the  $\text{NH}_3$  storage and slip, a series of systematic and comprehensive tests were carefully designed and conducted. Figure 1.2.18 shows the summary of the key results obtained, characterizing  $\text{NH}_3$  storage as a function of temperature and space velocity. In this series of tests, transient  $\text{NH}_3$  slip was accurately captured with a laser diode.

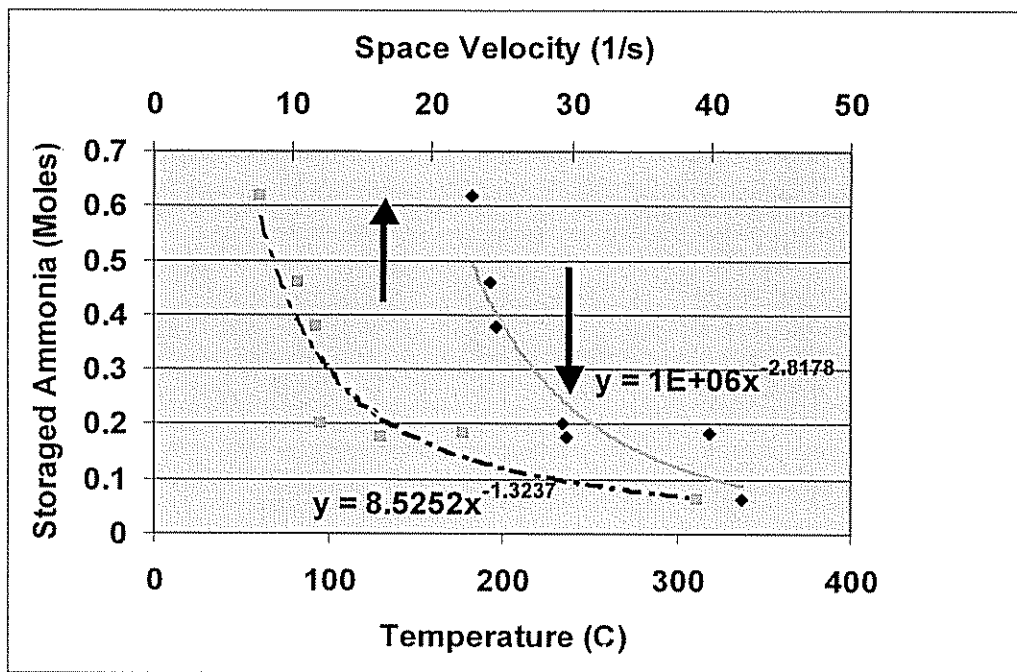


Figure 1.2.18 Ammonia Storage Capacity as Function of Temperature and Space Velocity

This strong ammonia storage capability as indicated in Figure 1.2.18 provides an opportunity to control the NOx emissions during cold operation and to enhance overall NOx conversion efficiency. To accomplish this enhancement in NOx reduction while simultaneously controlling NH<sub>3</sub> slip, a sophisticated control strategy was developed. The virtual lab played an instrumental role in this development. A new ammonia storage and release model based on global reaction mechanisms was developed and calibrated against testing data. Figures 1.2.19 and 1.2.20 show the NOx prediction and NH<sub>3</sub> balance, respectively, for a typical operating condition and indicate excellent agreement between simulated and experimental results.

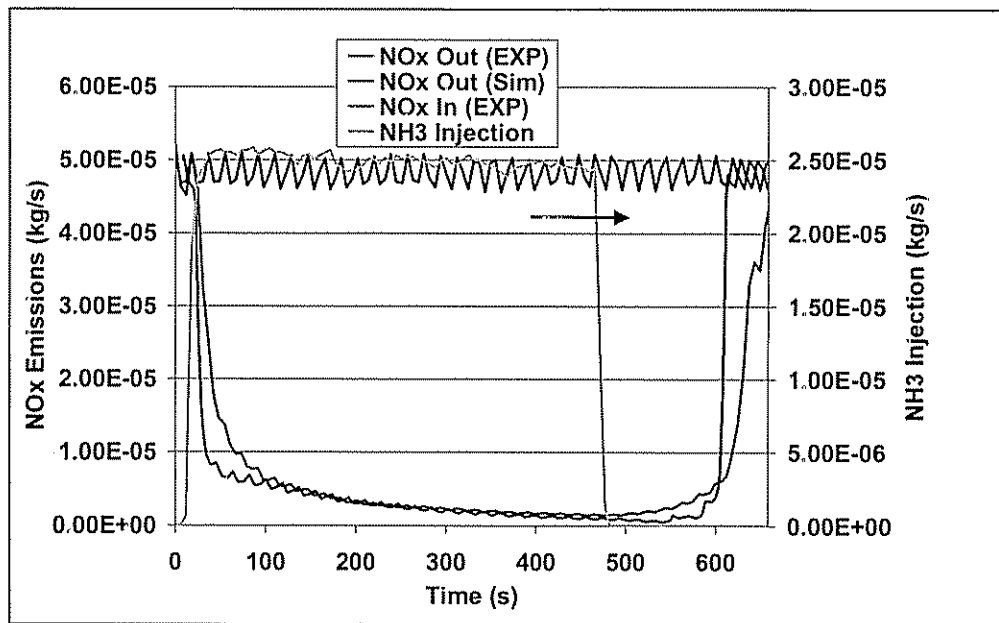


Figure 1.2.19 NOx Prediction During Storage and Release @ 2000 rpm and 308°C

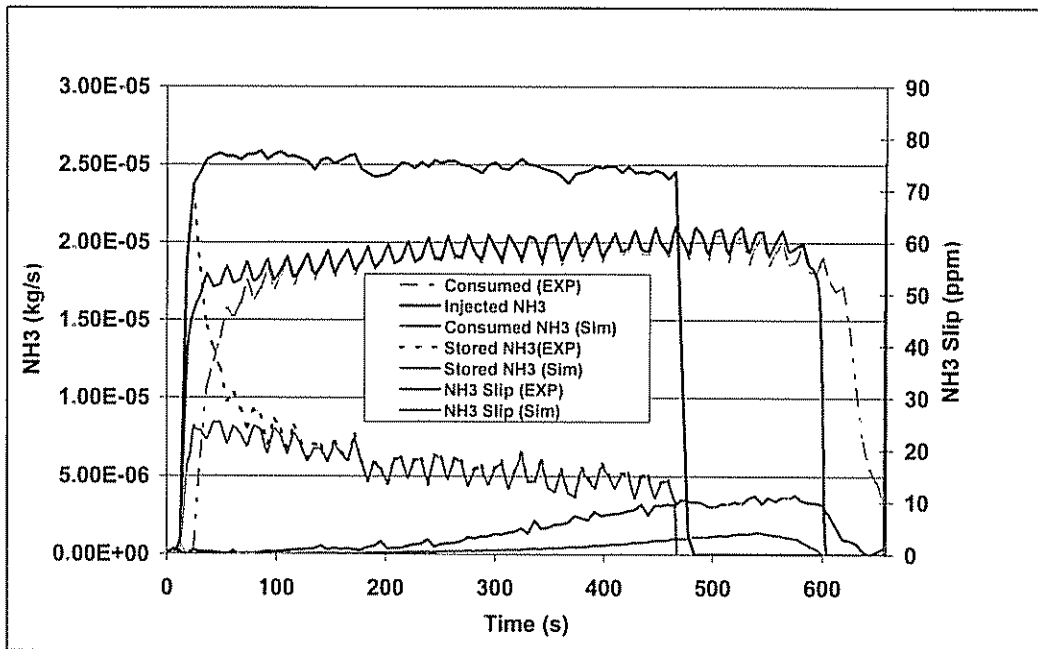


Figure 1.2.20 NH<sub>3</sub> Balance During Storage and Release @ 2000 rpm and 308°C

Utilizing this calibrated model, a sophisticated control strategy for urea injection was developed. Figure 1.2.21 shows the control logic diagram for urea injection. Figure 1.2.22 shows a trade-off analysis between ammonia slip and NOx reduction efficiency. The red oval shows the area that

was identified via the analytical tool as the optimization region of interest, characterized by high NOx reduction efficiency while controlling NH<sub>3</sub> slip.

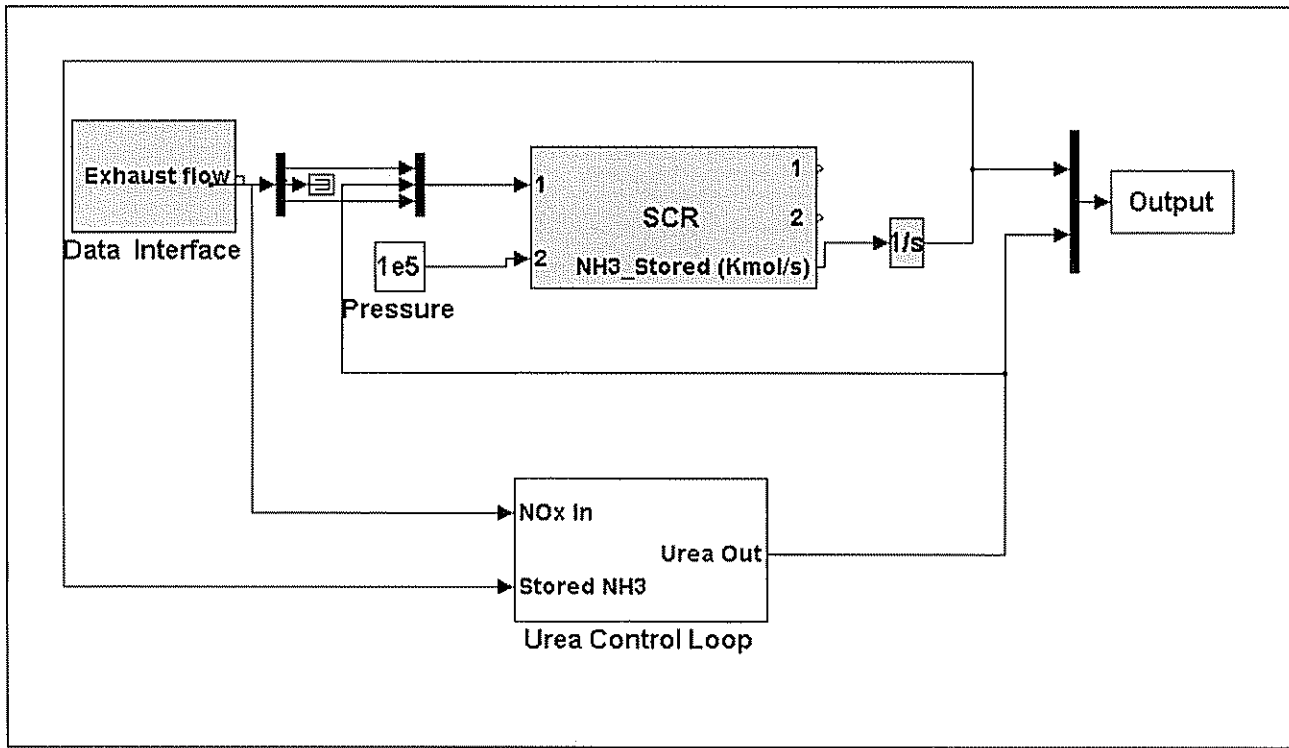


Figure 1.2.21 Urea Injection Control Logic Diagram

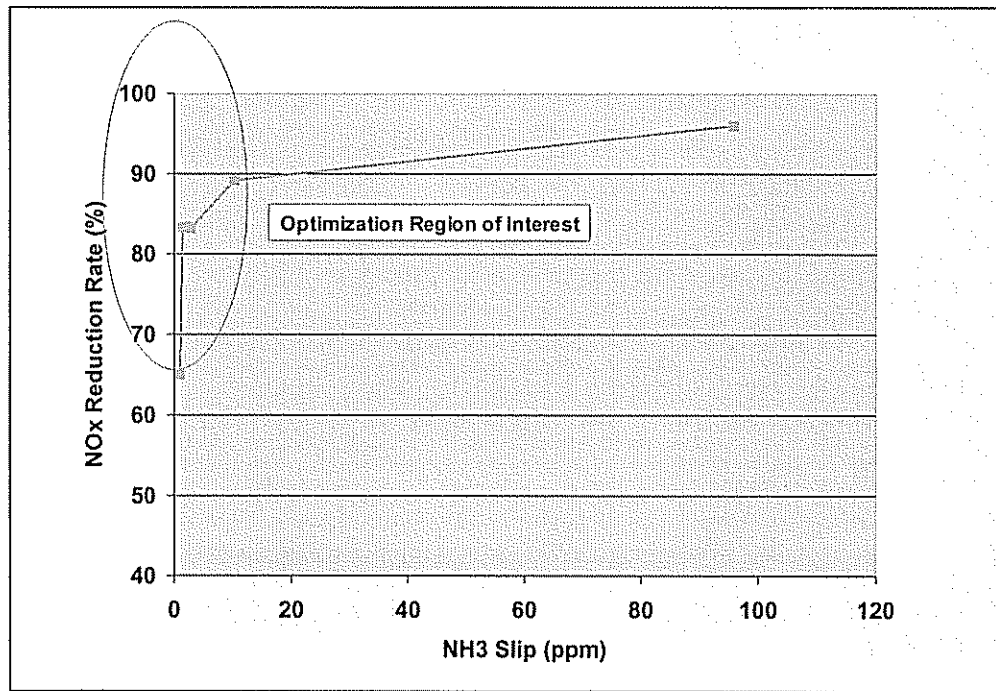


Figure 1.2.22 Optimization Region of Interest Identified via the Analytical Tool

This urea injection control strategy including real-time ammonia storage estimation was effectively utilized in vehicle testing, achieving Tier 2 Bin 3 emissions levels for both passenger car and LD truck platforms.

#### 1.2.1.4 Characterization of Urea Injection Mixing

To minimize urea (and thus "fuel") consumption and  $\text{NH}_3$  slip, it is important to maximize urea hydrolysis to  $\text{NH}_3$  and ensure uniform distribution of  $\text{NH}_3$  in the exhaust stream. Mal-distribution of ammonia is bound to lead to poor NOx conversion and increased risk of ammonia slip. Integrated transient 3D CFD along with other SCR models can be effectively utilized to assess nominal design performance. A critical design parameter is the injection nozzle hole-to-hole variation in urea flow. While the analytical tools were used to assess the impact of hole-to-hole flow variation on SCR performance, a rapid prototype spray fixture was designed and manufactured to qualitatively and quantitatively characterize the spray pattern and flow variation. The nozzle hole design was optimized to improve hole-to-hole urea flow and spray uniformity. Figure 1.2.23 shows the hole-to-hole flow distribution as a function of flow rate, before and after optimization. The spider chart has been normalized such that a flow number of "1" represents the average flow expected for each nozzle. For the optimized design, uniform flow distribution is attained for all flow rates tested except the lowest flow rate of 190 g/hour. This is critical for LD vehicle applications where high fidelity control of urea distribution at low flow rate is important, given the relatively low engine out emissions and exhaust flow rates.

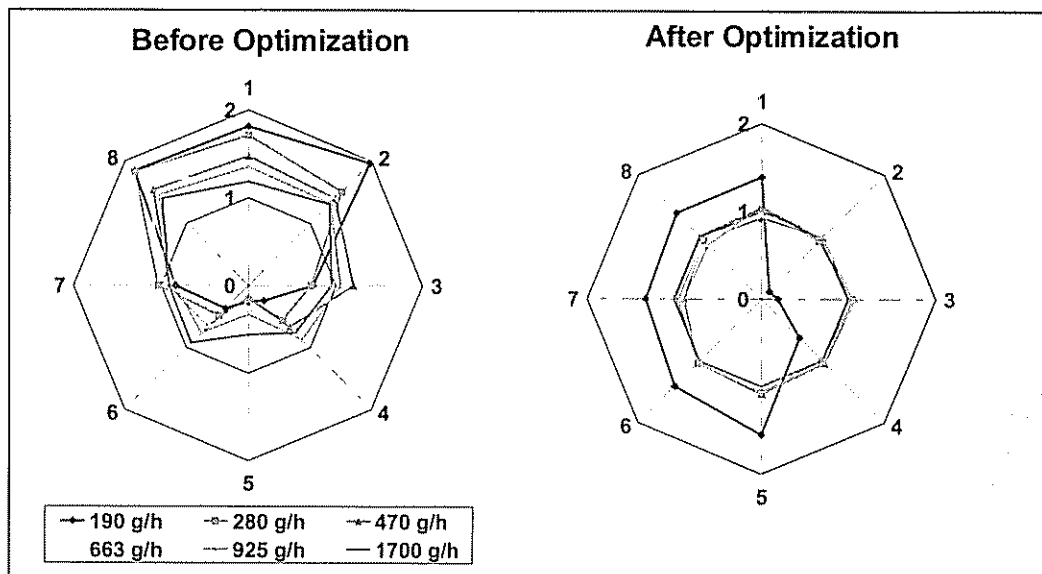


Figure 1.2.23 Urea Injection Control Issue - Hole-to-Hole Flow Rate Variation

Another important performance parameter is the  $\text{NH}_3$  distribution in the exhaust stream at the inlet of the SCR. In order to assess the impact of  $\text{NH}_3$  distribution with confidence, a 3D CFD simulation tool was used. The objectives of this study were twofold. First, it evaluated ammonia mixing and distribution in a SCR system, and second, it studied effects of non-uniform injection on ammonia distribution. Figure 1.2.24 shows the computational grids generated for this 3D CFD study.

During this investigation, a "mal-distribution index" was introduced to quantify the uniformity of NH<sub>3</sub> distribution along the exhaust pipe and to judge the NH<sub>3</sub>-exhaust mixing effectiveness. At any given cross-section normal to the axial flow direction in the computational model, the flow "mal-distribution index"  $\varphi$  is defined by

$$\varphi = \frac{1}{2N} \sum_{i=1}^N \left| \frac{m_i / A_i}{m_{total} / A_{total}} - 1 \right|$$

where  $m_i$  is mass flux through the  $i^{\text{th}}$  cell and  $A_i$  is the cross section area of the  $i^{\text{th}}$  cell;  $m_{total}$  and  $A_{total}$  are the total flux and total flow area at the selected cross-sectional plane, respectively; and  $N$  is the total number of cells in that cross-section.  $m_i$  is positive in forward flow and negative in reverse flow.  $\varphi$  reduces in value as the flow distribution becomes uniform and is 0 for an ideal uniform flow distribution.

Two cases, with uniform injection and with non-uniform injection, as shown in Figure 1.2.25, were analytically studied.

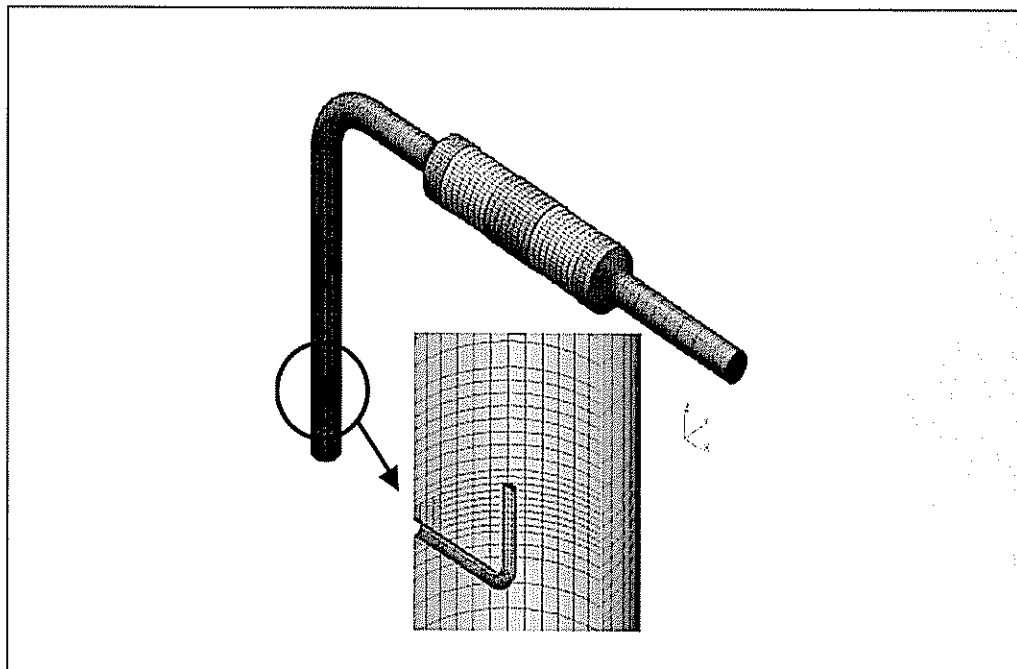
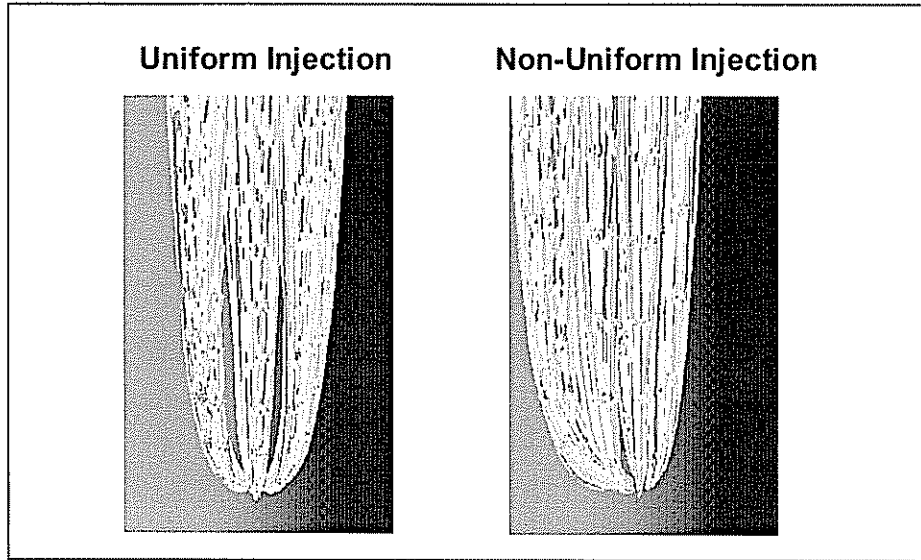
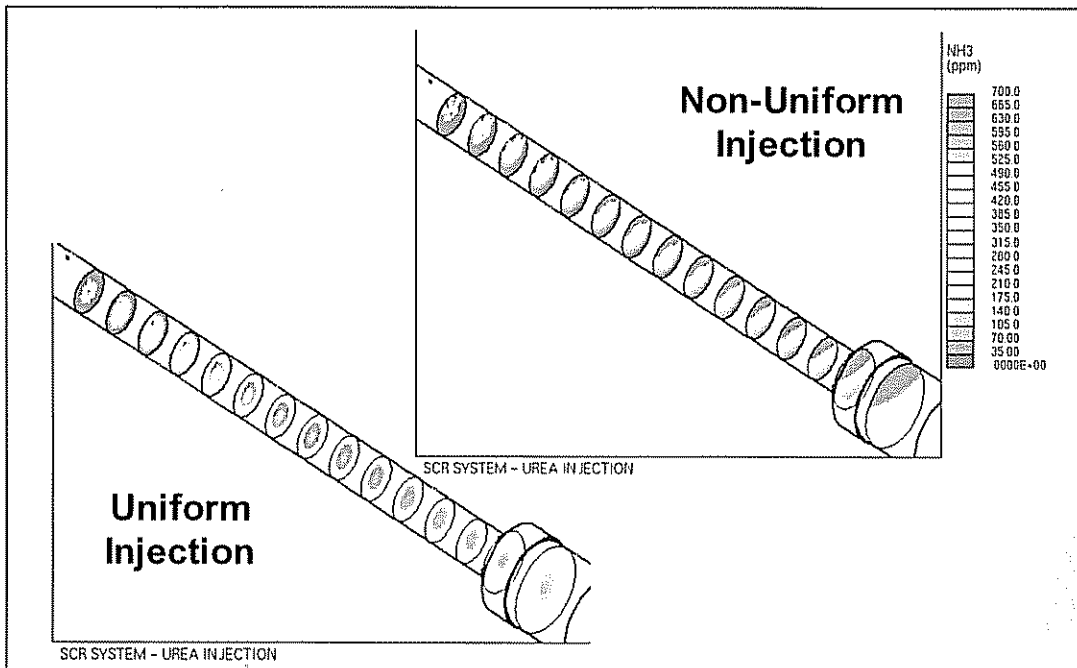


Figure 1.2.24 SCR Piping System and Computational Grid



**Figure 1.2.25 Two Urea Injection Distributions Obtained from CFD Simulations**

Two exhaust piping configurations were considered – a straight pipe and a pipe with a 90° elbow. Figure 1.2.26 shows the simulated results for the straight-pipe configuration with the uniform and non-uniform urea injection patterns.



**Figure 1.2.26 Ammonia Distribution for a Straight Pipe Configuration**

In reality, a completely uniform  $\text{NH}_3$  distribution with a mal-distribution index of 0 is difficult to obtain. A mal-distribution index of over 0.2 is high, showing strong non-uniform distribution of  $\text{NH}_3$ , as is the case for the straight pipe with non-uniform injection (Figure 1.2.27). Such a mal-distribution of  $\text{NH}_3$  is likely to result in less than optimum  $\text{NOx}$  conversion efficiency in the SCR and increased risk of  $\text{NH}_3$  slip.

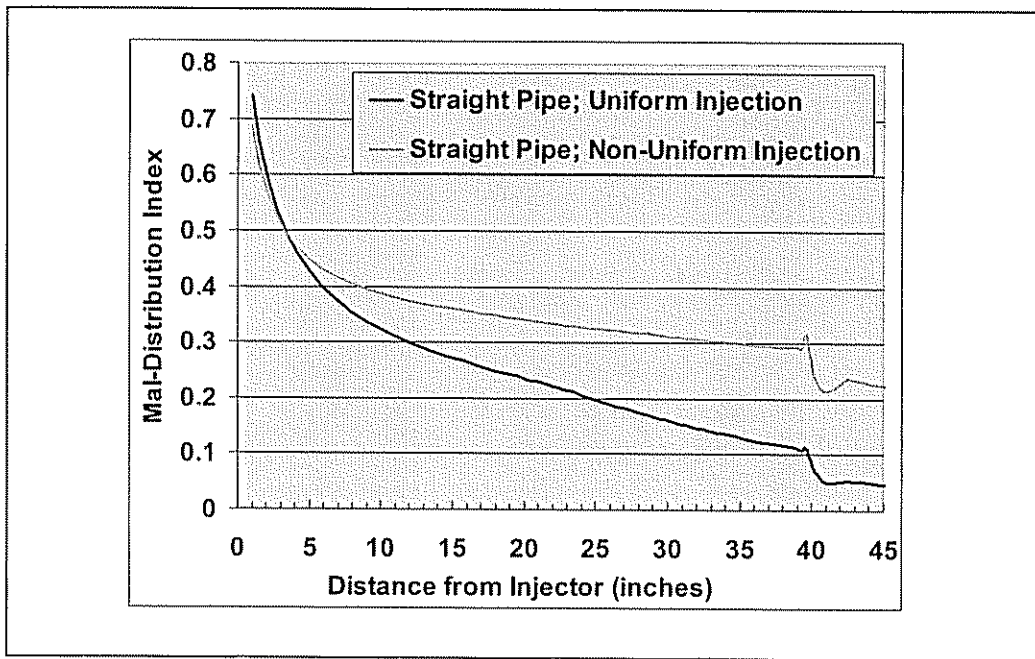


Figure 1.2.27 Mal-Distribution Index for a Straight Pipe Configuration

In order to improve urea mixing, several design modifications were considered. One of the approaches was the introduction of a  $90^\circ$  elbow in the exhaust pipe. Figure 1.2.28 shows the simulated results for the  $90^\circ$  elbow exhaust piping, with and without uniform urea injection. Compared to the straight pipe configuration, the  $90^\circ$  elbow configuration shows a significant improvement in  $\text{NH}_3$  distribution at the inlet of the SCR despite the non-uniform urea injection pattern. Figure 1.2.29 shows the mal-distribution index for the four different cases discussed above. The importance of the  $90^\circ$  elbow to enhance  $\text{NH}_3$  mixing in the exhaust stream is evident. A mal-distribution index of 0.05 was obtained at the inlet of the SCR for the  $90^\circ$  elbow configuration, for both the uniform and non-uniform urea injection cases.

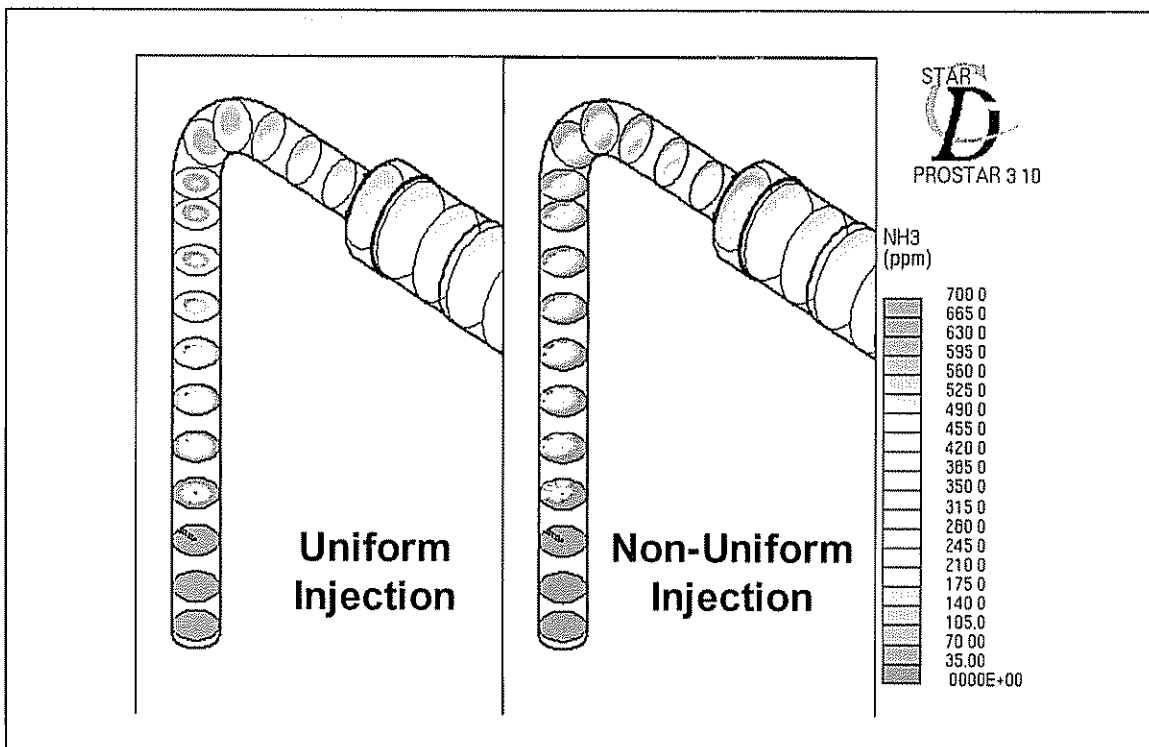


Figure 1.2.28 Ammonia Distribution for the 90° Elbow Configuration

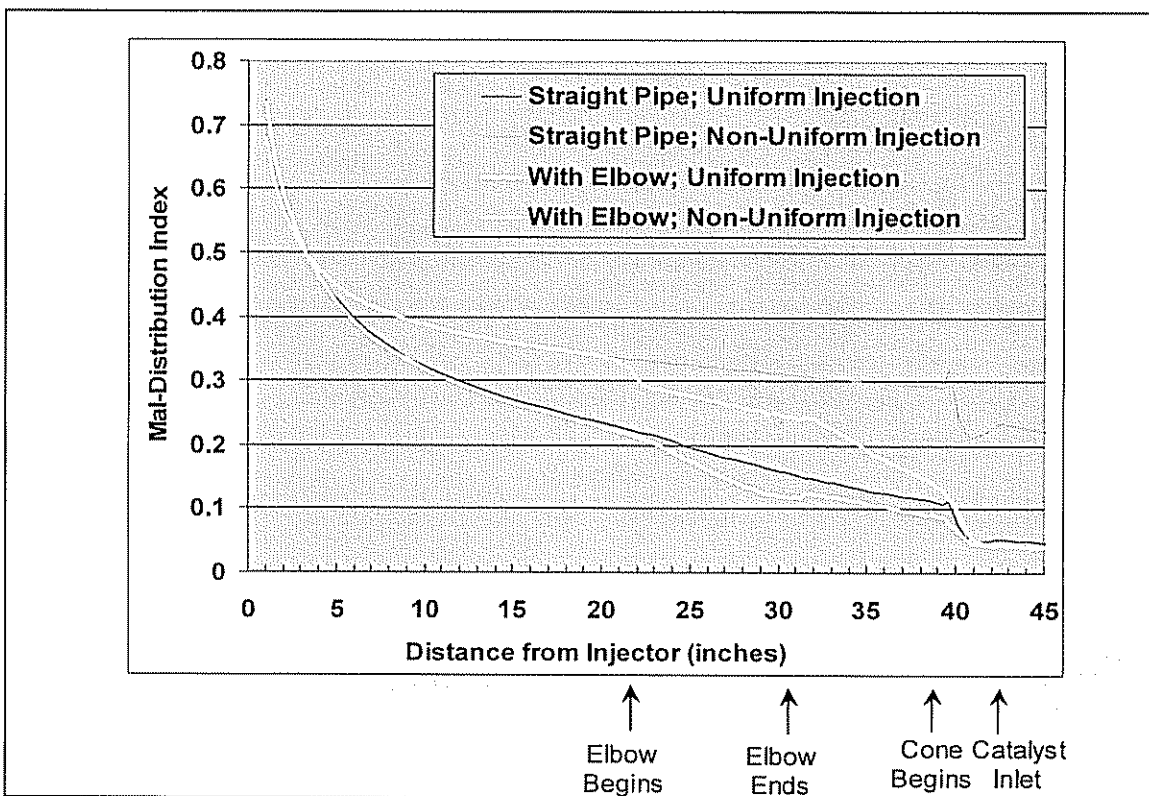


Figure 1.2.29 Mal-Distribution Index for Straight Pipe and Elbow Configurations

Interestingly, when additional approaches to further enhance mixing were attempted in the test cell, such as the addition of a butterfly valve upstream of the SCR, no further performance benefits were obtained, showing that the elbow design is adequate to provide uniform  $\text{NH}_3$  distribution at the SCR inlet. Figure 1.2.30 shows the NOx reduction efficiency as a function of alpha (a stoichiometric measure of  $\text{NH}_3/\text{NOx}$  ratios) for the elbow configuration case with and without additional mixing via an exhaust throttle valve. These experimental results validate the analytical prediction of the utility of the elbow configuration to obtain uniform  $\text{NH}_3$  distribution in the exhaust stream.

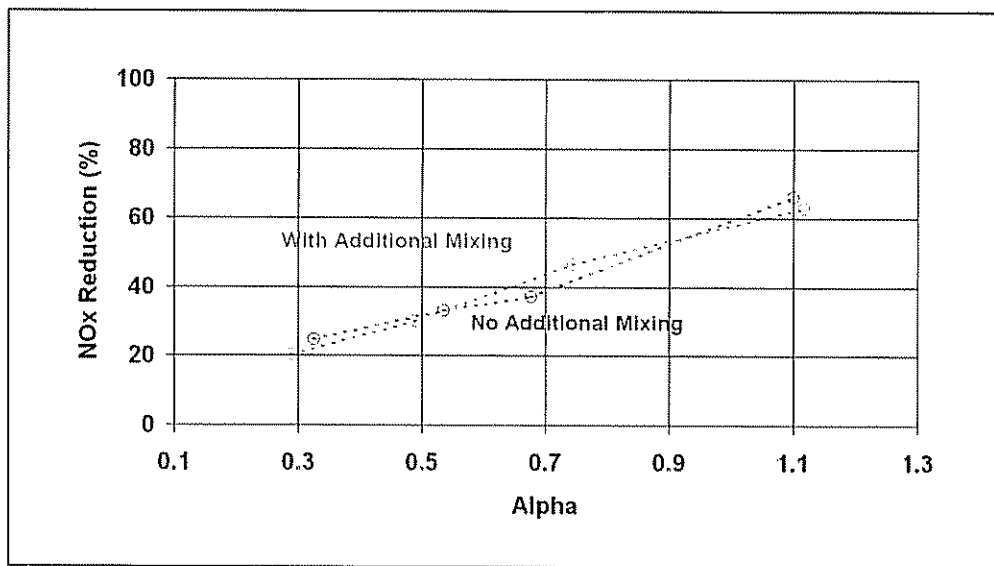


Figure 1.2.30 Effect of Additional Mixing on NOx Reduction for the 90° Elbow Configuration

### Task 1.2.2 CSF Characterization

State-of-the-art CSF technology was utilized in the LEADER program. The filter volume was 2.5 liter for the 1.5L HEV engine and 5.0 liter for the 4.0L DELTA engine. The filters used were ceramic, wall-flow substrates coated with precious and base metal components, targeting >80% filtration efficiency over the US FTP75 cycle.

#### 1.2.2.1 CSF Regeneration Characterization

Characterization of CSF regeneration is important given the impact of regeneration on fuel economy and filter durability. Figure 1.2.31 shows the impact of filter regeneration on vehicle fuel economy as a function of mileage. The fuel economy impact depends on initial PM loading, regeneration frequency, regeneration schemes, trap size and its geometry, and catalytic material for passive regeneration.

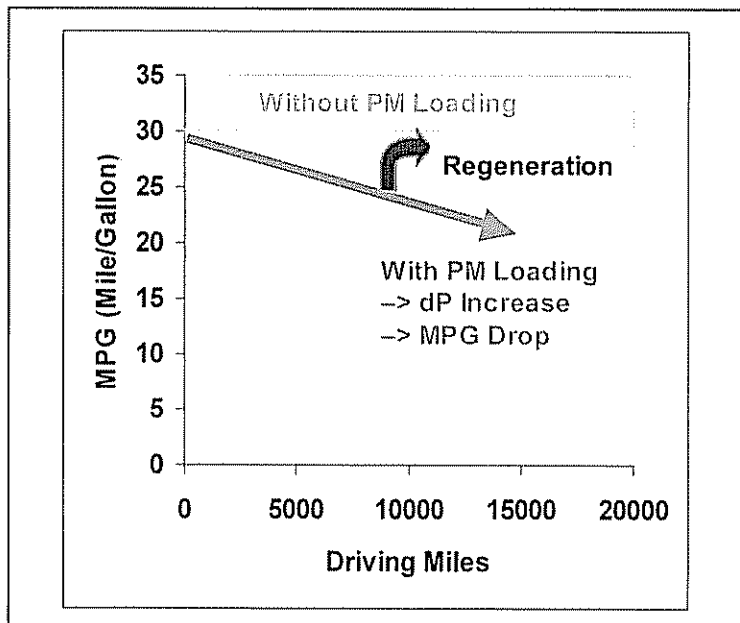


Figure 1.2.31 Impact of CSF Regeneration on Fuel Economy

The primary regeneration mechanism in this program was the use of catalytic-assisted approach ( $\text{NO}_2$  reaction mechanism with carbon). This passive regeneration typically happens at lower temperature compared to active regeneration. By properly selecting the  $\text{NO}_2$  level and temperature, the pressure drop across filters can be controlled and optimized, thus partially mitigating the fuel economy penalty. Without proper control schemes and adequate protection, the filter may undergo uncontrolled regeneration, possibly resulting in a failure. Figure 1.2.32 shows a cross-section of a failed CSF sample. This failure is attributed to internal damage caused by extreme temperatures ( $>1455^\circ\text{C}$ ) which are the result of an uncontrolled regeneration event.

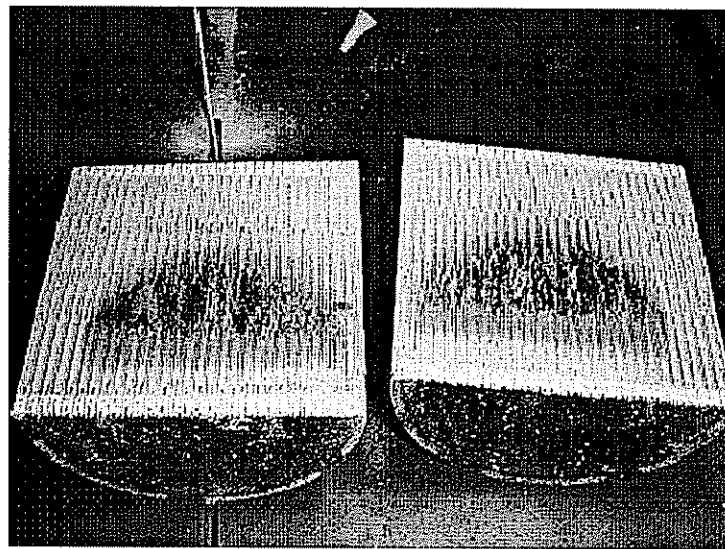


Figure 1.2.32 CSF Failure as a Result of Uncontrolled Regeneration

Figure 1.2.33 shows the apparent lack of correlation between the soot filter mass and pressure drop across the filter. Due to this lack of correlation, the pressure drop cannot be solely utilized to trigger active regeneration in a catalyzed soot filter. Figure 1.2.34 shows the baseline filter mass shift after multiple regenerations for a 2.5L CSF used for the 1.5L HEV engine. This baseline mass shift may be attributed to ash accumulation in the filter, but the correlation has not been quantified yet.

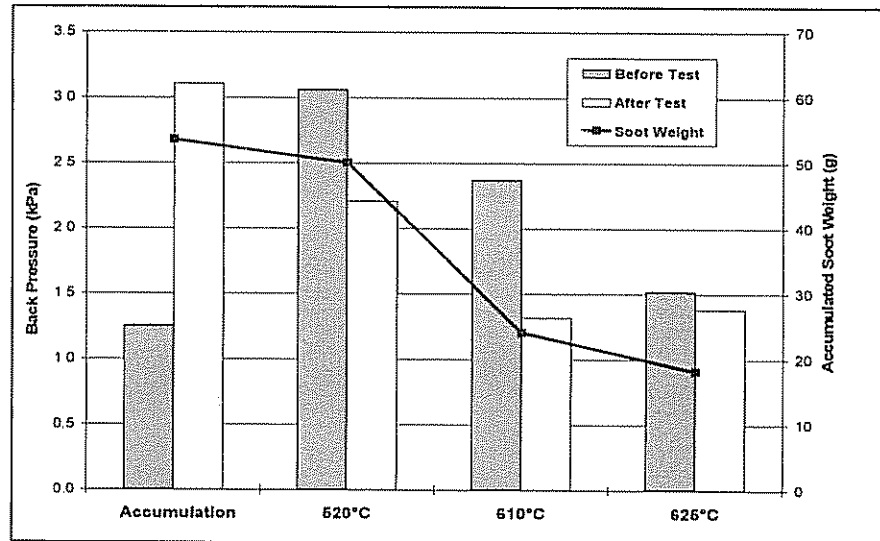


Figure 1.2.33 Apparent Lack of Correlation between Accumulated Soot and Pressure Drop

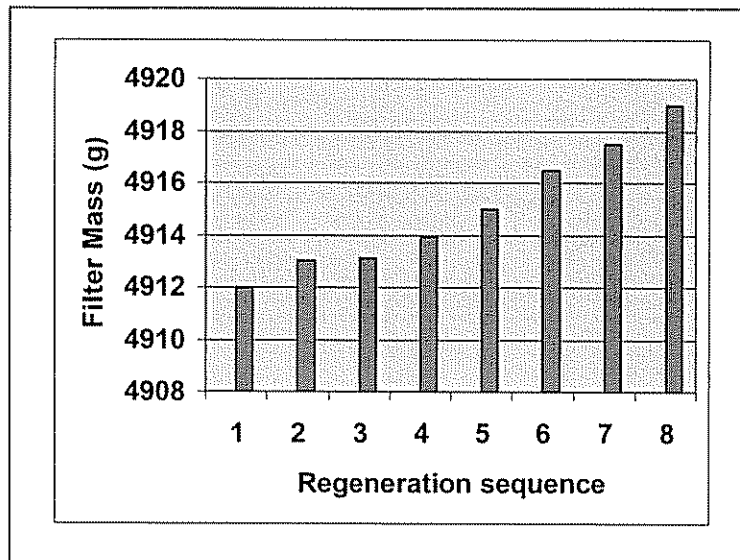


Figure 1.2.34 Baseline Mass Shift after Multiple Regenerations

It was observed that passive regeneration occurs very quickly once the CSF inlet reaches favorable conditions. Figure 1.2.35 shows regeneration occurrence under three different conditions with favorable temperature and  $\text{NO}_2$  characteristics at the inlet of the CSF. The pressure drop across the CSF reduces significantly during the first 15-20 minutes of passive regeneration.

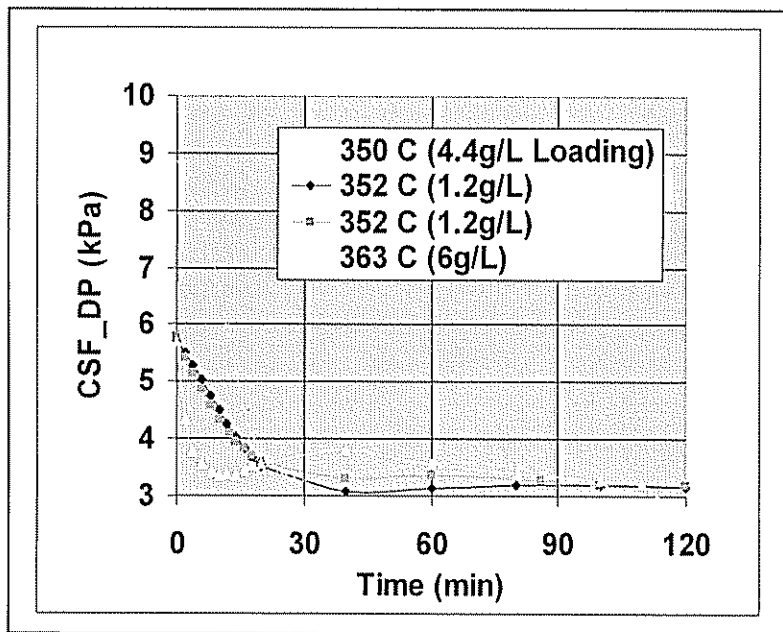


Figure 1.2.35 Passive Regeneration for the 1.5L HEV Engine

It was also observed that passive regeneration is a function of space velocity, as inferred by the balance point determination tests shown in Figures 1.2.36 and 1.2.37.

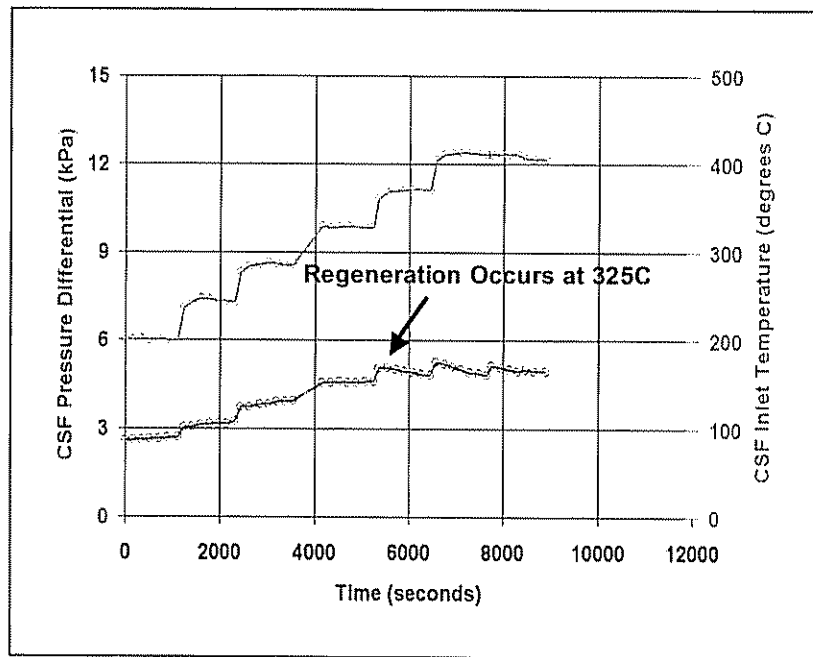


Figure 1.2.36 Balance Point Determination at 2200 rpm for a 1.5L HEV Engine Application

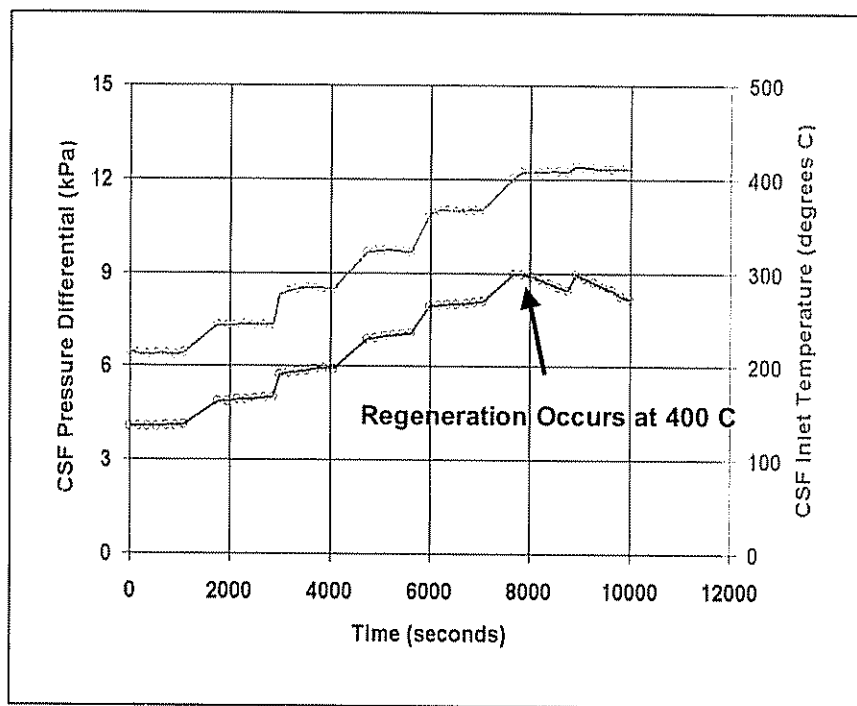


Figure 1.2.37 Balance Point Determination at 2700 rpm for a 1.5L HEV Engine Application

During the course of the program, state-of-the art CSF models were developed as discussed in the description of Task 1.1 (Modeling Development and Integration). More importantly, the models were used to provide a better understanding of aftertreatment characteristics and to provide testing directions. Figure 1.2.38 shows the temporal soot balance inside the filter at a typical engine operating condition. Such data was obtained using the validated CSF model and is impossible to obtain by conventional experiment means. The model is able to provide the temporal history of the soot balance in the filter, including soot oxidation and retention. The model is also able to identify favorable exhaust species and temperature conditions for a complete regeneration to occur.

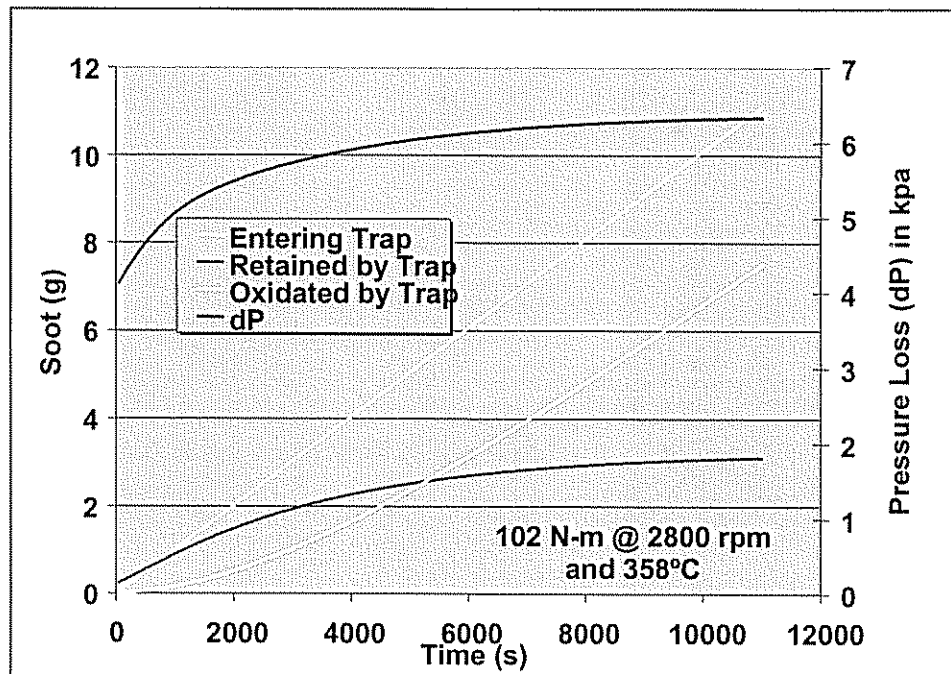


Figure 1.2.38 CSF Soot Balance Analysis Using DDC Developed CSF Model

CSF aging characterization was also carried out over 50, 300, 600 and 1000 hours. Table 1.2.3 shows NO to NO<sub>2</sub> conversion efficiency as a function of aging hours. Very little apparent loss of catalytic activities was observed after 1000 hours of aging.

Table 1.2.3 NO<sub>2</sub> Conversion Efficiency for Aged Catalyzed Soot Filters

% NO <sub>2</sub> Post CSF			
	1650 / 180	1500 / 140	1350 / 120
50 Hour Aged	75.4	75.5	64.7
300 Hour Aged	71.3	70	58.8
600 Hour Aged	68.5	60.8	53.3
1000 Hour Aged	67.8	70.4	64.7

### 1.2.2.2 CSF Regeneration Strategy Development

The failed CSF sample as shown in Figure 1.2.32 signifies the importance of a sophisticated regeneration control strategy with adequate protection features. In order to ensure a high ROI to the LEADER program, a comprehensive CSF regeneration strategy was developed and establishes an important milestone for future programs. The primary development focus was on regeneration start and stop triggers. Figure 1.2.39 shows the general concept of how the CSF regeneration is triggered depending on the soot mass trapped in the CSF.

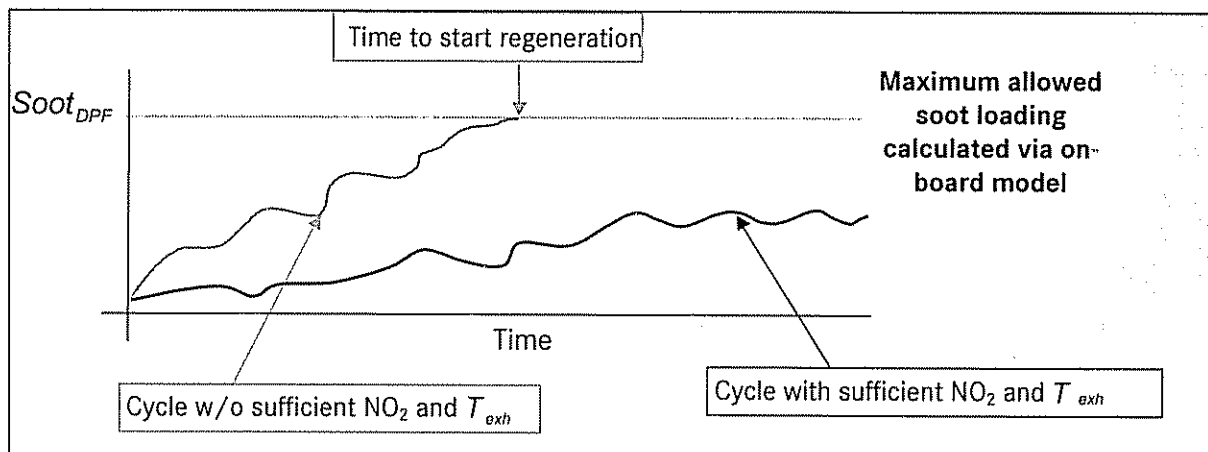


Figure 1.2.39 General Regeneration Strategy for Stop and Start Triggering

Targeting the general strategy laid out in Figure 1.2.39, an offline analytical model was developed with the intention of utilizing it for real-time control. This model was based on DDC's 2D CSF model, but with a few key simplifications to allow computational feasibility for real-time control. A single channel was assumed in the 0D real-time model, while maintaining the same filtration area as the actual CSF, as shown in Figure 1.2.40. A uniform soot distribution was assumed in the filter. Also, the NO<sub>2</sub> formation was assumed to be governed by the thermal equilibrium law.

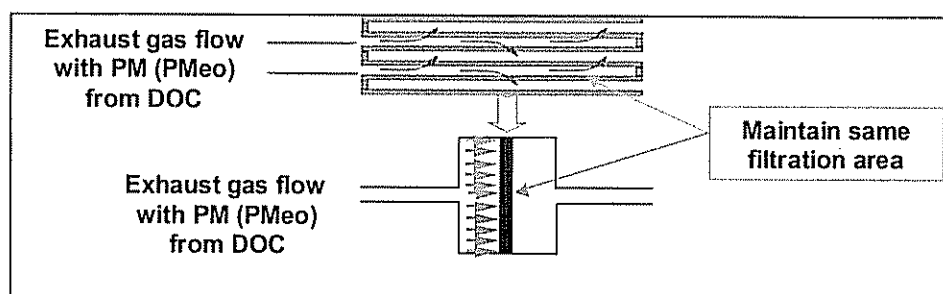


Figure 1.2.40 Simplification of a 2D CSF Model to a Real-Time 0D Model

Figure 1.2.41 shows the primary blocks in the regeneration control strategy model. This model was validated against existing testing data as well as other simulation data, and then was utilized to conduct parametric studies which looked at the impact of a few key parameters on regeneration. Figure 1.2.42 shows the filter behavior during regeneration using the late in-cylinder fuel injection approach, as calculated by this model.

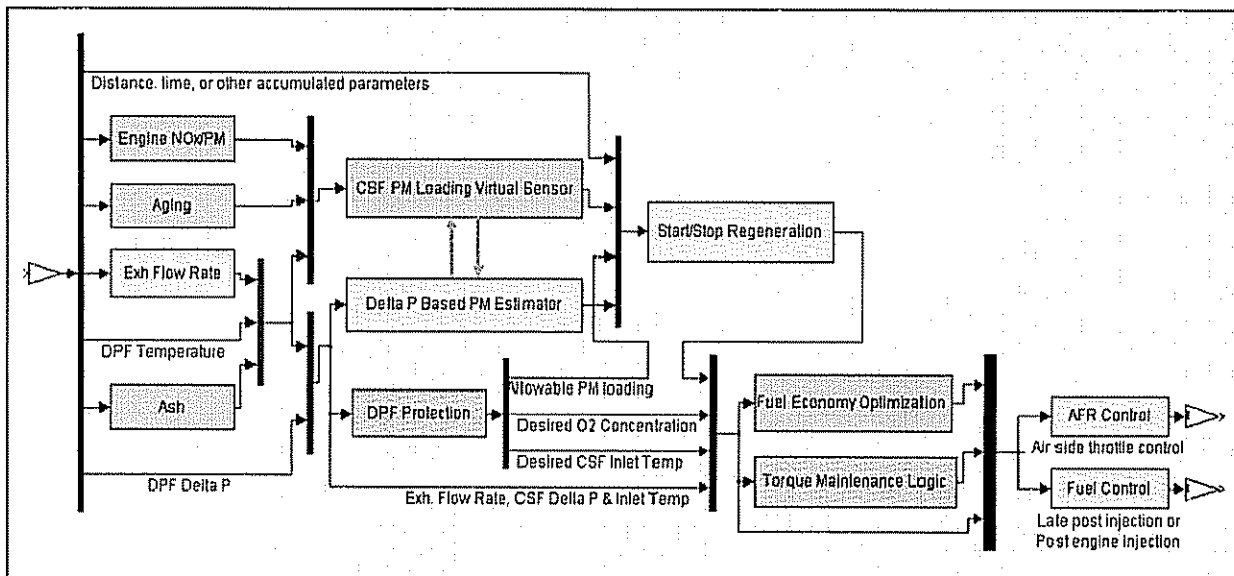


Figure 1.2.41 Regeneration Control Algorithm

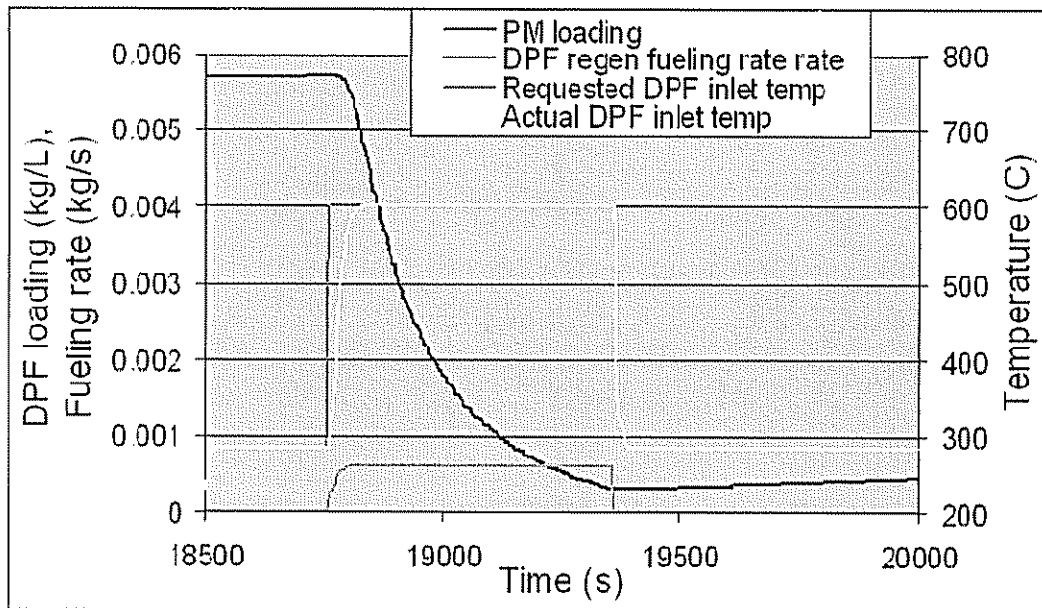
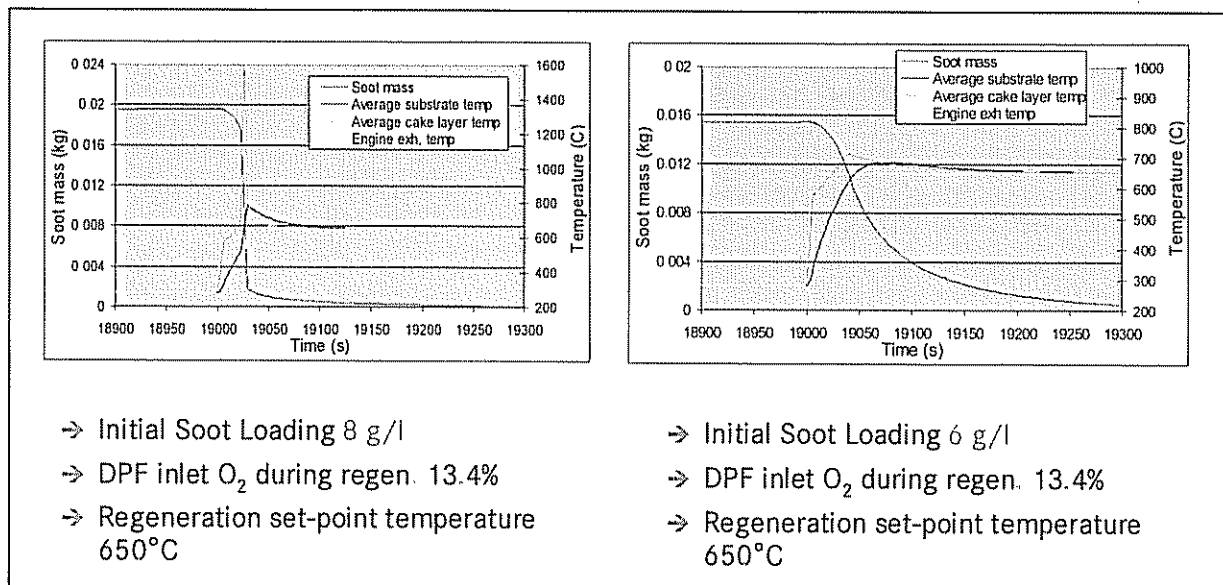


Figure 1.2.42 Regeneration Behavior Simulated in Real Time

Figure 1.2.43 shows the impact of CSF initial soot loading on the regeneration behavior. With an initial soot loading of 8 g/L and typical exhaust temperature and species conditions, the soot cake layer temperature reaches over 1500°C when regeneration is triggered. With an initial soot loading of 6 g/L, however, the regeneration temperatures are controlled to ~700°C. These results highlight the importance of soot loading in determining regeneration characteristics and the need for a sophisticated control strategy.



**Figure 1.2.43 Effect of Soot Loading on Regeneration**

### 1.2.2.3 Other CSF Projects

Additional CSF-related projects were also initiated under the LEADER program. These include fuel burner development, ash loading testing and reactor bench tests. However, due to programmatic issues, these projects were transferred to the DOE-DDC DELTA program (Contract #DE-FC26-02OR22909) after obtaining DOE's approval. The technology development conducted under these projects will be presented in the final report of the DELTA program.

### Task 1.2.3 Characterization of LNT+CSF System

State-of-the-art LNT technology was utilized in the LEADER program. The catalyst used was about 10L in volume for the 4.0L DELTA engine and included precious and base metal components coated on a ceramic flow through substrate targeting a NOx conversion of 50% over the US FTP75 driving cycle.

Two LNT configurations were considered as shown in Figure 1.2.44.

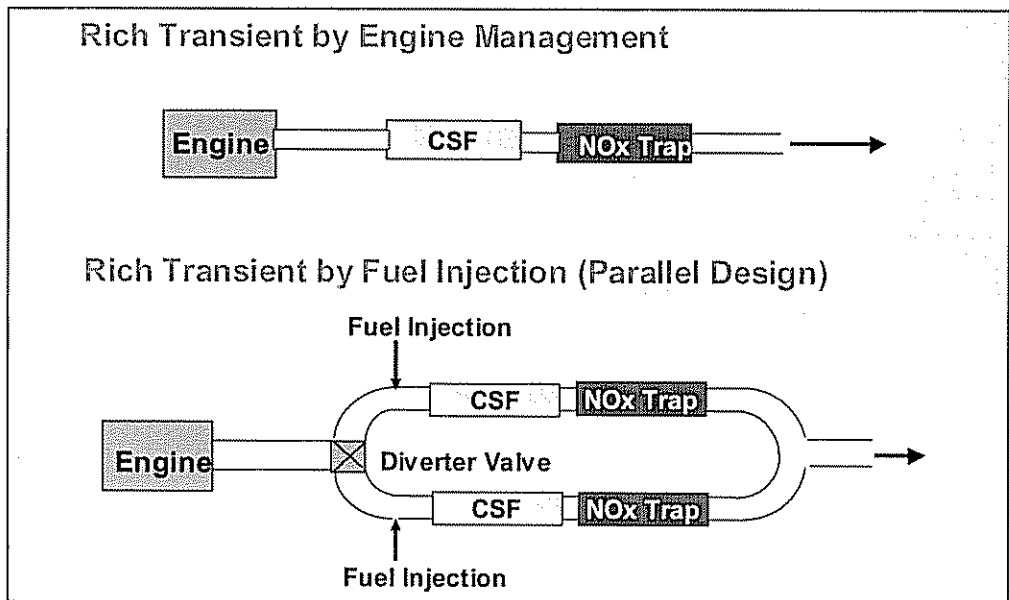


Figure 1.2.44 Two LNT Configurations Considered under the LEADER Program

The pros and cons of these two configurations are presented below.

<u>Engine Management</u>	<u>Exhaust Fuel Injection</u>
✓ Very active rich mixture (high CO). Effective for cool exhaust regeneration. Good for most passenger cars.	✓ Simplicity in engine set up - minimum change in engine operating parameters
✓ Avoids fuel condensation at low temperatures	✓ Works well at higher temperatures ( $>300^{\circ}\text{C}$ )
✓ Requires small space for catalyst system	✓ Low temperature ( $<250^{\circ}\text{C}$ ) activity is limited. Fuel condensation may occur at low temperatures.
✓ Possible to achieve high exhaust temperatures	✓ Space limitation for the parallel design may be an issue for some applications
✓ Engine Management Development required	

The program's goal was to test both approaches. Engine management strategies, including combustion and air management, were tested at DDC's facility, while the exhaust fuel injection configuration testing was conducted at the EC facility. The engine management results will be presented in the description of Task 2 which covered other engine-related development activities as well. This section will only cover the results of the exhaust fuel injection development study.

Figure 1.2.45 shows a picture of the test set-up, utilizing the exhaust fuel injection approach. Figure 1.2.46 shows a close-up view of one of the fuel injectors located in the exhaust stream.

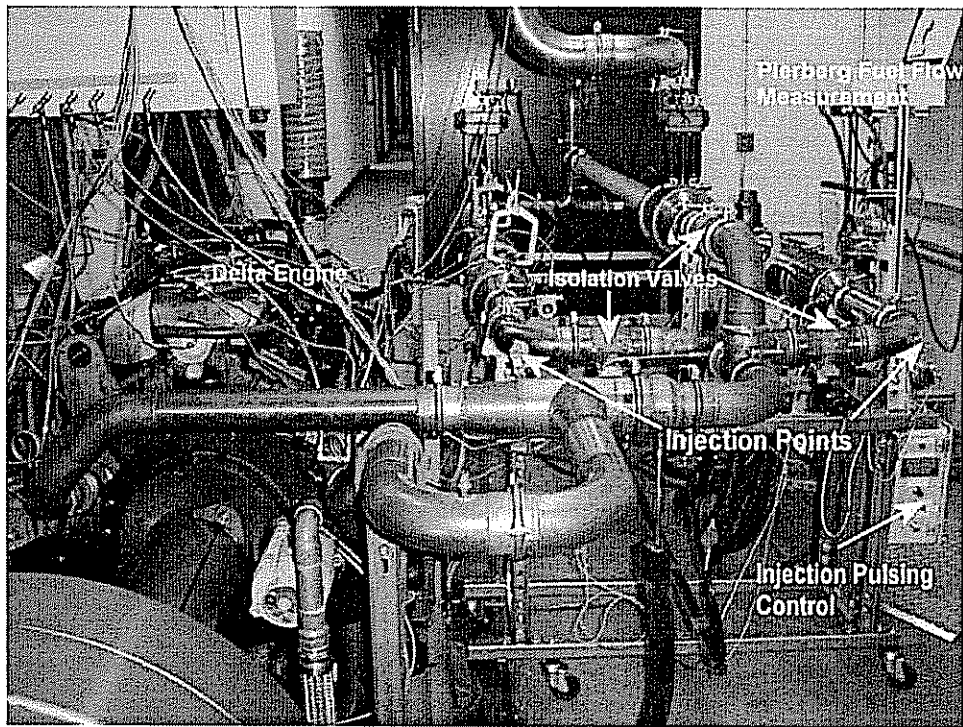


Figure 1.2.45 Dual Parallel-Leg LNT/CSF System Using Exhaust Fuel Injection

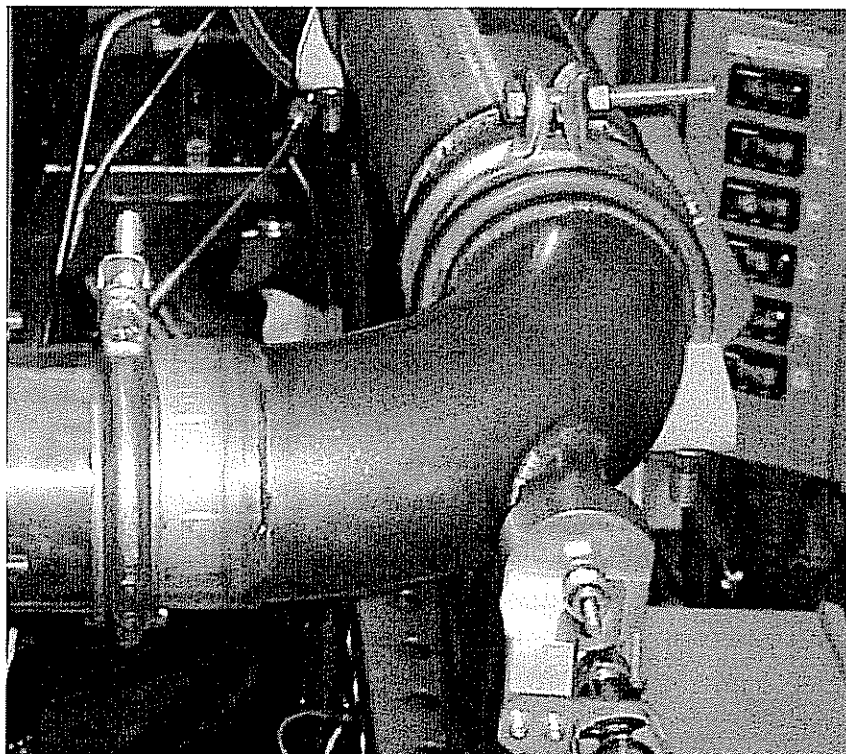


Figure 1.2.46 Exhaust Fuel Injector

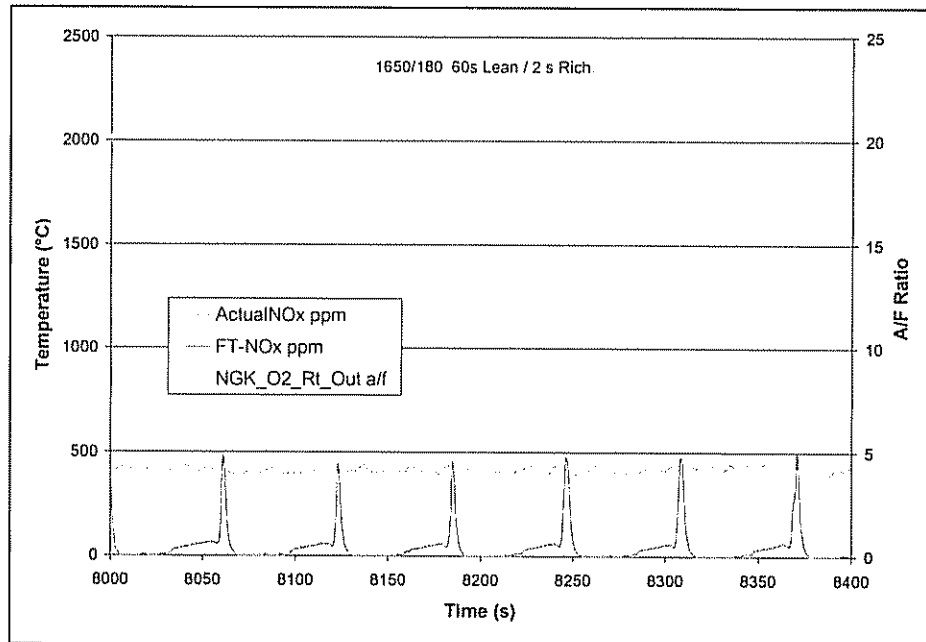
During the tests, the exhaust flow was controlled approximately in the 10%-90% ratio, with 10% flow rate used for rich regeneration, and 90% flow rate used for lean operation.

Seven steady state modes were selected to characterize the LNT system. These operating conditions are listed in Table 1.2.4.

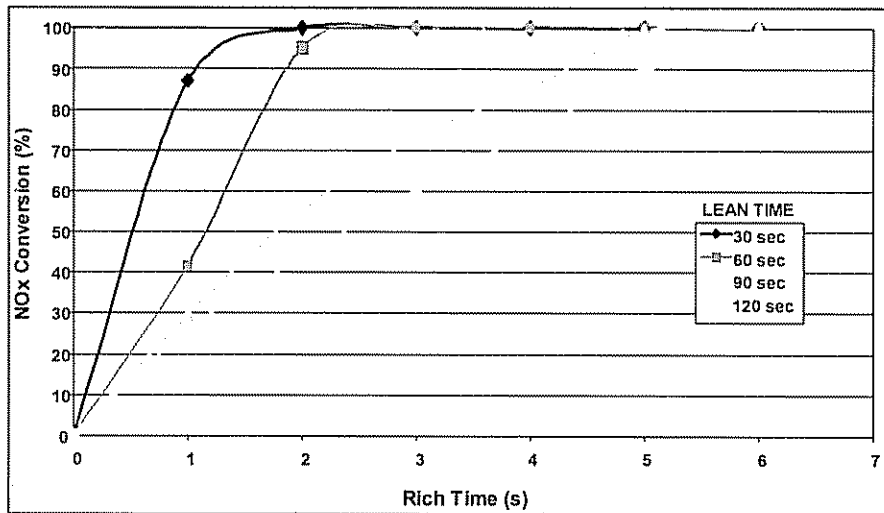
**Table 1.2.4 Steady State Modes for Characterization of LNT/CSF System**

Set Point	Engine Speed (rpm)	Engine Load (Nm)	Turbo Out Temp (°C)	NOx Rate (g/min)
1	2200	235	470	2.8
2	1650	180	355	1.9
3	1500	140	300	1.0
4	1350	120	273	0.8
5	1400	80	207	0.7
6	1150	80	207	0.5
7	1550	60	195	0.7

Figure 1.2.47 shows example results from the dual leg LNT system with 60 s lean and 2 s rich operation, resulting in over 90% reduction in NOx. During the course of the program, many different lean and rich ratios were tested in order to optimize the LNT performance. Figure 1.2.48 shows example results of the optimization study conducted at 1500 rpm and 140 N·m torque. As can be seen, a lean time operation of 30 seconds yields the best performance for NOx conversion.

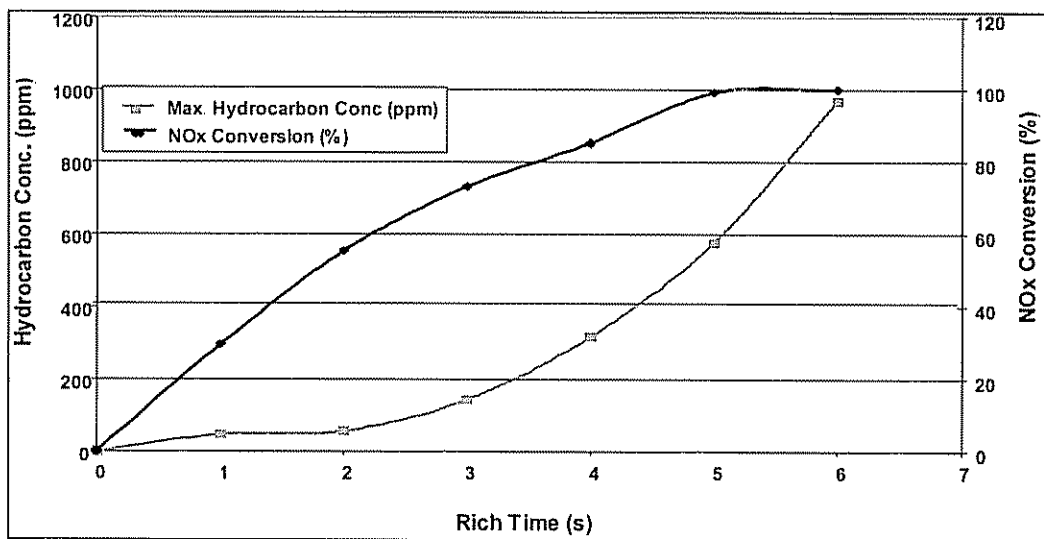


**Figure 1.2.47 Example Results from a Dual Leg LNT System with 60s Lean / 2s Rich Operation Resulting in over 90% NOx Conversion**



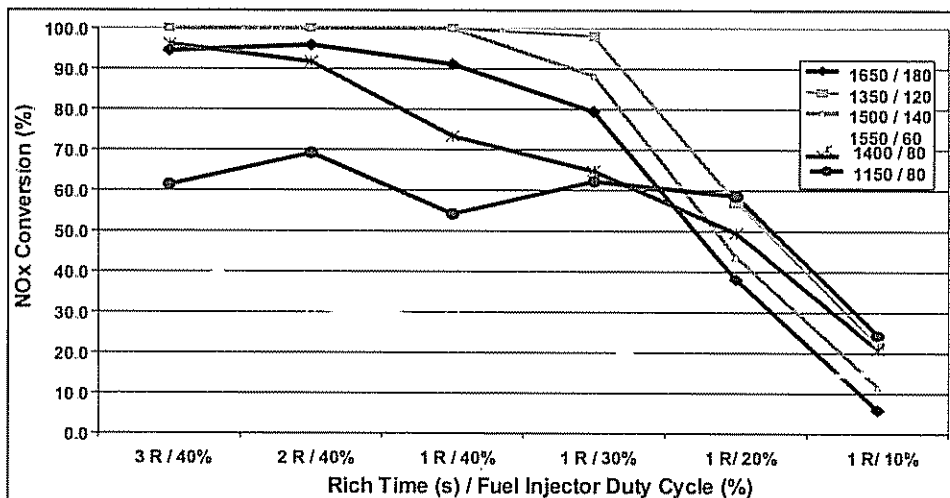
**Figure 1.2.48 Example Results of NOx Conversion with Lean/Rich Operation Optimization at 1500 rpm / 140 N·m**

Figure 1.2.49 summarizes the impact of rich operation time on the NOx conversion and HC slip. This study suggests that for a lean operation time of about 90 s, the rich time should be in the range of 4-5 seconds in order to achieve the best NOx reduction at this operating condition.



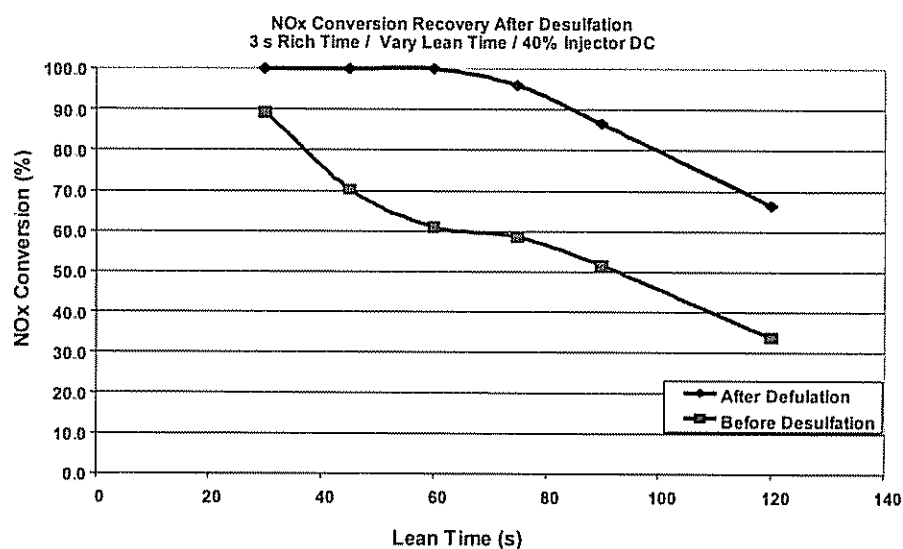
**Figure 1.2.49 Example of Trade-off of Hydrocarbon Slip and NOx Conversion at 1500 rpm / 140 N·m**

Figure 1.2.50 shows the sensitivity of NO<sub>x</sub> conversion to rich operation time for six steady state modes. High NO<sub>x</sub> conversion efficiency for the high loads can be attributed to the high exhaust temperatures. The low efficiency at 1550 rpm and 60 N·m is due to the relatively low exhaust temperature.



**Figure 1.2.50 Sensitivity of NO<sub>x</sub> Conversion to Rich Operation Time and Injector Duty Cycle for Six Steady State Modes**

The LEADER program also carried out a desulfation investigation. Figure 1.2.51 shows example results of NO<sub>x</sub> conversion recovery after desulfation. The desulfation was conducted by maintaining 700°C at the inlet of the LNT. These results suggest that for a given 3 s rich time, the lean time should be maintained in the range of 40-60 s in order to have high NO<sub>x</sub> conversion recovery after desulfation.



**Figure 1.2.51 NO<sub>x</sub> Conversion Recovery after Desulfation at 700°C**

Experimental studies to evaluate the fuel economy penalty resulting from the rich regeneration operation were also conducted. Figure 1.2.52 shows the fuel economy penalty versus NOx conversion efficiency at six operating conditions. In general, the fuel economy penalty was maintained below 5%, while maintaining 50%-90% NOx conversion efficiencies for 5 of the 6 operation modes. For the low temperature operation condition, the fuel economy penalty was high and the NOx conversion efficiency was also poor.

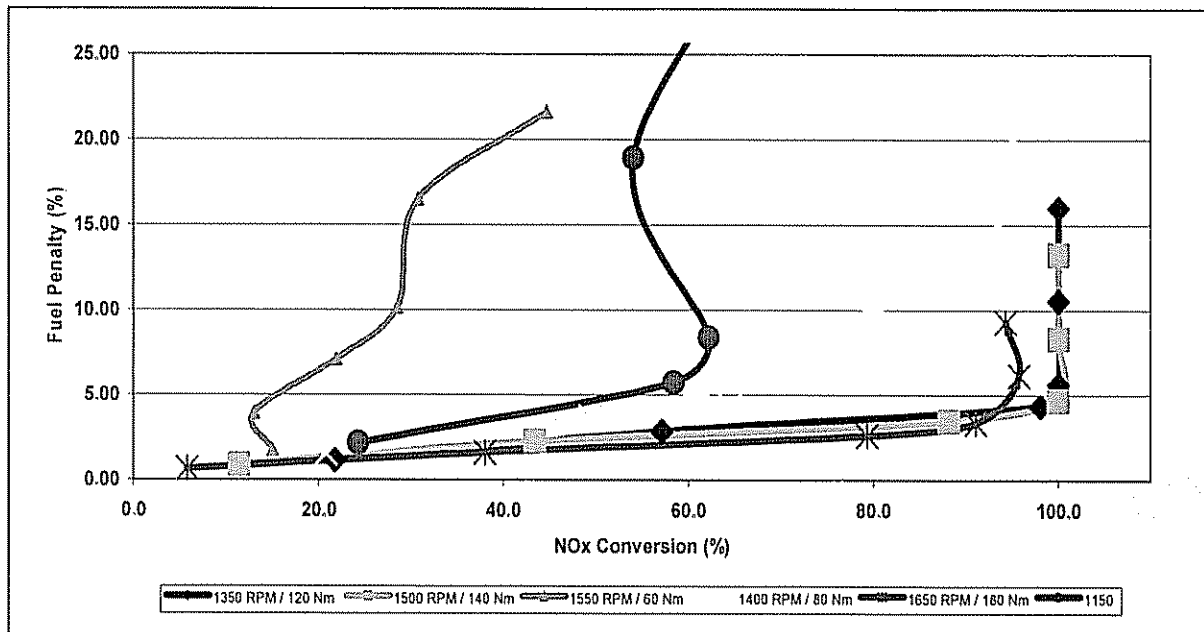


Figure 1.2.52 Summary of Fuel Economy Penalty versus NOx Conversion Efficiency

Some of the other findings of this study using a dual leg LNT system with external exhaust fuel injection are listed below:

- NOx conversion efficiency using a dual leg NOx-trap configuration correlates with the catalyst temperature.
- Performance is expected to deteriorate at temperatures below 200°C based on laboratory experiments.
- Efficiency for activation of injected diesel fuel over the CSF is relatively poor at temperatures below 200°C, even at low space velocity.
- Fuel economy penalty can be minimized by avoiding over injection of fuel and by optimizing the injection quantity based on the stored NOx.
- In most cases 90%+ NOx conversion efficiency results in a fuel penalty of 4-5%, with 90% by-pass control strategy.

### Task 1.2.4 DOC Characterization

The LEADER program benefited from the use of reactor bench tests to characterize DOC performance. A small representative DOC sample with 10 mm x 18 mm was used instead of a full DOC sample. The reactor bench tests allowed a comprehensive and systematic study to be conducted with the objective of characterizing DOC performance as a function of space velocity, temperature and species concentration and obtaining fundamental reaction data for DOC model calibration. This allowed a broad range of conditions to be tested in a relatively inexpensive manner, compared to the tedious and expensive engine dynamometer tests that would have been required to obtain similar data. The tests were carried out at the state-of-the-art research facility of DaimlerChrysler. Table 1.2.5 shows the 10 operating points tested, which cover a range of temperature, space velocity and species conditions. These included six different exhaust species mixtures and are referred to as Mix 1 through Mix 6.

Table 1.2.5 Reactor Bench Test Matrix

DOC Test Point	SV [1/h]	Temp [°C]	NO [ppm]	NO <sub>2</sub> [ppm]	HC [ppm]	CO [ppm]	H <sub>2</sub> O [%]	O <sub>2</sub> [%]	Generated Mixtures
1	44500	175	340	35	24	85	4	20	Mix 1
2	44500	200	340	35	24	85	4	20	Mix 1
3	44500	250	340	35	24	85	4	20	Mix 1
4	44500	250	340	35	5000	3500	4	10	Mix 3
5	44500	350	340	35	24	85	4	20	Mix 1
6	44500	350	600	60	24	85	4	20	Mix 4
7	187000	250	765	80	10	160	4	10	Mix 5
8	187000	350	130	15	10	160	4	10	Mix 6
9	187000	350	765	80	10	160	4	10	Mix 5
10	187000	450	130	15	10	160	4	10	Mix 6

Figure 1.2.53 shows the experimental setup using the reactor test bench. The DOC test samples were placed in the reactor section.

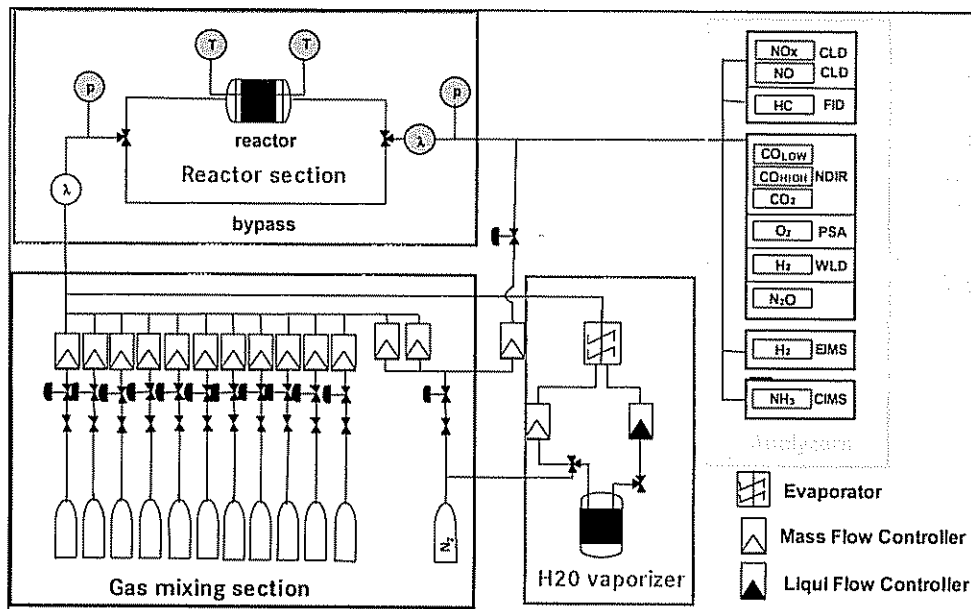


Figure 1.2.53 Experimental Setup Used for DOC Characterization

Figures 1.2.54a – 1.2.54e show example results of NO, NO<sub>2</sub> conversion as a function of temperature for the different mixtures. It is observed that:

- NO<sub>2</sub> formation is function of space velocity as evidenced by the test results of Mix 1 and Mix 6. Higher space velocity reduces NO<sub>2</sub> formation.
- NO<sub>2</sub> formation is function of HC and CO. High HC and CO reduces the NO<sub>2</sub> formation as evidenced in the test results of Mix 3 in the temperature range of 200° to 300°C.

These results will be utilized to calibrate DDC's DOC model developed as part of the LEADER program.

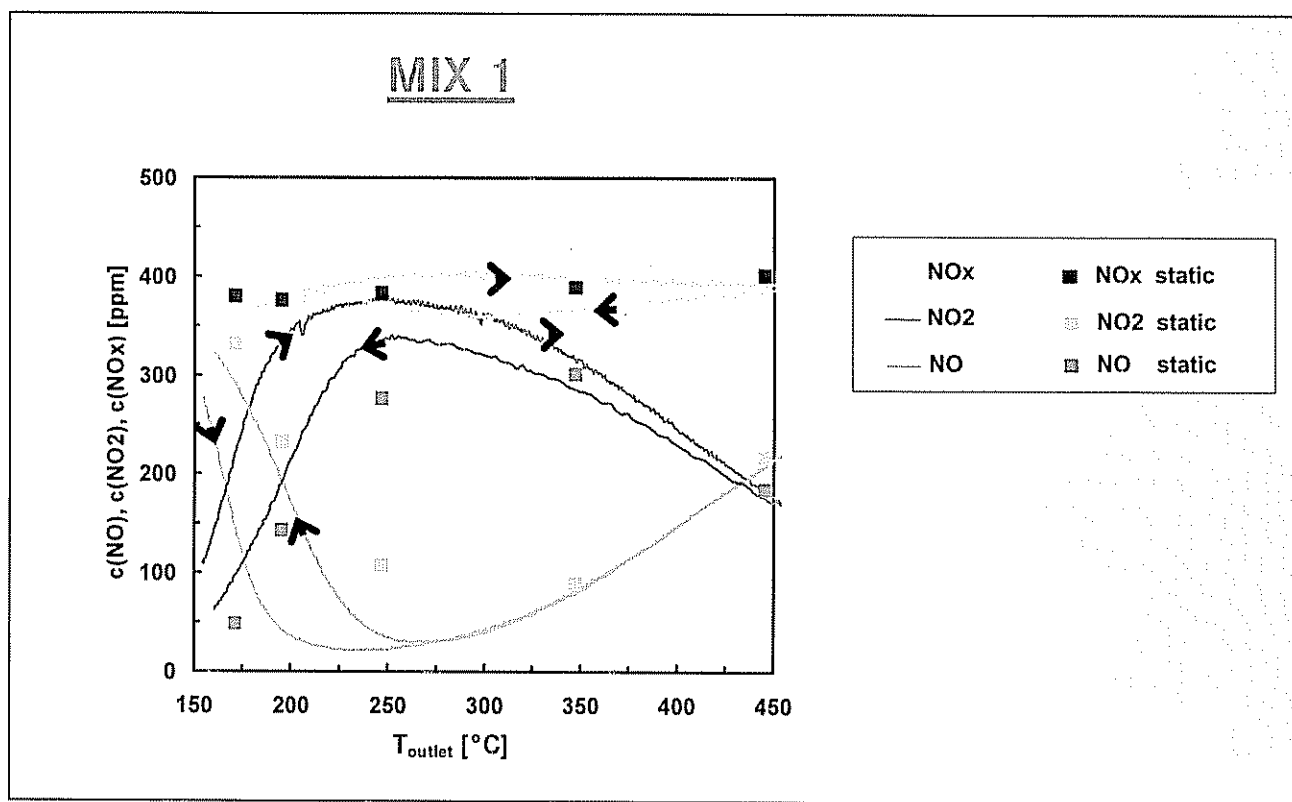


Figure 1.2.54a NOx Concentration versus Inlet Temperature of DOC for Mix 1

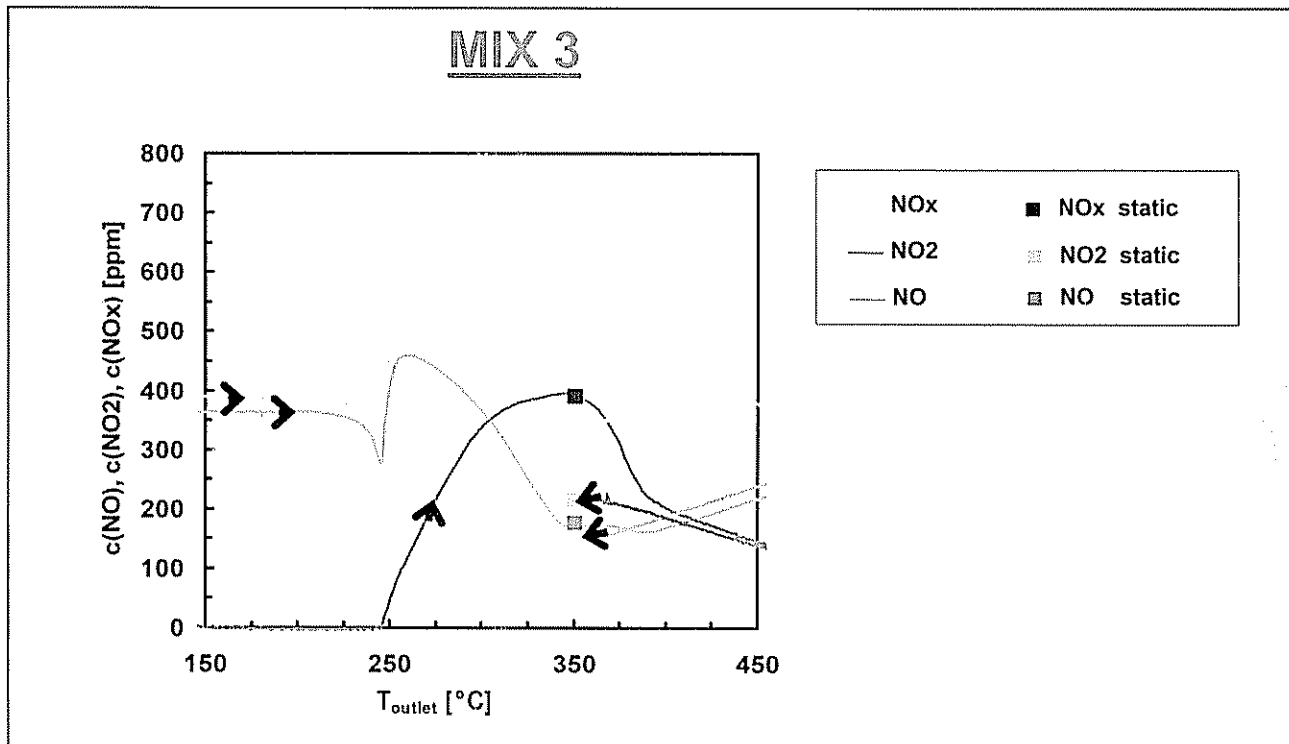


Figure 1.2.54b NOx Concentration versus Inlet Temperature of DOC for Mix 3

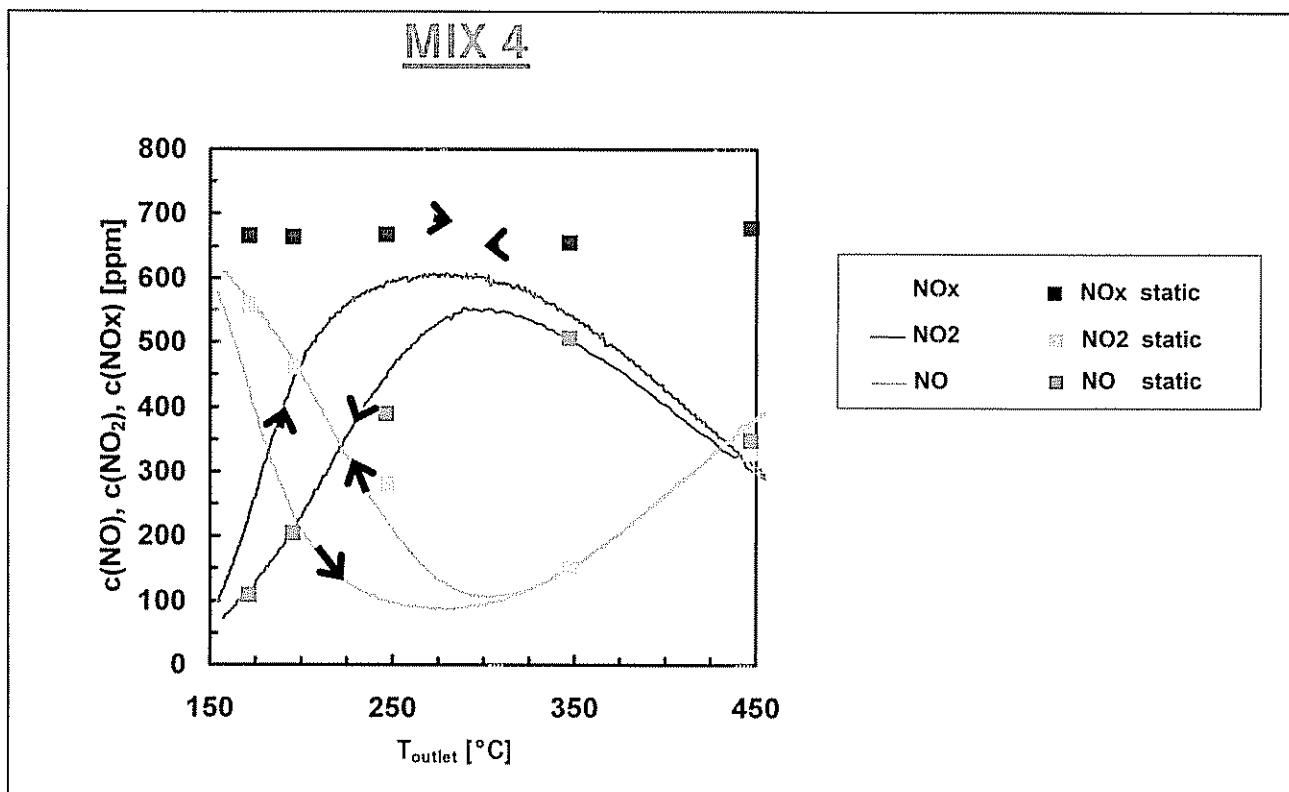


Figure 1.2.54c NOx Concentration versus Inlet Temperature of DOC for Mix 4

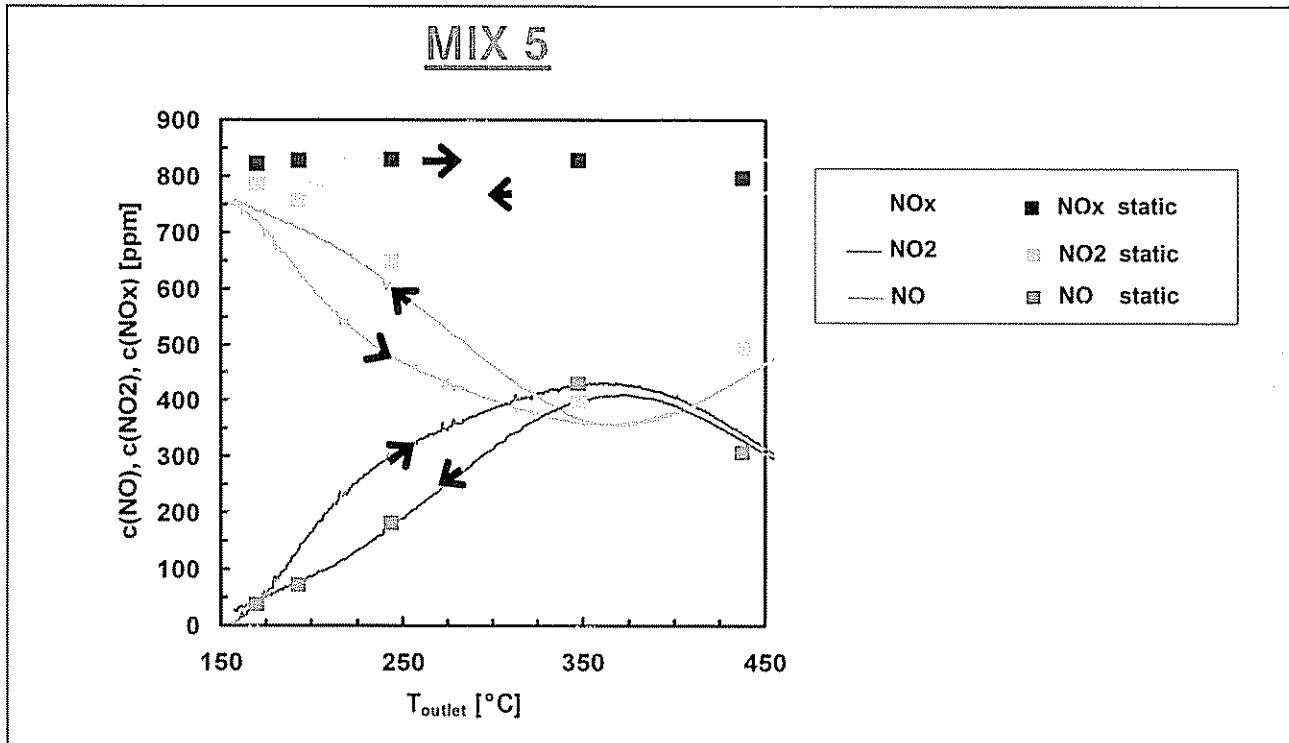


Figure 1.2.54d NOx Concentration versus Inlet Temperature of DOC for Mix 5

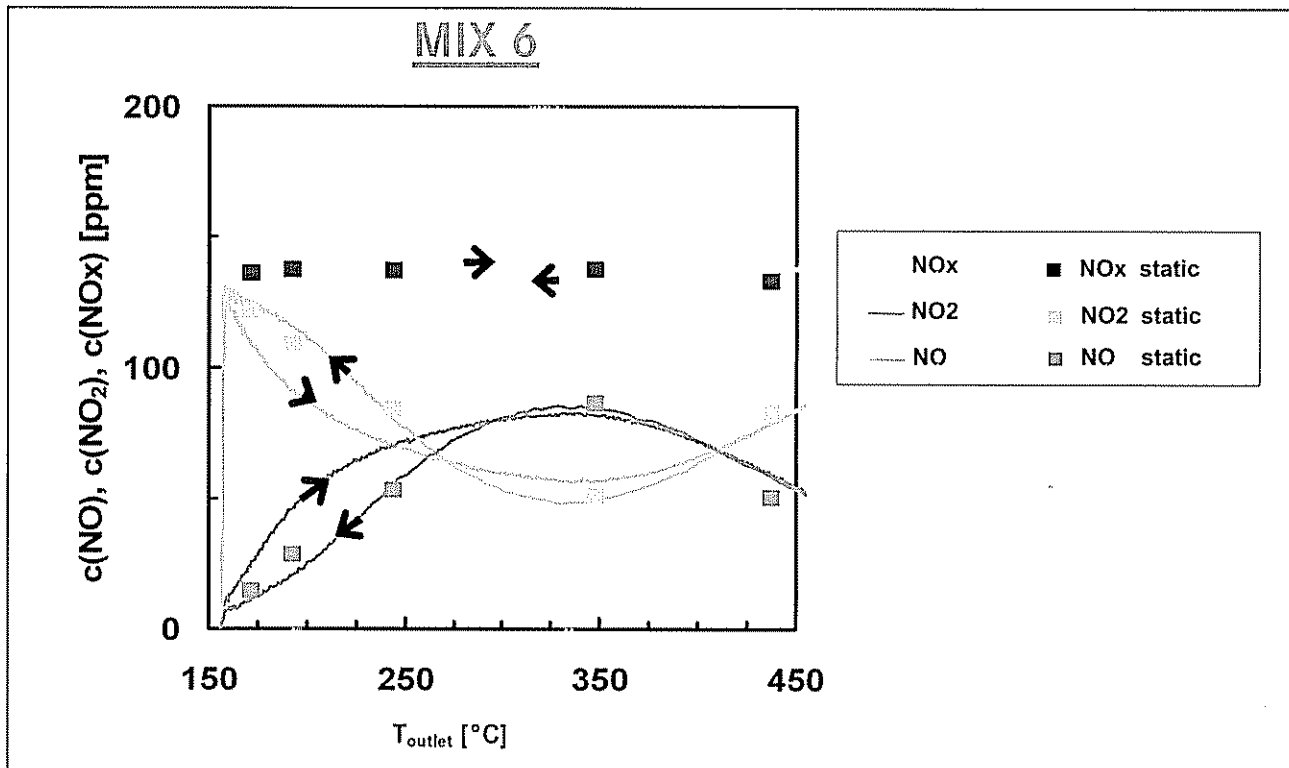


Figure 1.2.54e NOx Concentration versus Inlet Temperature of DOC for Mix 6

## Task 2 Engine-Based Development

The engine-based development focused on two specific areas: (a) advanced combustion development to reduce engine out emissions and (b) air management for regeneration control of aftertreatment devices. The air management development primarily utilized the DELTA engine platform.

The LEADER program placed increased emphasis on system integration and recognized the importance of engine out emissions reduction in addition to aftertreatment development. This engine out emissions reduction based on in-cylinder combustion optimization was a key contributor in achieving Tier 2 Bin 3 results for both the 1.5L HEV and 4.0L DELTA engines. Figure 2.1 shows a picture of these two engines.

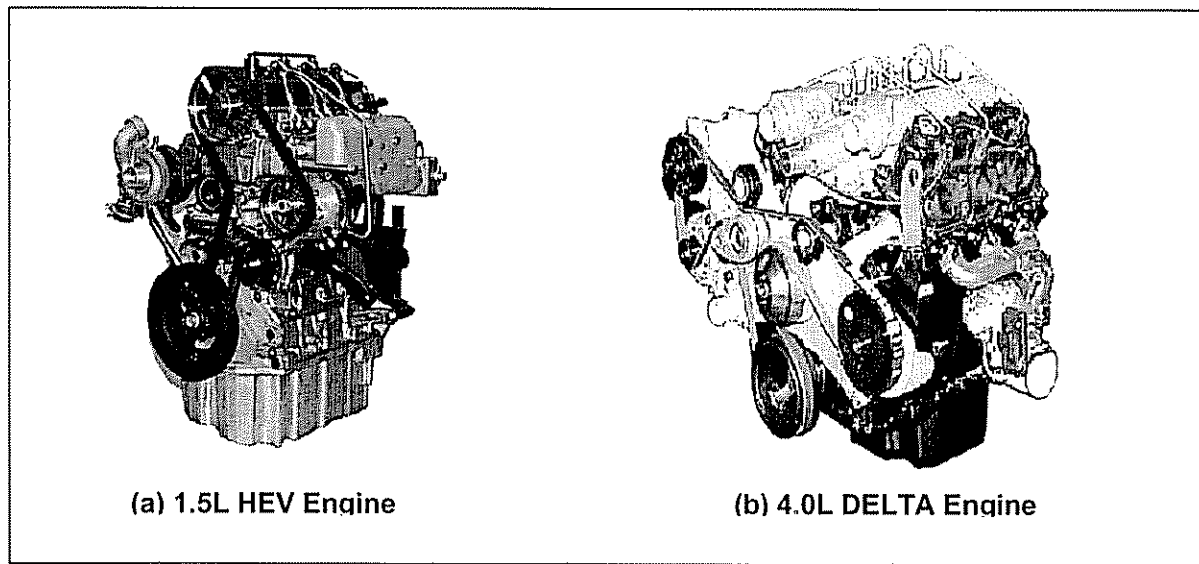


Figure 2.1 Personal Transportation LEADER Engines

## Task 2.1 Advanced Combustion Development

In synergy with the DOE-DDC DELTA program, DDC developed a unique combustion concept, CLEAN Combustion®, which results in low engine out emissions while improving engine and aftertreatment integration. CLEAN Combustion® is characterized by a low temperature and low equivalence ratio combustion process, which results in simultaneous reduction of NO<sub>x</sub> and PM while controlling carbon monoxide (CO) and hydrocarbon (HC) to desired levels for aftertreatment integration. Figure 2.2 shows a typical simultaneous reduction in NO<sub>x</sub> and PM using CLEAN Combustion®, compared to the classical emissions trade-off obtained with conventional combustion. This benefit has been demonstrated over steady-state as well as transient operation with the availability of advanced enabling technologies related to the fuel system, air-EGR system and controls integration. This technology has been successfully applied to both the HEV and DELTA engines on the engine dynamometer test-bed as well as the chassis dynamometer test-bed.

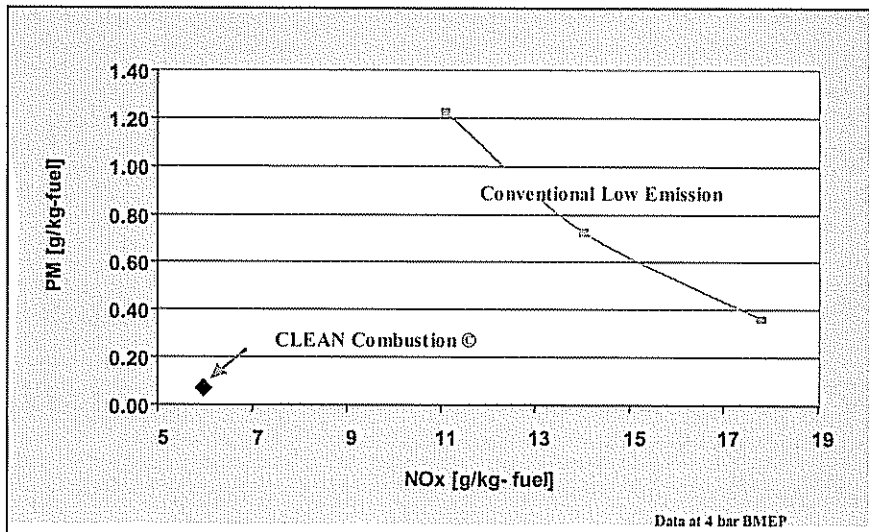


Figure 2.2 DDC's CLEAN Combustion<sup>®</sup> Development

Figure 2.3 explains how CLEAN Combustion<sup>®</sup> results in simultaneous NOx and PM reduction. The figure shows the NOx and PM formation regions in the background as a function of equivalence ratio and temperature [Akihama et al., SAE Paper 2001-01-0655]. Superimposed on this figure are two sets of data, one for CLEAN Combustion<sup>®</sup> in green and the other for conventional combustion in red. This data represents the local in-cylinder equivalence ratio and temperature conditions corresponding to the point of maximum heat release in the power stroke. It is observed that CLEAN Combustion<sup>®</sup> occurs at lower temperatures and lower equivalence ratios compared to conventional combustion and avoids the formation of NOx and PM emissions.

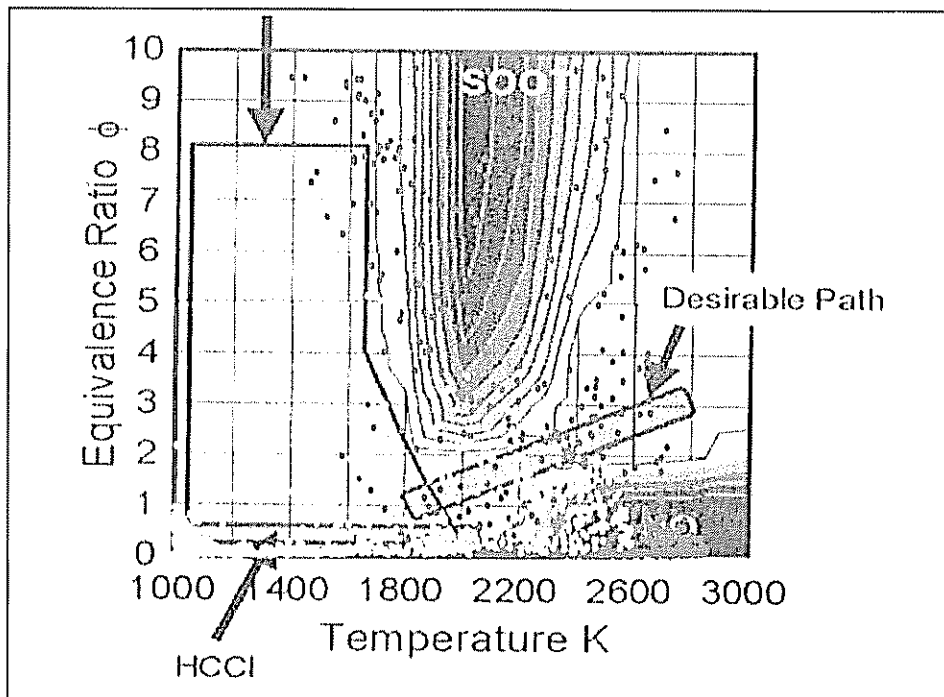


Figure 2.3 CLEAN Combustion<sup>®</sup> Concept

Figures 2.4 and 2.5 show the ability to produce controllable CO and HC emissions by utilizing CLEAN Combustion<sup>®</sup>. If desired, the engine out CO and HC levels can be controlled to relatively high levels and thus provide synergies for aftertreatment regeneration. It is also possible to control the HC and CO levels to lower levels via engine control strategies. The data shown in Figures 2.4 and 2.5 were generated on the DELTA engine. Similar behavior was also seen in the 1.5L HEV engine.

CLEAN Combustion<sup>®</sup> also provides favorable engine out NO<sub>2</sub>/NOx ratios, compared to conventional combustion. Figure 2.6 shows the NO<sub>2</sub> formation as a function of BMEP for both conventional combustion and CLEAN Combustion<sup>®</sup>. The results obtained for conventional combustion agree well with the results available in literature. The increased NO<sub>2</sub> formation in CLEAN Combustion<sup>®</sup> is beneficial for passive CSF regeneration as well as SCR and LNT performance. If engine out NO<sub>2</sub> is not high enough, precious metals are typically used in aftertreatment catalysts to enhance NO to NO<sub>2</sub> conversion. CLEAN Combustion<sup>®</sup> offers potential to reduce precious metal cost of aftertreatment devices by providing high engine out NO<sub>2</sub> concentrations.

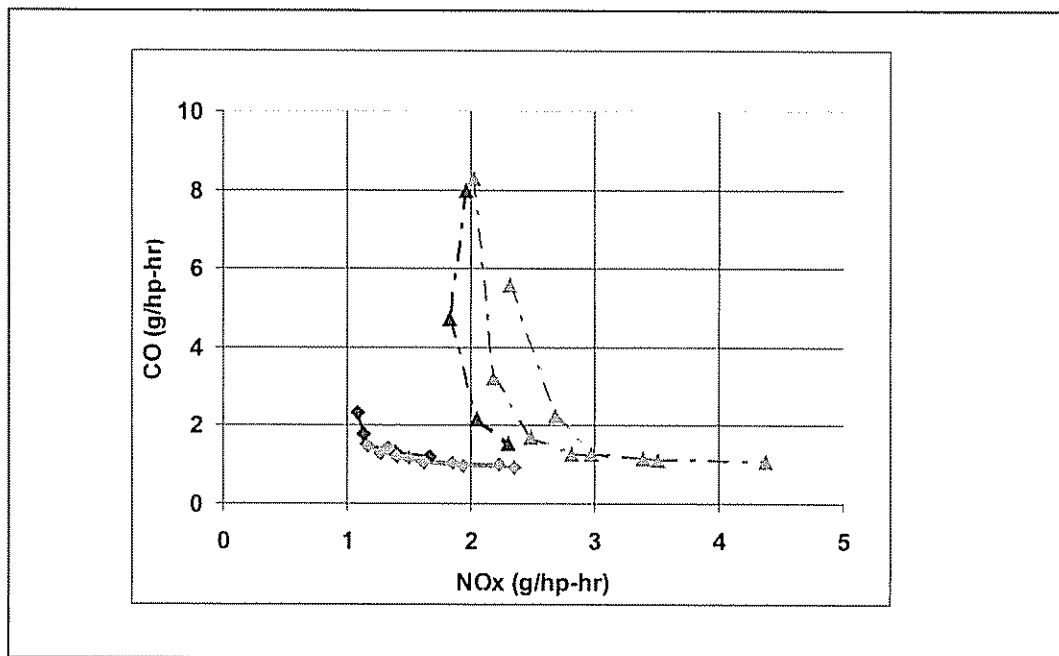


Figure 2.4 Controllable CO Emissions Produced by CLEAN Combustion<sup>®</sup>

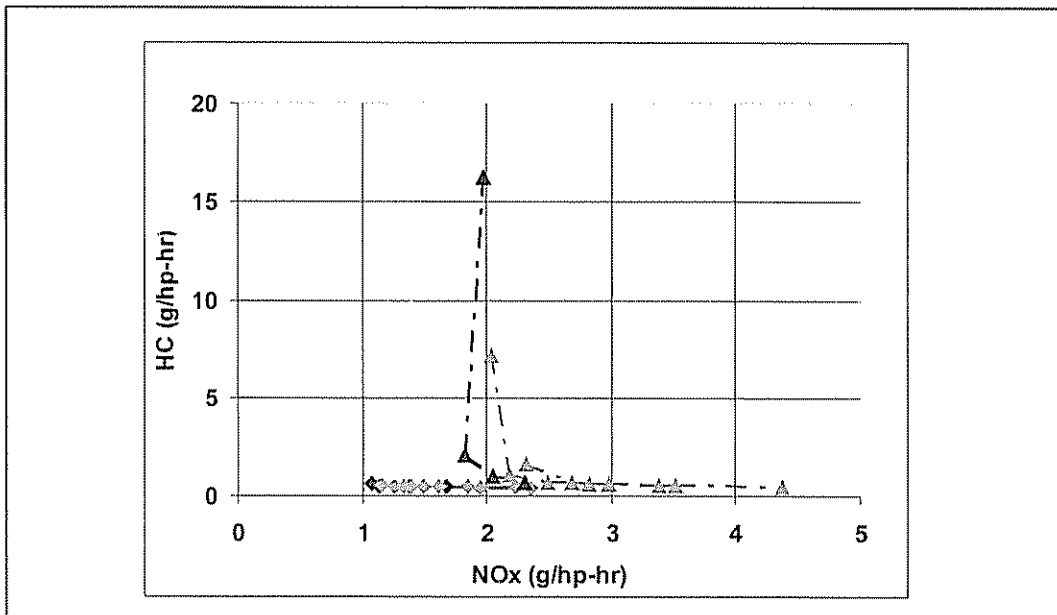


Figure 2.5 Controllable HC Emissions Produced by CLEAN Combustion®

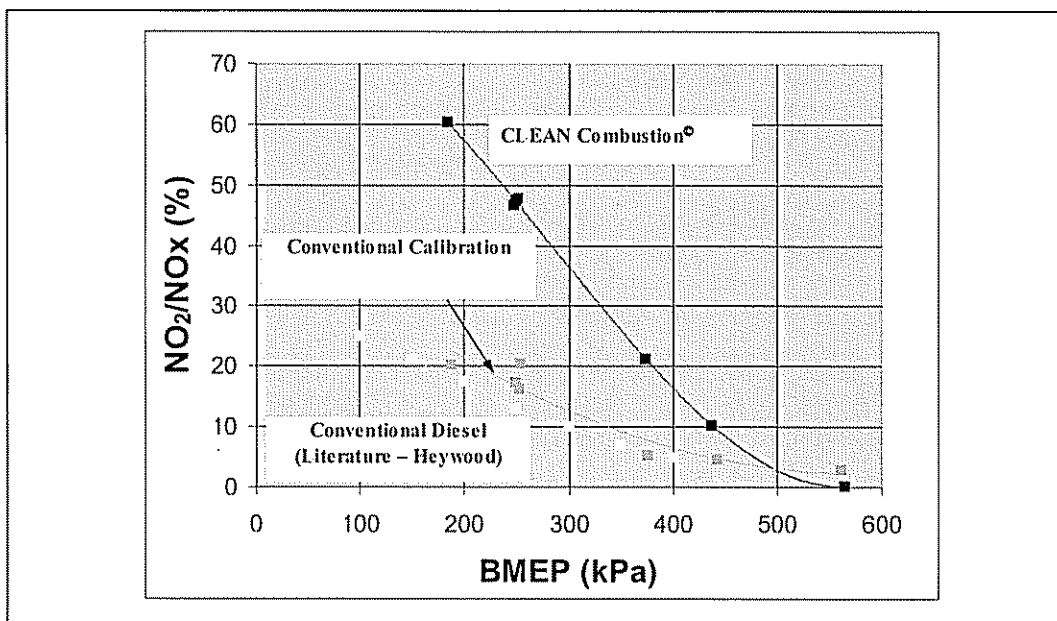


Figure 2.6 High Engine Out NO<sub>2</sub>/NOx Ratios Due to CLEAN Combustion®

CLEAN Combustion® also offers the ability to raise exhaust temperature by about 50°C. This increase in temperature, coupled with the exhaust species management strategy described above, is an ideal platform for synergistic engine and aftertreatment integration.

## Task 2.2 Air Management Development

Another critical technology development area is air system management to provide favorable exhaust temperatures for LNT or CSF regeneration. Air management strategies developed in this program primarily focused on the DELTA engine. These include air by-pass, post in-cylinder injection and a combination of the two to achieve favorable exhaust temperature conditions. The air by-pass system utilized a by-pass pipe between the compressor inlet and the intercooler outlet. A valve was used to control the amount of the by-pass flow depending on the operating conditions. In order to quantify the potential of the air by-pass system, seven modes were selected, as shown in Figure 2.7. The emphasis was on light load conditions, which are critical conditions for LNT or CSF regeneration due to their low exhaust temperature.

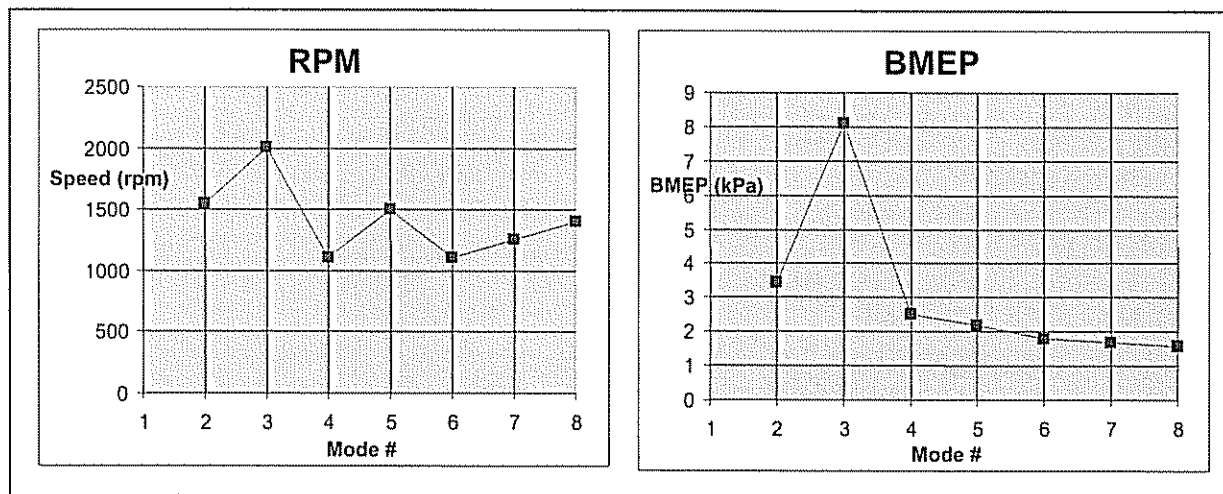


Figure 2.7 Seven Selected Modes for Air Management Strategy Development

Figure 2.8 compares the air/fuel ratio for the different strategies over the seven operating modes, while Figure 2.9 compares the corresponding exhaust temperatures at the turbine outlet. The use of air by-pass was found to be effective in reducing the air/fuel ratio and increasing the exhaust temperature for the operating modes under investigation. Combination of air by-pass and post in-cylinder injection results in a further increase in exhaust temperatures for Modes 2 through 4, but interestingly the temperature decreases for Modes 5 through 8. The reason for this is not entirely clear, but it may be attributed to over-injection of the fuel during the post injection process, which may cool down the exhaust flow. This indicates the potential opportunity to further optimize the in-cylinder post injection event, since, in theory, the post injection process is expected to increase the exhaust temperatures.

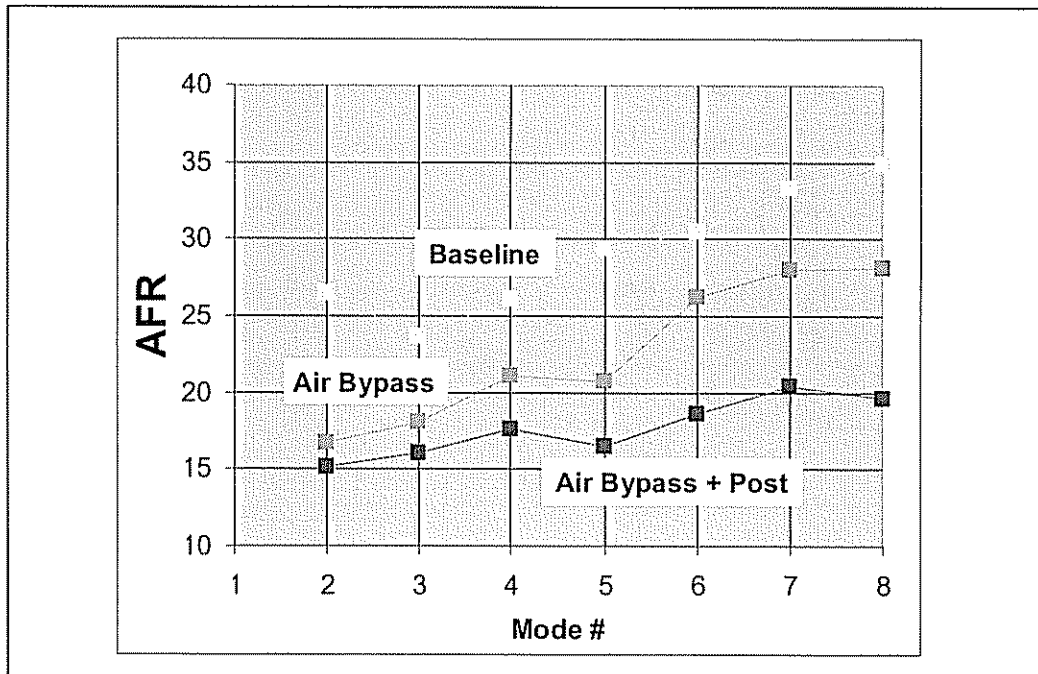


Figure 2.8 Air Fuel Ratio Comparisons Using Different Air Management Strategies

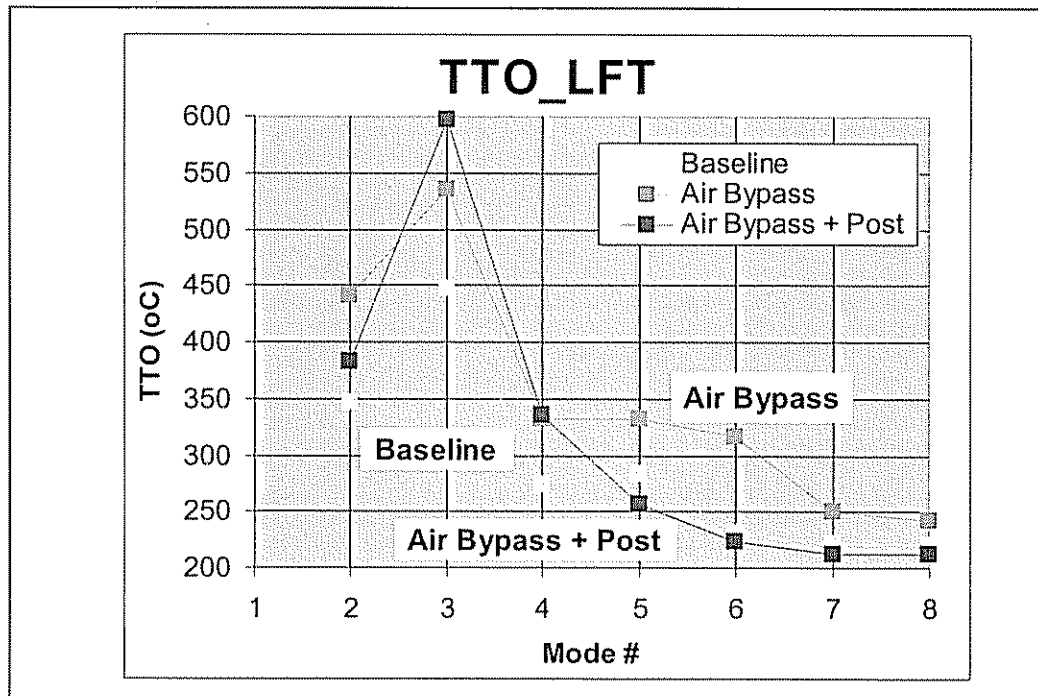


Figure 2.9 Turbine-Out Exhaust Temperature Comparisons with Different Air Management Strategies

### Task 3 Aftertreatment System Development and Integration for a Neon Passenger Car

This task will report on the chassis dynamometer testing and development conducted with a Dodge Neon which served as a mule vehicle to simulate a 2250-lb PNGV-type vehicle. A detailed description of this PNGV mule vehicle can be seen in Appendix 3. The vehicle was equipped with a 1.5 liter high speed direct injection (HSDI) diesel engine as shown in Figure 2.1, a catalyzed soot filter (CSF) and a urea-based selective catalytic reduction (SCR) device. The vehicle was tested over different test cycles including Federal Test Procedure 75 (FTP75), Hot 505 (H-505), and Highway Fuel Economy (HWYFE). The cycle descriptions are given in Appendix 4.

#### Task 3.1 Test Preparation

In addition to the aftertreatment systems, the vehicle was equipped with insulated exhaust pipes (Figure 3.1). These tests were conducted in the December 2001 – January 2002 time frame. A low sulfur fuel, with a maximum sulfur content of 10 ppm, was used for this testing. Additional properties of the low sulfur fuel are listed in Table 3.1. Urea was injected through a pre-prototype urea system provided by Engelhard and modified by DDC (Figure 1.2.4). This urea dosing system was developed to enable the testing of the urea SCR fairly early in the LEADER program. The vehicle test set-up is shown in Figure 3.2. Ammonia slip was measured by utilizing wet chemistry on samples collected from the diluted exhaust. Additional information on the vehicle set up can be viewed in Appendix 5.

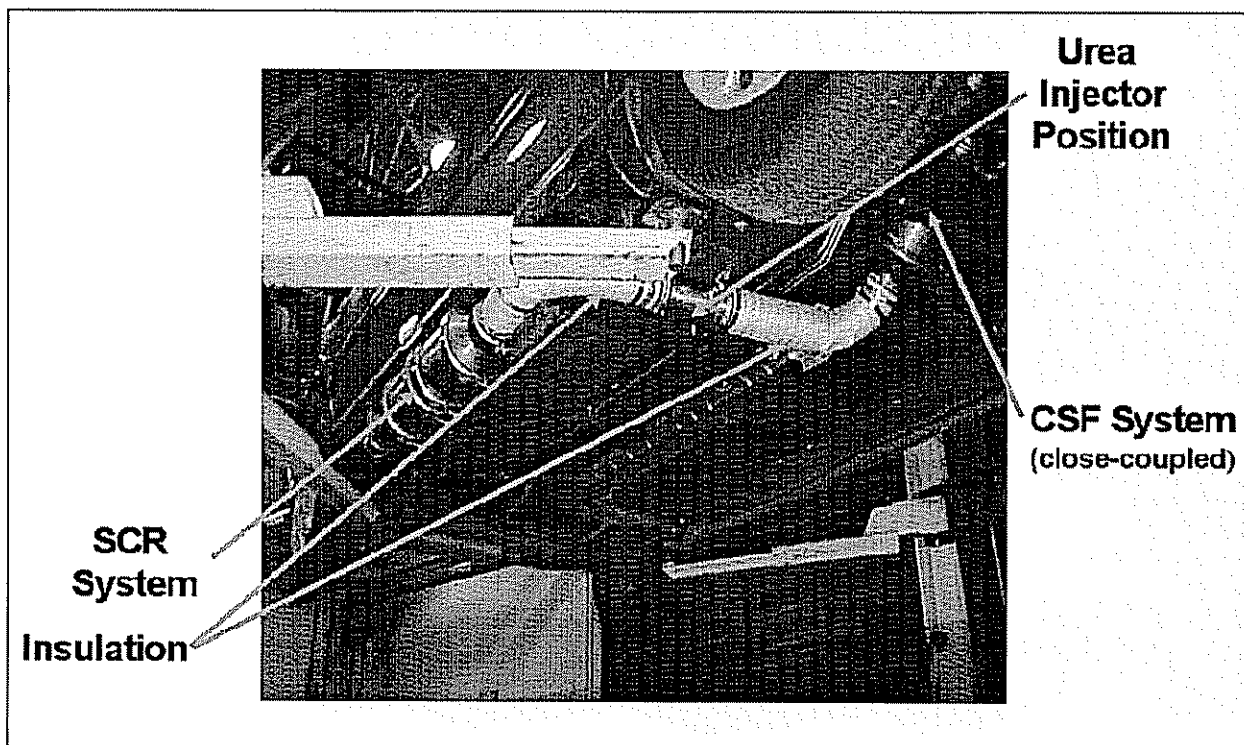
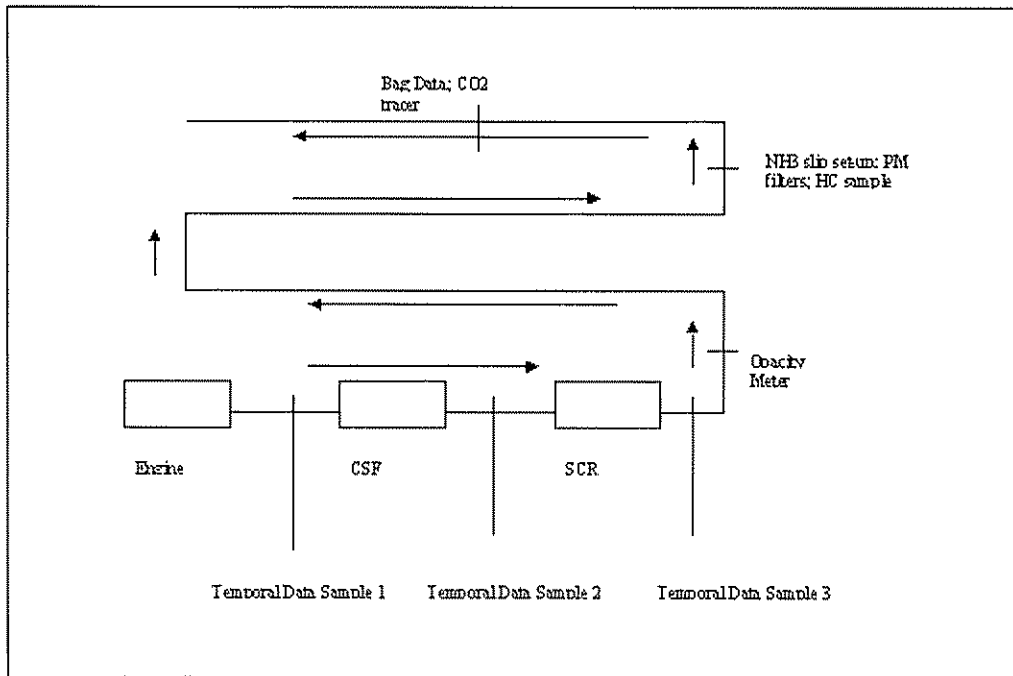


Figure 3.1 Dodge Neon CSF-SCR Exhaust Aftertreatment System



**Figure 3.2 Schematic of the Vehicle Test Set-Up**

**Table 3.1 Low Sulfur Fuel Properties**

<b>Sulfur</b>	<b>&lt;10 ppmw</b>
<b>Aromatics</b>	<b>&lt;10 %v</b>
<b>PNA</b>	<b>0.5</b>
<b>Natural Cetane Number</b>	<b>60</b>
<b>Nitrogen</b>	<b>5 ppmw</b>
<b>API Gravity</b>	<b>37-42</b>
<b>Distillation IBP (D-86)</b>	<b>375°F</b>
<b>Cloud Point</b>	<b>32°F</b>

### **Task 3.2 Vehicle Test Results**

One of the key deliverables of the LEADER program was to demonstrate Tier 2 Bin 5 emissions levels using an integrated engine and aftertreatment system. Appendix 6 describes the Tier 2 emissions regulations which are being phased in since 2004. During the course of the program, Tier 2 Bin 3 emissions levels were demonstrated for both the mule PNGV vehicle and the LD truck platform. Several of these results have also been reported in the past in various DOE-

sponsored DEER Conferences<sup>11,12</sup>. Figure 3.3 represents a summary of the Tier 2 emissions milestones achieved with the 2250-lb Dodge Neon vehicle over the FTP75 test cycle. The aggressive Tier 2 Bin 3 emissions levels were obtained with no NH<sub>3</sub> slip and a combined fuel economy of 63 miles per gallon, integrating FTP75 and highway fuel economy cycle test results.

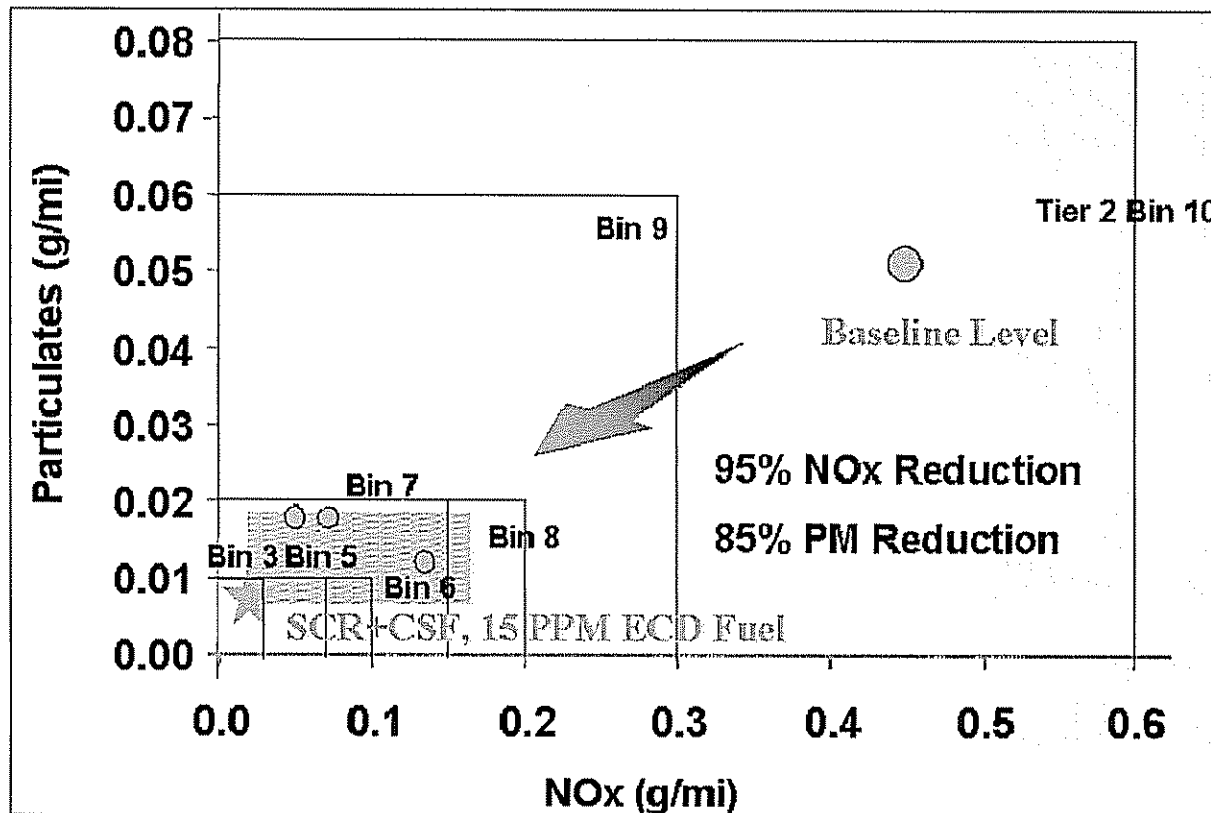


Figure 3.3 FTP75 Emissions Milestones for the PNGV Mule Vehicle

Figure 3.4 shows the combined city and highway fuel economy versus FTP75 tailpipe out NOx emissions for several data-sets. The data obtained in August 2001 is shown in blue and that obtained in January 2002 is shown in red. These results show that, depending on the maturity of the engine and aftertreatment calibration, reducing NOx is not necessarily combined with a fuel economy penalty. The fuel economy can be selectively recovered by calibration refinement. There is further potential to improve fuel economy and maintain or even enhance the miles-per-gallon advantage of diesel-powered vehicles over their gasoline counterparts while meeting Tier 2 emissions.

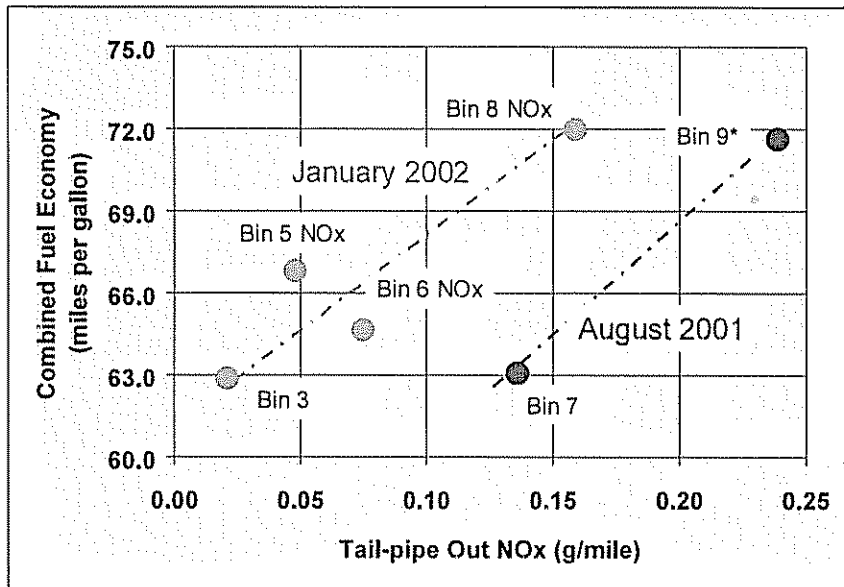


Figure 3.4 Combined Fuel Economy for Tier 2 Emissions Milestones

Figure 3.5 shows the tailpipe out NOx (g/mile) versus engine out NOx (g/mile) for the FTP75 milestone results. These results highlight the importance of sub-system optimization and system integration to achieve the aggressive Bin 3 results. Compared to the Bin 9 data-set, the Bin 3 data-set represents nearly 50% reduction in engine out emissions. This was primarily achieved via advanced combustion strategies as described earlier. The Bin 3 data-set represents an aftertreatment NOx reduction efficiency of about 90% compared to about 35% for the Bin 9 results. Incremental improvements in the aftertreatment system efficiency applied to the Bin 6 results yielded Bin 3 emissions levels, for the same engine out NOx level. The NOx reduction efficiency of the aftertreatment system and the SCR inlet temperature levels for these data points are shown in Figures 3.6 and 3.7, respectively.

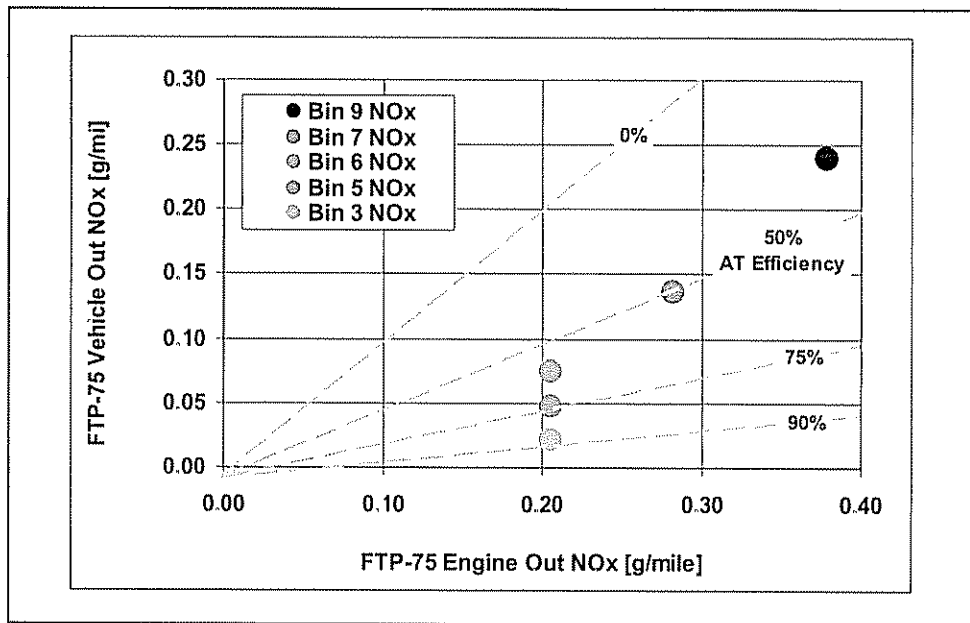


Figure 3.5 FTP75 Vehicle Out NOx versus Engine Out NOx

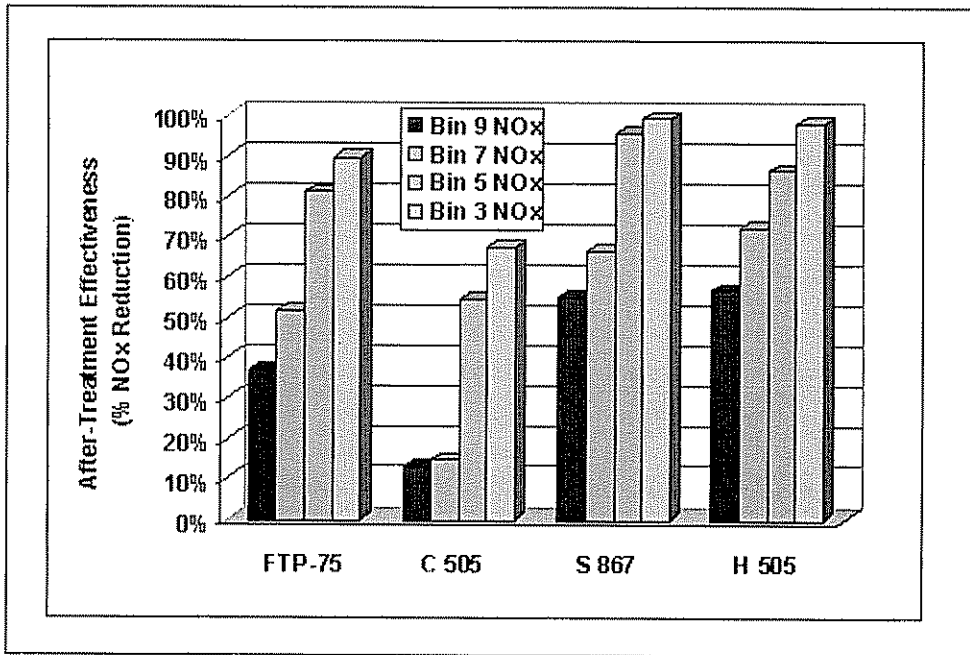


Figure 3.6 Aftertreatment Effectiveness During FTP75

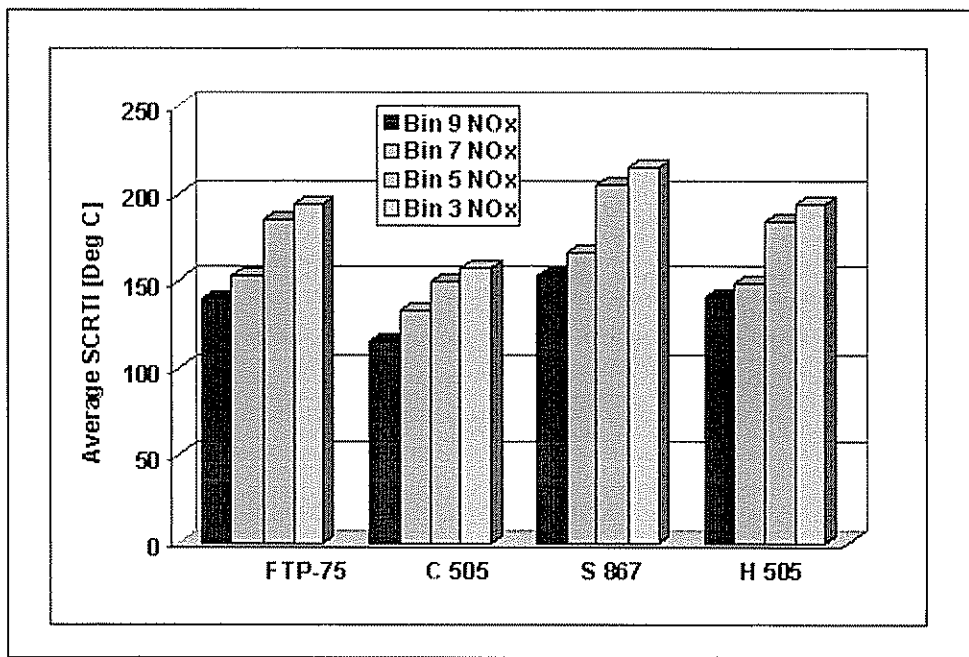


Figure 3.7 Average SCR Inlet Temperature During FTP75

Figure 3.8 shows the vehicle testing results for the highway fuel economy cycle. Impressively, a fuel economy of about 95 miles per gallon was obtained over the highway fuel economy cycle for the relatively light PNGV mule vehicle. The cycle description can be seen in Appendix 4.

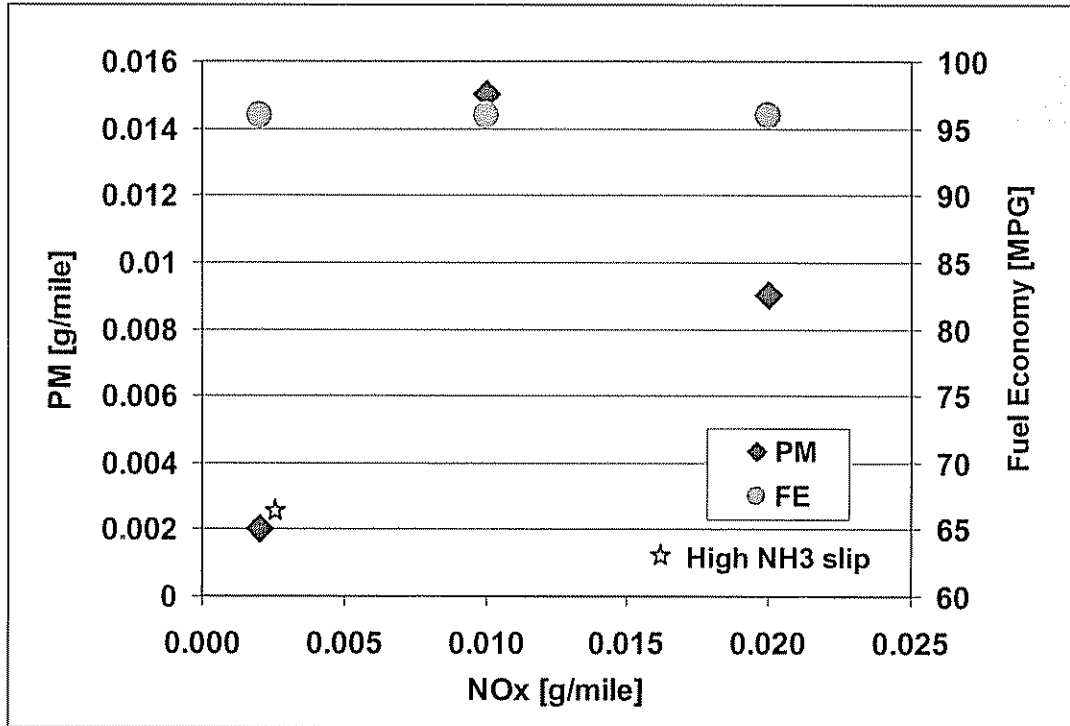


Figure 3.8 NOx, PM, MPG for Highway Fuel Economy Test Cycle

A significant contributing factor in improving the NOx reduction efficiency of the SCR device to about 90% levels was the development and application of a sophisticated urea injection control strategy that also accounts for the NH<sub>3</sub> stored on the SCR device. This control strategy development was accomplished by utilizing the 1D SCR analytical model developed under the LEADER program.

Figure 3.9 shows several SCR out NOx emission traces over a typical Hot 505 transient cycle for the same engine out NOx trace. In addition to the baseline SCR out NOx trace, two additional NOx traces (denoted by X and Y) are shown. These two NOx traces correspond to different control strategies. Both of the control strategies are effective in significantly reducing the tailpipe out NOx emissions compared to the baseline, while maintaining acceptable NH<sub>3</sub> slip levels.

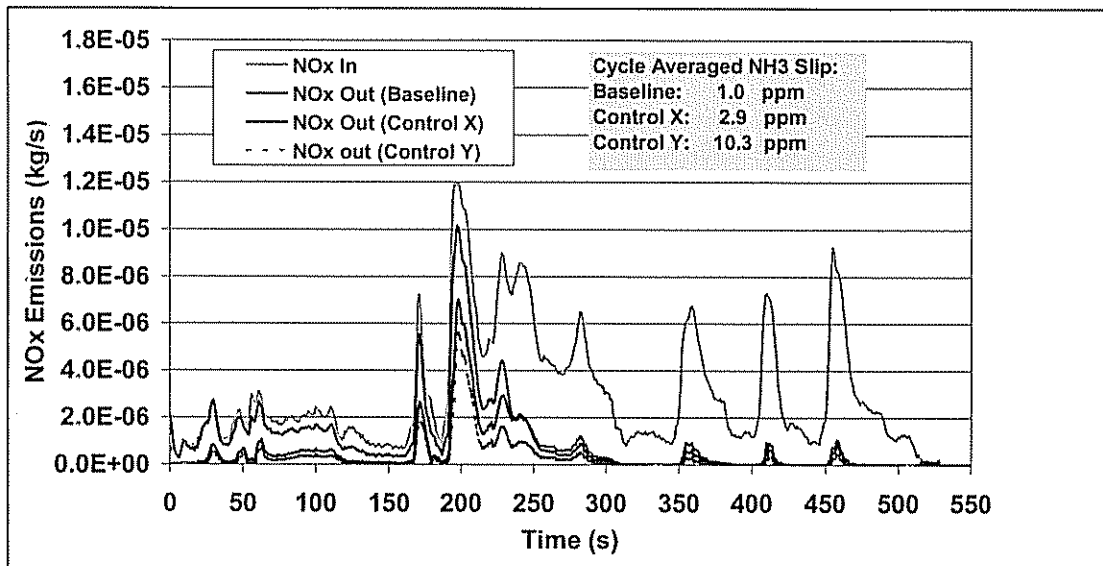


Figure 3.9 Urea Control Strategy Development over Hot 505 Transient Cycle Using 1D SCR Model

The analytical tool is effective in exploring various control strategies and identifying the trade-off between NOx reduction efficiency and NH<sub>3</sub> slip as shown in Figure 3.10. This is a powerful development tool and identifies an optimization area for the development to focus on for further refinement.

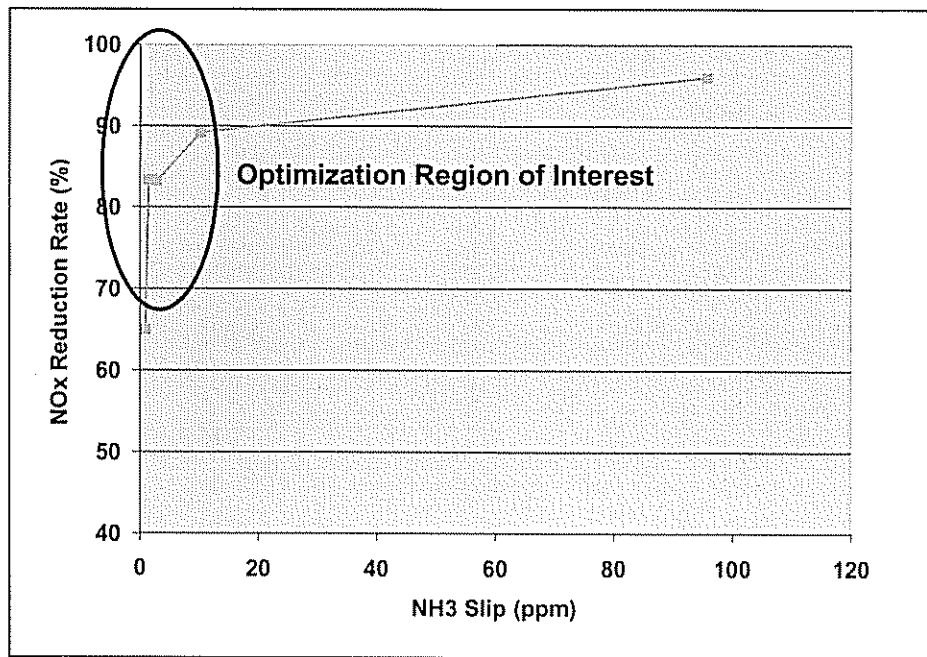


Figure 3.10 NOx Reduction and NH<sub>3</sub> Slip Trade-Off Identified via the Analytical Tool

These results, as shown in Figures 3.9 and 3.10, laid a strong foundation for the Tier 2 Bin 3 emissions demonstration. Figure 3.11 shows the cumulative NOx emissions obtained on a vehicle chassis dynamometer for the Tier 2 Bin 5 and Tier 2 Bin 3 results. The control strategies used for these two data-sets are denoted as X' and Y', respectively, and are based on the control strategies developed via the analytical tool.

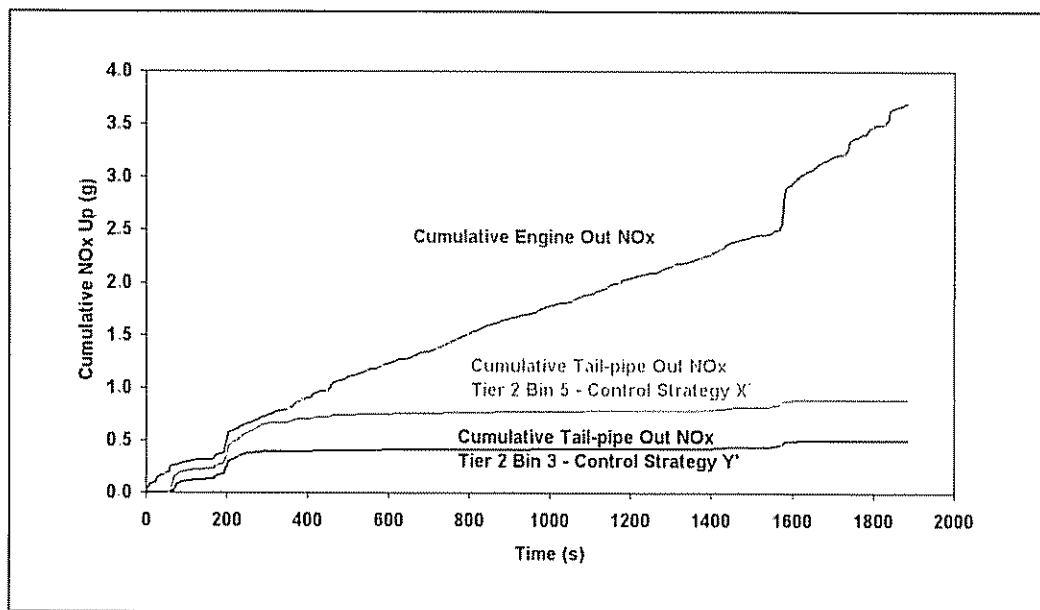


Figure 3.11 Experimental Validation of the Urea Injection Control Strategy Development

### Task 3.3 Data Repeatability

A significant challenge during the course of this program was to ensure accurate tailpipe out emissions measurement at the very low Tier 2 Bin 5 emissions levels. This is particularly true for PM measurements. Figure 3.12 shows the amount of scatter in typical PM filter data (total, primary and secondary) over the Hot 505 cycle. This scatter is significantly larger than the industry standard of about 5%. As the data (NOx and/or PM) approaches zero, the variation becomes large. Today's methods for measuring NOx and PM appear insufficient to provide the measurement accuracy required for the Tier 2 Bin 5 and below emissions levels. Without some improved method, engineering development targets would be forced to focus on zero system out emissions to ensure that the "production solution" variation would fall below the emission limits.

Figure 3.13 shows the mean PM filter loading levels (total, primary and secondary) over typical Hot 505 runs. The secondary filter has deposits of only single digit micrograms. This is more than 100 times lower than the minimum desired loading level of 1 mg. While the loading on the primary soot filter is approximately 100  $\mu\text{g}$ , it still is 10 times lower than the minimum desired mass deposit. As a result of the small loading levels, the variability or standard deviation over mean value becomes much larger than the standard industry acceptance of 5%.

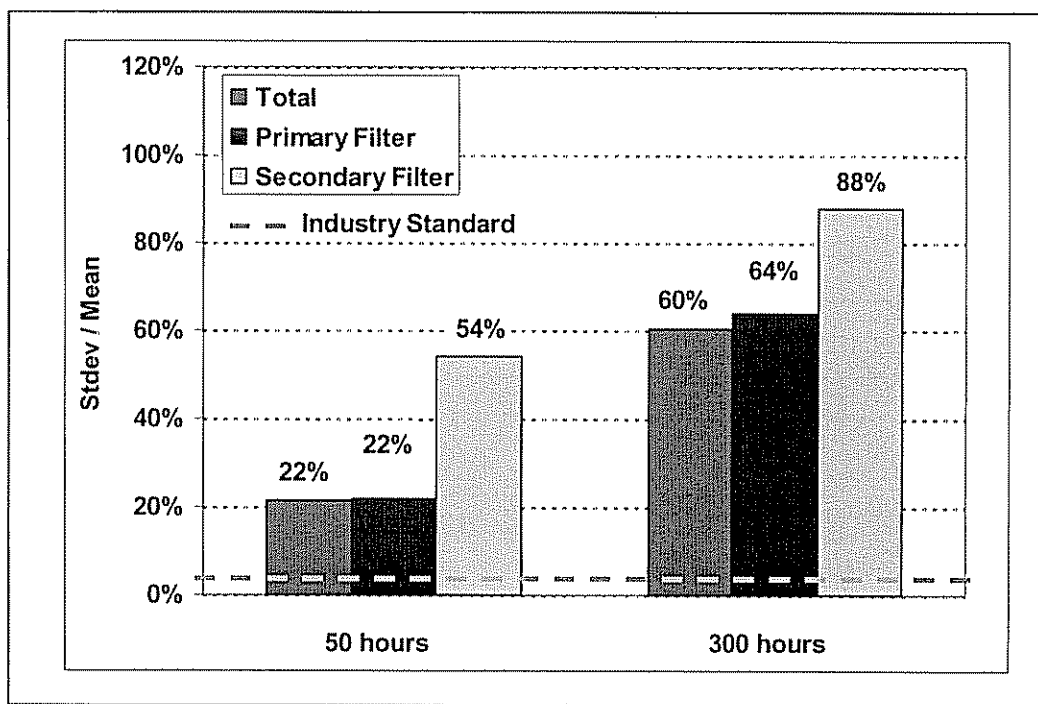


Figure 3.12 PM Loading Standard Deviation Over Mean Value, Hot 505

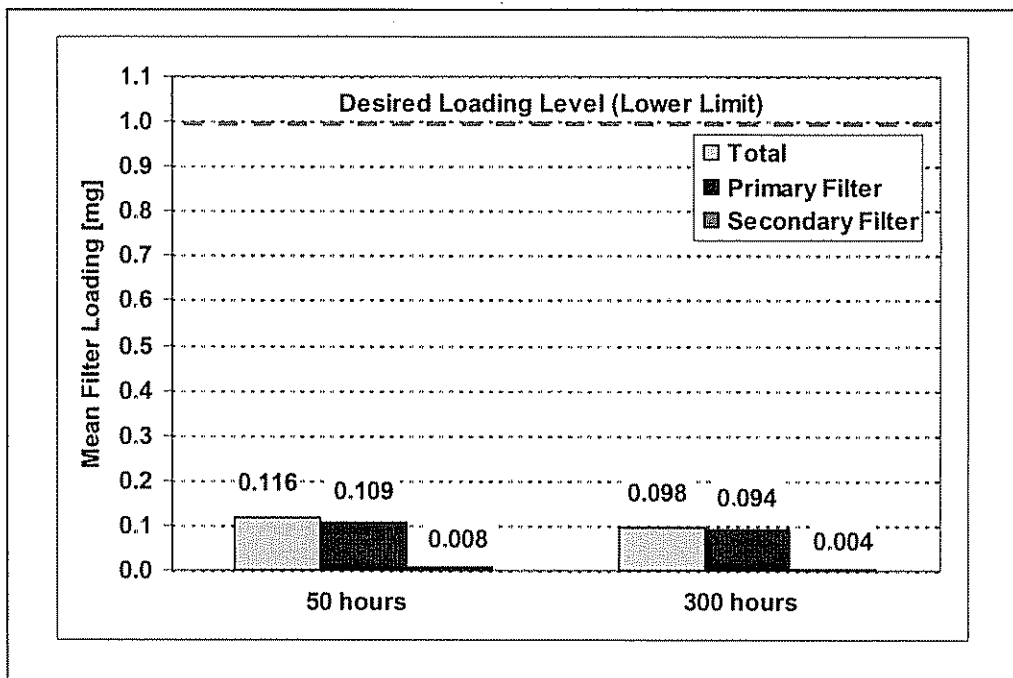


Figure 3.13 Mean Filter Mass Loading, Hot 505

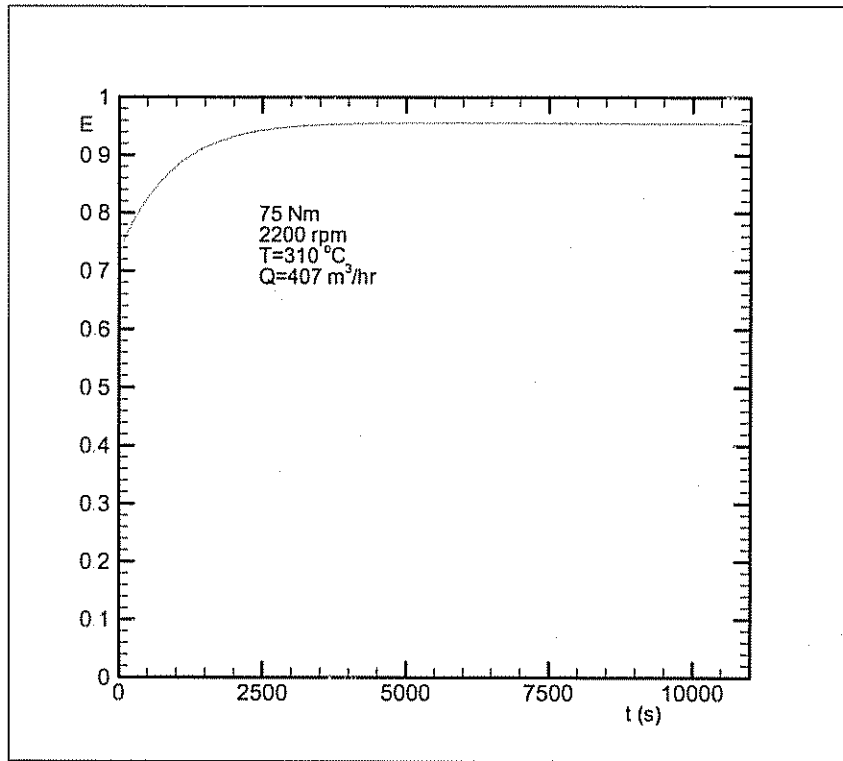
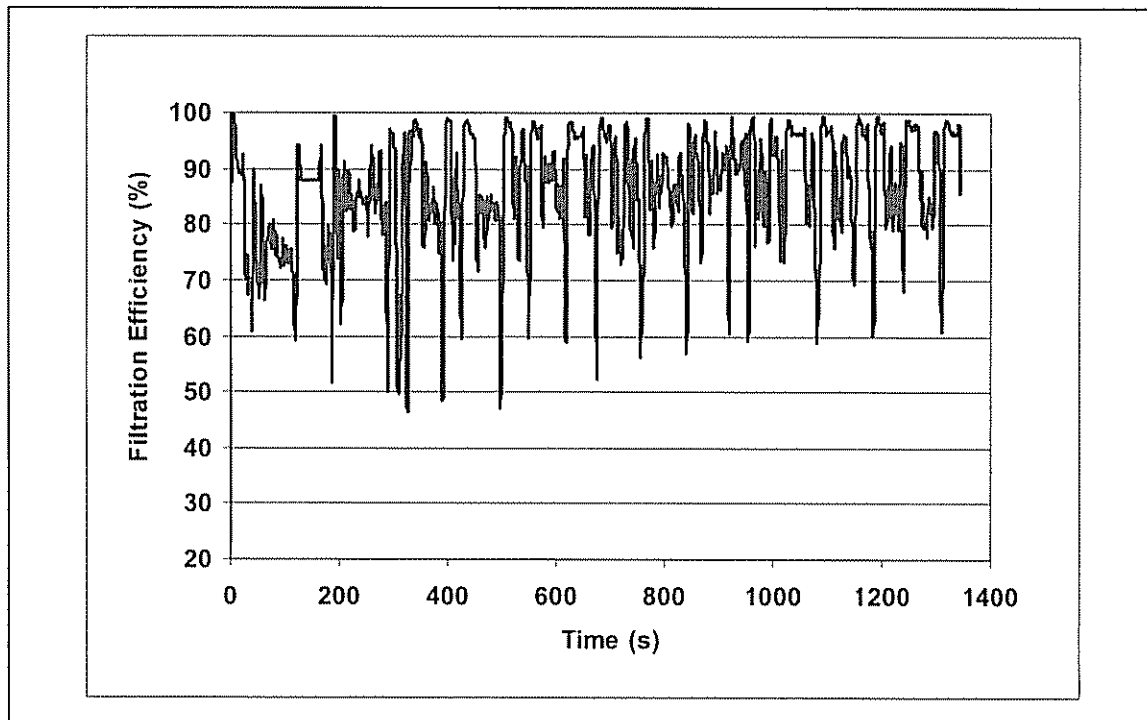


Figure 3.14 Simulated CSF Filtration Efficiency During Particulate Loading

Figure 3.14 illustrates CSF simulation model prediction of the relationship between CSF filtration efficiency and time, or rather the trapped soot mass, at a steady state operating condition. The PM reduction across the CSF initially increases with increasing particulate loading until it reaches a plateau and stays there until the next regeneration takes place, reducing the soot mass loading. Therefore, at any operating condition, the CSF filtration efficiency varies depending on the trapped soot mass at that moment in time. Figure 3.15 shows a prediction of the CSF soot trapping efficiency over the C-505 and S867 portions of the FTP75 test cycle for a certain initial trapped mass condition. The fluctuation in predicted filtration efficiency is significant and explains the likely source of PM emission variation. The model suggests low transient filtration efficiencies at high exhaust flow conditions, where the engine out soot emission flow rate is high.



**Figure 3.15 Simulation Model-Predicted CSF Filtration Efficiency, C-505 and S867 Portions of FTP75**

#### Task 4 Scalability Confirmation

One of the major tasks in this program was “scalability confirmation”, which involved “scaling up” and application of the 1.5L engine and aftertreatment system technology to the 4.0L engine and aftertreatment system. Consistent with the technology development methodology shown in Figure 0.7, a transient dynamometer test-bed was used extensively to “simulate” vehicle chassis dynamometer test cycles. This systematic approach shortened the development cycle considerably and thus reduced cost by ensuring that the vehicle goals were met nearly “out-of-

the-box", due to the strong foundation established by the analytical and experimental results, and particularly the transient dynamometer test-bed results.

#### Task 4.1 Simulated Vehicle Tests in a Transient Engine Testing Cell

This task involved extensive calibration development utilizing different engine and aftertreatment strategies. In this development work, an integrated SCR + CSF system was used to carry out the performance tests and catalyst characterization. A dual leg SCR/CSF system was used to maximize performance, taking advantage of the Vee engine configuration, where a dual exhaust manifold with twin-turbochargers was used. In this transient engine testing cell, the wet chemistry method was used to measure ammonia slip.

Figure 4.1 shows several emissions data-sets obtained over the Hot 505 cycle during the course of development. The data points shown within the oval were obtained with no  $\text{NH}_3$  slip. This effort was beneficial in identifying a technical road-map for transient emissions development and in down-selecting strategies for vehicle tests.

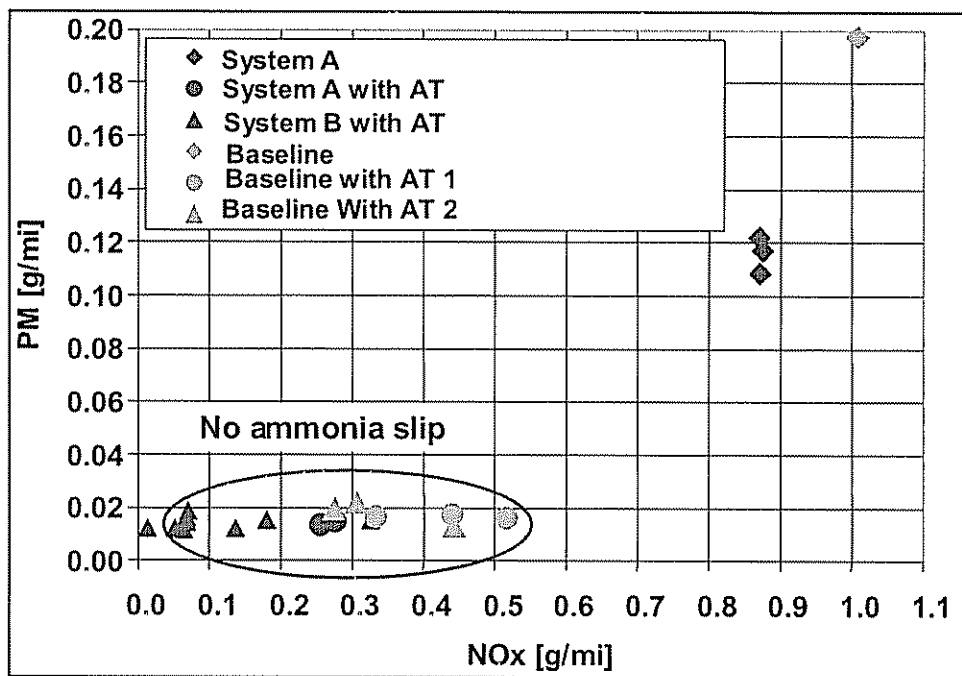


Figure 4.1 Simulated Hot 505 Cycle for Optimization of Different Calibration Packages

Figure 4.2 summarizes the technical path that evolved during the course of the program. This included systematic development of in-cylinder combustion, aftertreatment system and urea injection optimization.

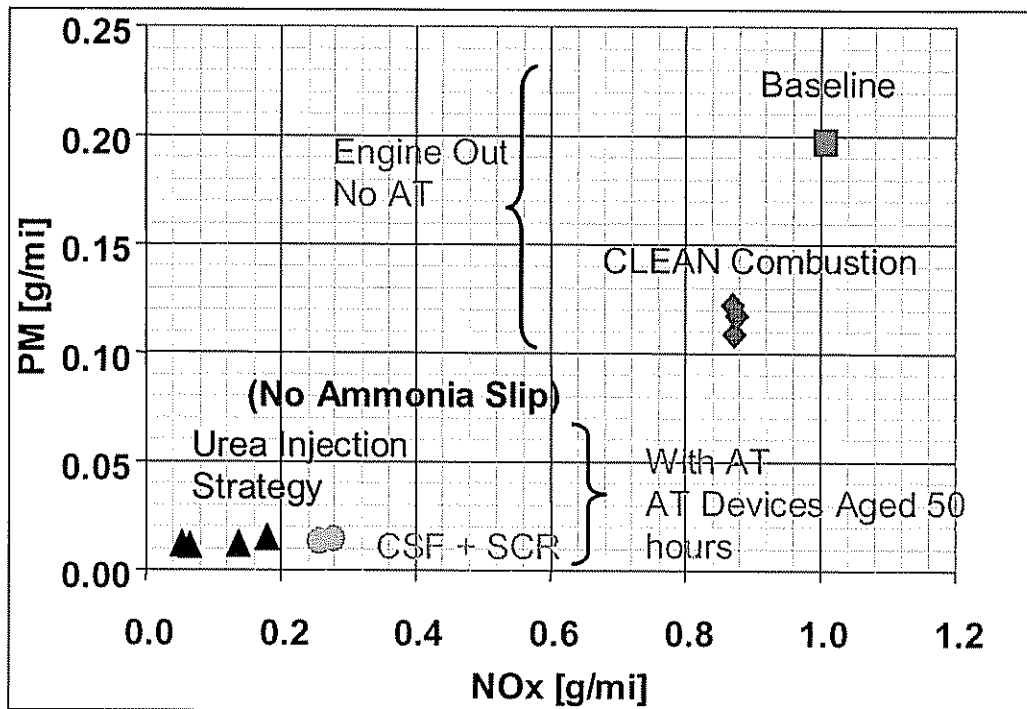


Figure 4.2 Calibration Strategy Development Path in a Transient Engine Testing Cell

#### Task 4.2 Vehicle Tests

A 2001 Dakota Quad Cap Sport 4x2 vehicle was selected as the vehicle test-bed for the program. A picture of the vehicle is shown in Figure 4.3. A 4.0L DELTA engine was used to replace the stock gasoline engine. A dual leg SCR and CSF aftertreatment system was used for this task. Figure 4.4 shows the layout of the aftertreatment system.

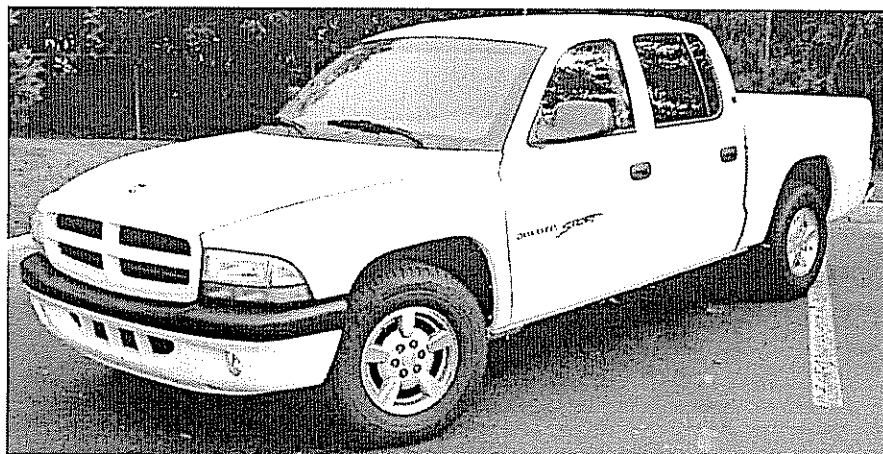


Figure 4.3 2001 Dakota Quad Cap Sport 4x2 Vehicle

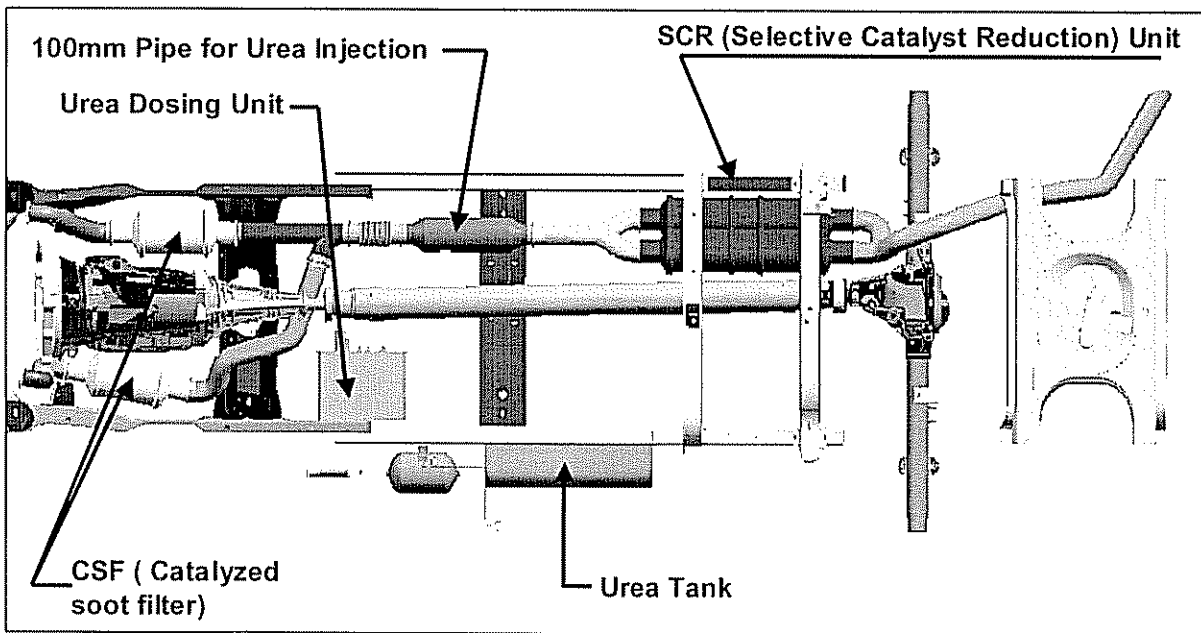


Figure 4.4 CSF and SCR System Layout in the Dakota Vehicle

In the first set of vehicle tests, Tier 2 Bin 6 emissions levels were obtained as shown in Figure 4.5. These results were obtained with a 45% fuel economy improvement compared to the gasoline engine baseline. Through the iterative development process and incremental improvements in engine and aftertreatment system calibration, near-Bin 9 emissions levels were obtained without the use of any active aftertreatment devices (Figure 4.6). Figure 4.7 shows the Tier 2 Bin 3 emissions results that were subsequently demonstrated. This aggressive reduction in tailpipe out emissions was achieved with no ammonia slip and a 41% fuel economy improvement, compared to the equivalent gasoline engine-equipped vehicle. Tier 2 Bin 3 emissions were demonstrated earlier on a PNGV-type mule passenger car application as shown in the description of Task 3.2.

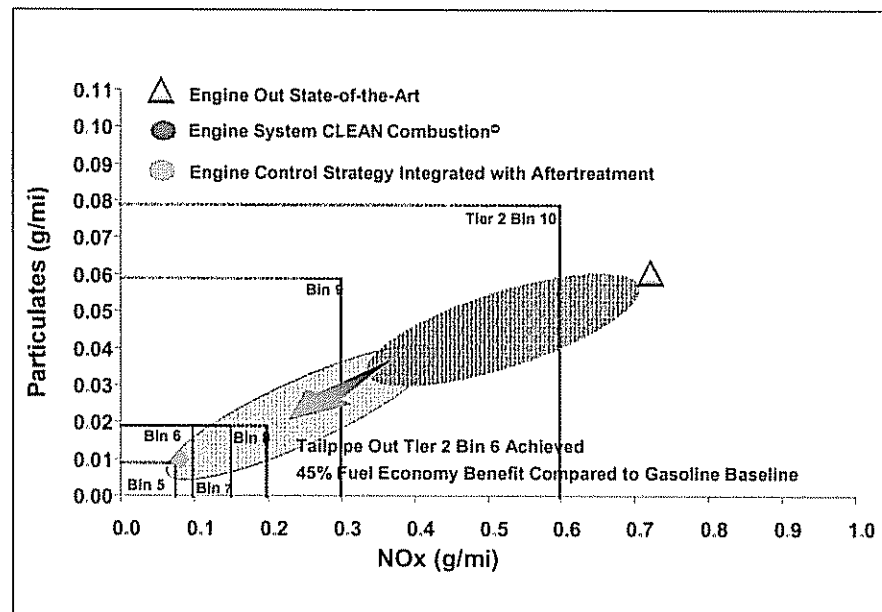


Figure 4.5 Light Truck Chassis Dynamometer Results (Bin 6)

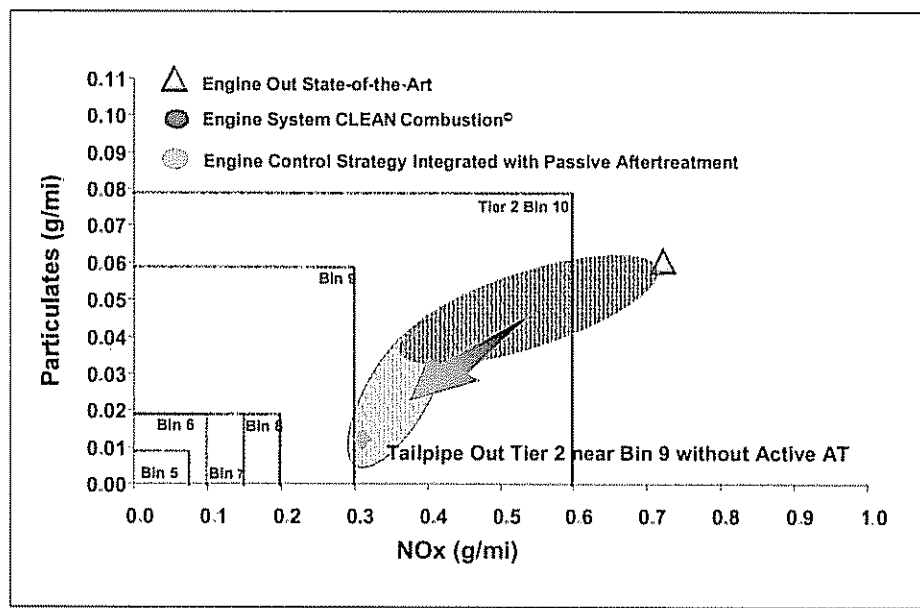


Figure 4.6 Light Truck Chassis Dynamometer Results (Near Tier 2 Bin 9 without Active AT)

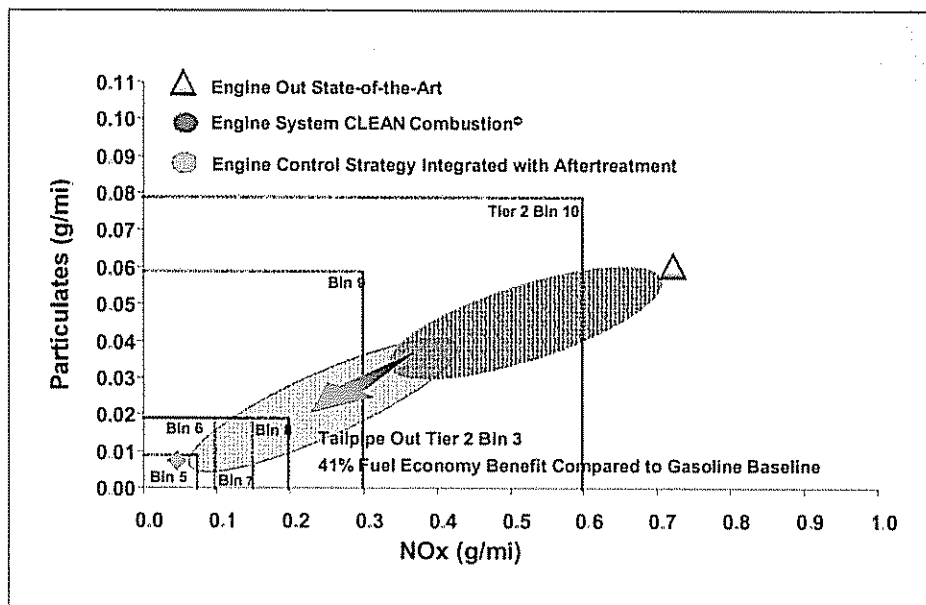


Figure 4.7 Light Truck Chassis Dynamometer Results (Tier 2 Bin 3)

#### IV. DEVELOPMENT CHALLENGES

The LEADER program has successfully demonstrated the aggressive performance and emissions targets for both the passenger car as well as the LD truck platform. However, significant challenges still remain, especially pertaining to product development targeting eventual commercialization of such technologies. Some of the key challenges are listed below:

- CSF Regeneration control strategy
- Packaging
- System simplification
- Integration of vehicle, engine, and aftertreatment
- Ash loading and cleaning
- Virtual lab applications

Figure 5.1 shows the impact of CSF regeneration frequency on fuel economy (MPG). It appears that the regeneration frequency is related to initial PM loading, catalytic material, regeneration schemes, and trap size and geometry (cell density, ratio of length and volume, pore size and wall thickness, etc.). Significant development effort is required to establish a robust regeneration control strategy that optimizes system performance to mitigate the fuel economy penalty over a range of driving conditions.

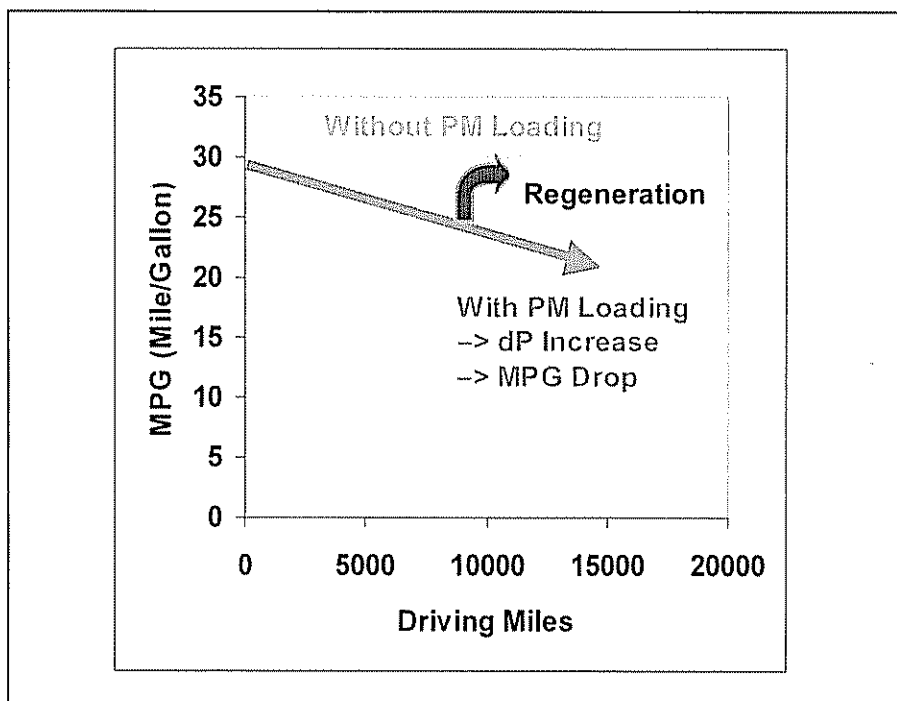
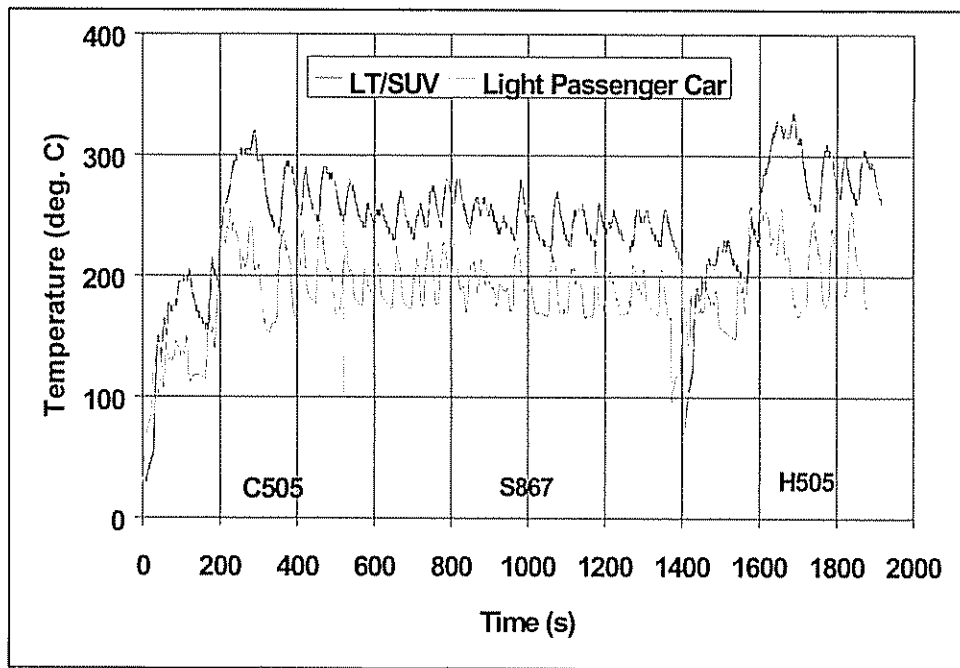


Figure 5.1 Impact of CSF Regeneration Frequency on Fuel Economy

Low exhaust temperatures, particularly during vehicle warm-up periods, present a substantial challenge for CSF regeneration in LD applications, and specifically for passenger cars. Figure 5.2 shows the temperature traces for LT/SUV and passenger car applications over the FTP75 test cycle. It can be seen that the passenger car exhaust temperature is in the range of 200°C for the majority of the operating period. This temperature is below the light off temperature for a typical DOC. The exhaust temperatures are much lower during the warm up period before 200 seconds.



**Figure 5.2 Temperature Profiles for LT/SUV and Passenger Car Applications over FTP75 Cycle**

These low exhaust temperatures render passive CSF regeneration nearly impossible. Figure 5.3 shows the soot balance inside a filter, including soot oxidation and trapped soot for a typical FTP75 cycle. These results were obtained utilizing DDC's proprietary CSF model and show nearly zero oxidation rate of soot due to the extremely low exhaust temperatures. This suggests the necessity to use active regeneration at the expense of system cost and control strategy complication. Alternative, though also challenging, approaches would be to develop engine management strategies to increase the exhaust temperatures or to develop catalyst technologies that are effective at lower temperatures. DDC's CLEAN Combustion® technology is one example of an engine-based strategy that increases the exhaust temperature by about 50°C compared to conventional combustion. However, additional effort is required to develop this temperature management strategy into a production-viable control scheme over a broad range of engine operation conditions without sacrificing fuel economy.

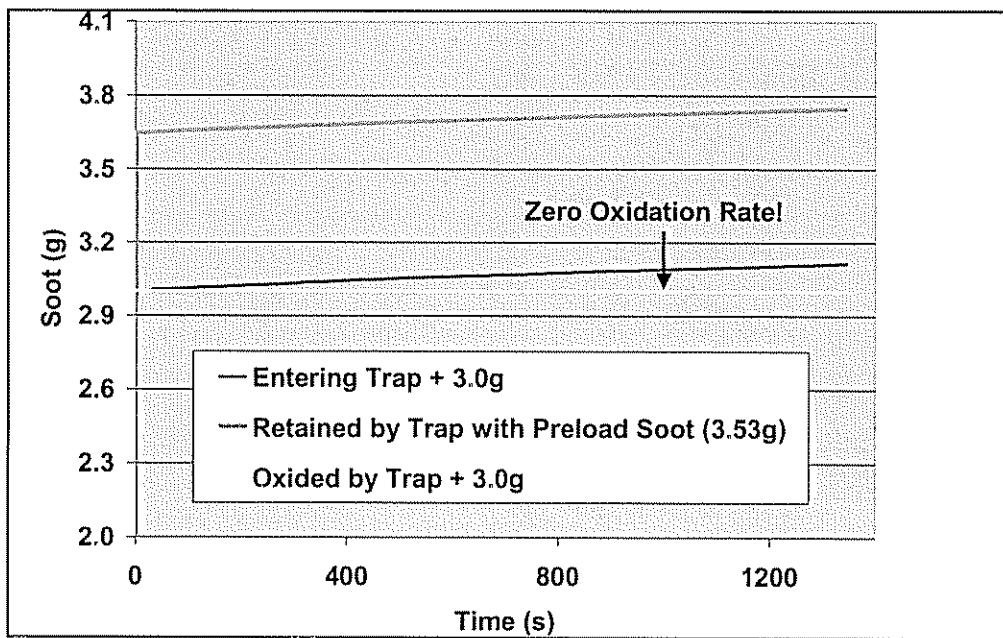


Figure 5.3 Soot Oxidation and Trapped Soot inside a Filter over a FTP75 Cycle

Packaging is a significant challenge for potential commercialization of these technologies, especially when a NOx aftertreatment device must be used in conjunction with a CSF. This is particularly true for passenger car applications. Figure 5.4 shows the pre-prototype SCR and CSF system developed and installed on the Neon vehicle as part of this program. As can be seen, substantial developments are required to reduce the size of the aftertreatment devices for commercial viability.

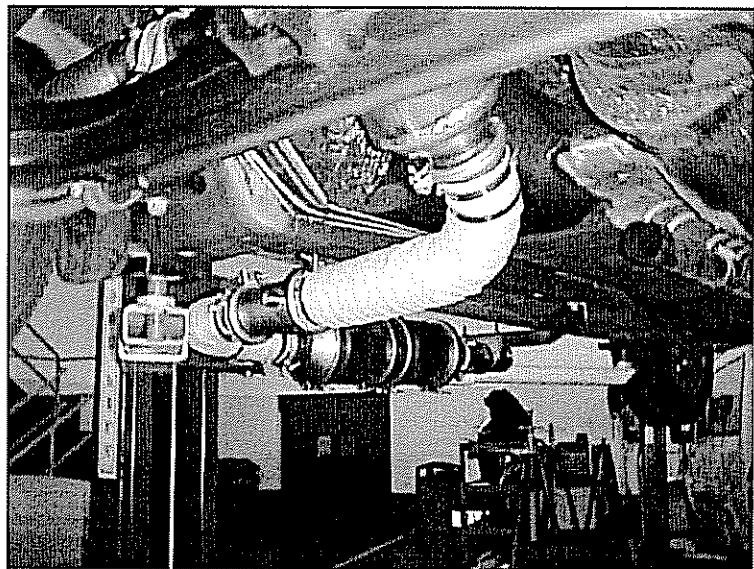
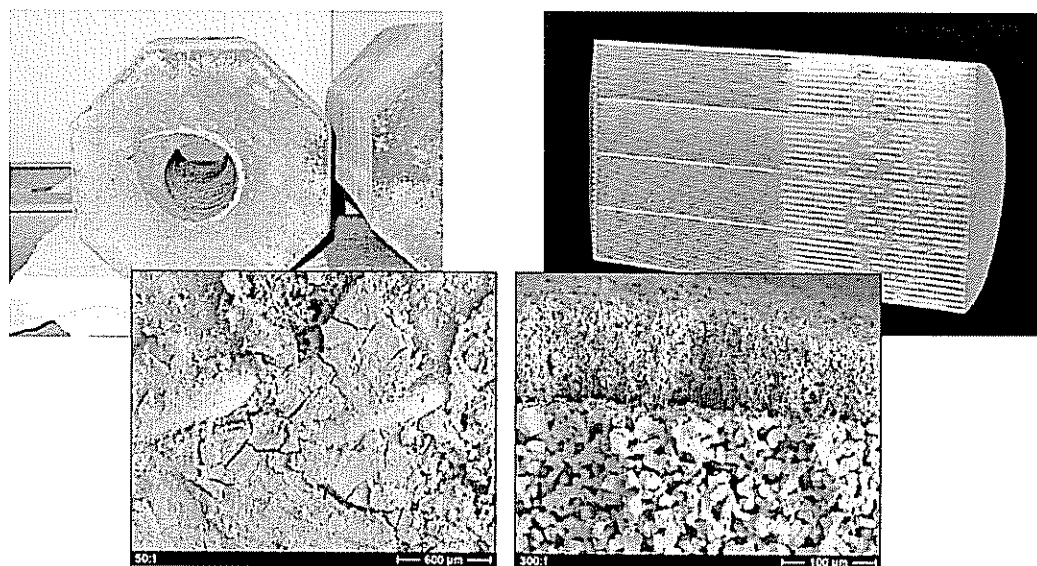


Figure 5.4 Packaging Challenging for Passenger Car Applications with Complicated NOx Aftertreatment and CSF System

Simplification of aftertreatment systems should be a key focus for further development with emphasis on reducing system cost. This requires increased emphasis on integrated engine, aftertreatment and vehicle system development. As described earlier, CLEAN Combustion® technology offers the potential for synergistic integration of the engine and aftertreatment system by controlling the exhaust species and temperatures to favorable conditions. This offers potential reduction in the aftertreatment system precious metal content and cost. Further development should continue to focus on simplification of the aftertreatment system, particularly catalyst volumes and cost.

Ash loading and cleaning is another significant challenge. Figure 5.5 shows a few examples of ash loading in typical filters. The pictures on the left side are for an SMF and the pictures on the right side are for a cordierite filter. The ash load in the cordierite filter occupies half of the filter volume and is likely to result in a significant pressure loss. Figure 5.6 shows the impact of ash loading on pressure loss. The pressure drop increases by 200% when the filter is 50% full of ash and has a soot loading of 6 g/liter.



**Figure 5.5 Ash Loading in Sintered Metal Filter (Left Side) and Cordierite Filter (Right Side)**

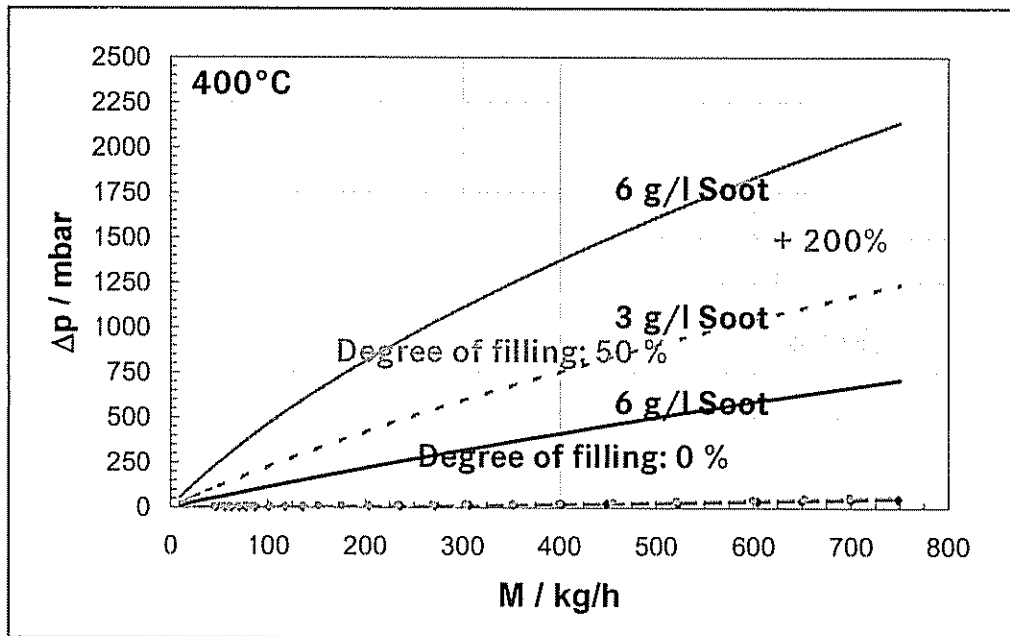


Figure 5.6 Pressure Loss Comparisons for a Filter with Ash Filling from 0% to 50%.

Increasing use of the virtual lab for system integration and its control development will result in a shortened developmental cycle, thus reducing cost. Virtual sensors, if developed and calibrated, would greatly simplify the system, thus reducing material cost. However, modeling maturity is still in question. One of the key issues is the availability of fundamental kinetic data for aftertreatment modeling. Typically, industrial modeling applications use global reaction mechanisms, lumping all unknown factors into an inhibition term. Derivation of a reliable global reaction mechanism with high fidelity requires comprehensive reactor bench tests to determine reaction rates as well as detailed kinetics. To resolve this issue, industry, catalyst suppliers, National Laboratories and universities should work together in a pre-competitive collaboration.

Additional challenges related to product development and commercialization of these technologies include:

- Urea mixing and control for SCR system
  - Low SCR NOx reduction efficiency due to urea injection instability issues
  - Unstable ammonia slip if appropriate urea injection control strategy is not applied
  - Reliability of ammonia slip measurement method
  - Uncertain urea conversion to NH<sub>3</sub> before SCR
  - Uniform NH<sub>3</sub> distribution to SCR catalyst
  - Urea deposit on wall surface at low temperature and release at high temperature
  - Mal-distribution leading to poor NOx conversion and ammonia slip
- LNT development and control related issues
  - Diesel fuel reductant needs

- Low temperature NOx reduction
  - Robust on-board de-sulfurization
  - Robust transient LNT control capability
  - Combustion/LNT synergies
- PM reduction technology issues
  - High PM variation downstream of CSF as indicated in Figures 3.12 and 3.13
  - Today's measurement methods insufficient for required Tier 2 Bin 5 measurement accuracy
  - PM variation due to shift in trapped mass based on soot loading / regeneration levels and filtration efficiency variation with exhaust flow rate under transient conditions

## V. REFERENCES

1. EIA Annual Energy Outlook 2003, DOE/EIA-0383 (2004), January 2004.
2. Transportation Energy Data Book: Edition 23, DOE/ORNL-6970, October 2003.
3. DDC Final Report, "DELTA – Diesel Engine Light-Duty Application," prepared for Department of Energy, May, 2003.
4. Zhang, H. and Bolton, B., "Application of Advanced Emission Control Sub-System to State-of-the-Art Diesel Engine," Combustion and Emission Control for Advanced CIDI Engines, 2000 Annual Progress Report, U.S. Department of Energy, November, 2000.
5. Zhang, H., "Demonstration of Integrated NOx and PM Emissions for Advanced CIDI Engines," Combustion and Emission Control for Advanced CIDI Engines, 2001 Annual Progress Report, U.S. Department of Energy, November, 2001.
6. Bolton, B., Hakim, N., Sisken, K. and Zhang, H., "Integrated Virtual Lab for Aftertreatment Simulations," 7th Diesel Engine Emissions Reduction Workshop, DEER 2001, August, 2001.
7. Bolton, B., Hakim, N., Fan, X., Sisken, K. and Zhang, H., "Update on Modeling for Effective Diesel Engine Aftertreatment Implementation – Master Plan, Status, and Critical Needs," 2002, " 8th Diesel Engine Emissions Reduction Workshop (DEER), August 25-29, 2002.
8. Bolton, B., Fan, A., Goney, K., Pavlova-MacKinnon, Z., Sisken K., Zhang, H., "Analytical Tool Development for Aftertreatment Sub-Systems Integration," 2003, " 9th Diesel Engine Emissions Reduction Workshop (DEER), August 24-28, 2003.
9. Zhang, H. "Aftertreatment Modeling Status, Future Potential and Application Issues," 10th Diesel Engine Emissions Reduction Workshop (DEER), August 29-September 3, 2004.
10. Konstandopoulos A.G., Johnson J.H., [1989] "Wall-Flow Diesel Particulate Filters – Their Pressure Drop and Collection Efficiency," SAE Tech. Paper 890405.
11. Aneja, R., Bolton, B. Hakim, N., and Pavlova-MacKinnon, Z. "Attaining Tier 2 Emissions through Diesel Engine and Aftertreatment Integration – Strategy and Experimental Results," 8th Diesel Engine Emissions Reduction Workshop (DEER), August 25-29, 2002.
12. Aneja, R. Bolton, B., Oladipo, B., Pavlova-MacKinnon, Z., and Radwan, A. "Advanced Diesel Engine and Aftertreatment Technology Development for Tier 2 Emissions," 2003 DEER Conference, August 24-28, 2003.

## APPENDIX 1: WET CHEMISTRY SET-UP

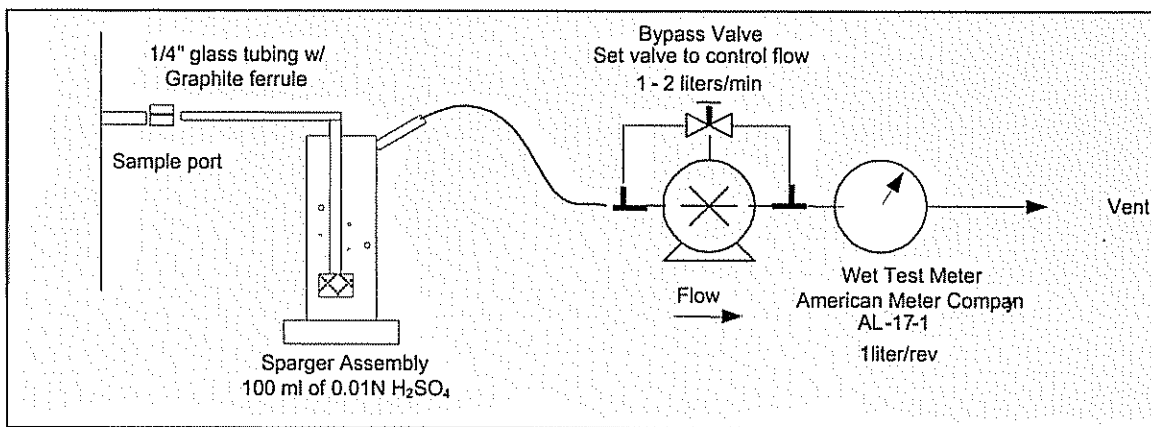


Figure A1 Wet Chemistry Test Set-Up

## APPENDIX 2: AMA TEST CYCLE

In the LEADER program, Detroit Diesel Corporation chose the AMA "Exhaust Emission Mileage Accumulation for Emissions Certification" cycle for characterization and aging of the aftertreatment devices. The AMA cycle driving schedule consists of 11 laps on a 3.75-mile durability track. Six out of the 11 laps are unique. The vehicle speed changes over time for the different laps are illustrated in Figure A2. Instructions on how to perform the test are also given in this Appendix.

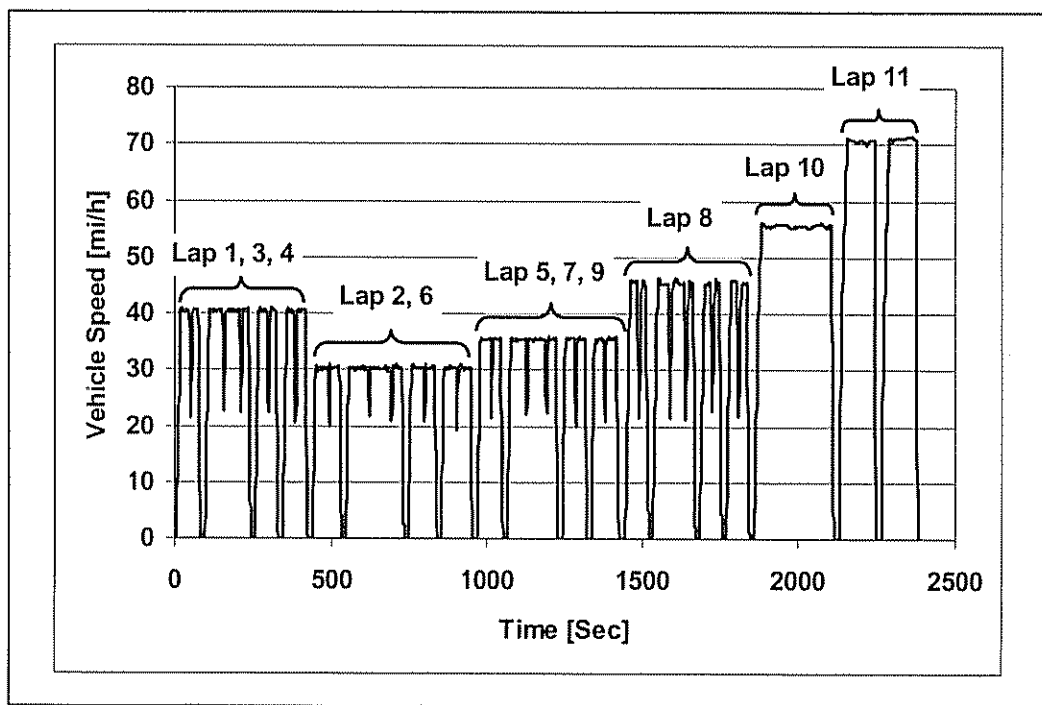


Figure A2 Vehicle Speed During AMA Driving Cycle

### 1. Driving Instructions

- 1.1. For transport from and to the Emission Laboratory, a vehicle transport must be used.
- 1.2. Bring the vehicle to a complete stop before shifting into first and reverse gears.
- 1.3. Operate automatic transmission in the range that gives the maximum number of forward gears.
- 1.4. No downshifts are to be conducted during decelerations to stop.
- 1.5. Conduct up and down shifts with manual gearboxes at the speeds specified on the test request.

## 2. Circuit Instructions

2.1 The schedule consists of 11 laps on a 3.75-mile durability track.

Lap No.	Step Speed	No. of Decelerations (D) to 20 mi/h	No. of Stops (S) for 15 sec. engine idle (mi/hr)
1	40	5	4
2	30	5	4
3	40	5	4
4	40	5	4
5	35	5	4
6	30	5	4
7	35	5	4
8	45	5	4
9	35	5	4
10	55	5	1
11	70	5	2

2.2 During each of the first 9 laps, conduct five decelerations at the indicated positions with 27 percent from the basic lap speed down to 20 mi/h, then accelerate at half throttle up to basic lap speed.

2.3 During each of the first 9 laps, conduct four stops at the positions shown on the circuit map. Accelerations to be made at half throttle. Decelerations to stop to be made with 27 percent.

2.4 Allow the engine to idle for a period of 15 seconds after each stop. Manual transmission: first gear engaged and clutch disengaged. Automatic transmissions in "Drive".

2.5 At the start of the 10th lap, accelerate at half throttle to 55 mi/h and drive the 10th lap at a constant speed of 55 mi/h.

2.6 Brake to a stop with 27 percent deceleration at the end of the 10th lap and idle for 15 seconds in first gear (or "Drive").

2.7 At the 11th lap, accelerate at full throttle to 70 mi/h and maintain this speed.

2.8 Stop at stop sign "S2" with 27 percent deceleration. Idle for 15 seconds.

2.9 Repeat 2.7 and 2.8 once, stopping at the start/finish sign. Idle for 15 seconds.

2.10 Repeat 2.1 to 2.9 to accumulate the mileage specified on the test request.

### APPENDIX 3: PNGV MULE VEHICLE DESCRIPTION

The light passenger car application of the DDC PNGV mule vehicle has demonstrated compliance with 2007 emissions regulations and beyond. The PNGV mule vehicle weight and aerodynamic targets are historical and were the basis for integrating the 1.5 liter HSDI engine and developing appropriate engine calibration strategy. The power electronics of a hybrid electric system would partially compensate for the small engine displacement. Comparison of a few key parameters of the DDC mule vehicle with the production Volkswagen Lupo (for the European market) is shown in Table A1. The Lupo offers lower power density and total vehicle weight than the DDC mule vehicle without the power electronics. Also, there are differences between the production Lupo certification and the DDC mule vehicle. The DDC PNGV mule vehicle with its advanced diesel and aftertreatment technologies demonstrates state-of-the-art emissions and fuel economy. The DDC PNGV mule vehicle data shown represents intermediate program results demonstrating Tier 2 Bin 7 emissions. Subsequently, further reduction in tailpipe out emissions was demonstrated while selectively improving the fuel economy.

Table A1 Comparison of the DDC PNGV Mule Vehicle with the Production VW Lupo

	VW Lupo TDI	DDC PNGV Mule
	Production	Early Prototype - Tech Demo
Vehicle Weight, kg	854-904, empty 2-door	1004
Engine	In-line 3 (CIDI)	In-line 3 (CIDI)
Displacement, L	1.2	1.5
BoreXStroke, mm	76.5X86.4	82X92
Power, kW	45	56
Torque, N·m	140	180
Specific Weight, kg/kw	19-21	18
Rated Speed, rpm	4000	4200
Rc	19.5:1	18.5:1
Air System	VGT/EGR	VGT/EGR
Aftertreatment	DOC	CSF+SCR
MPG	78.7 (driving cycle?)	70.5 (FTP75 Combined MPG)
Emissions	EURO2?	2007 0.14 g/mile NOx 0.013 g/mile PM FTP75

#### APPENDIX 4: FTP75 AND HIGHWAY FUEL ECONOMY TEST CYCLES

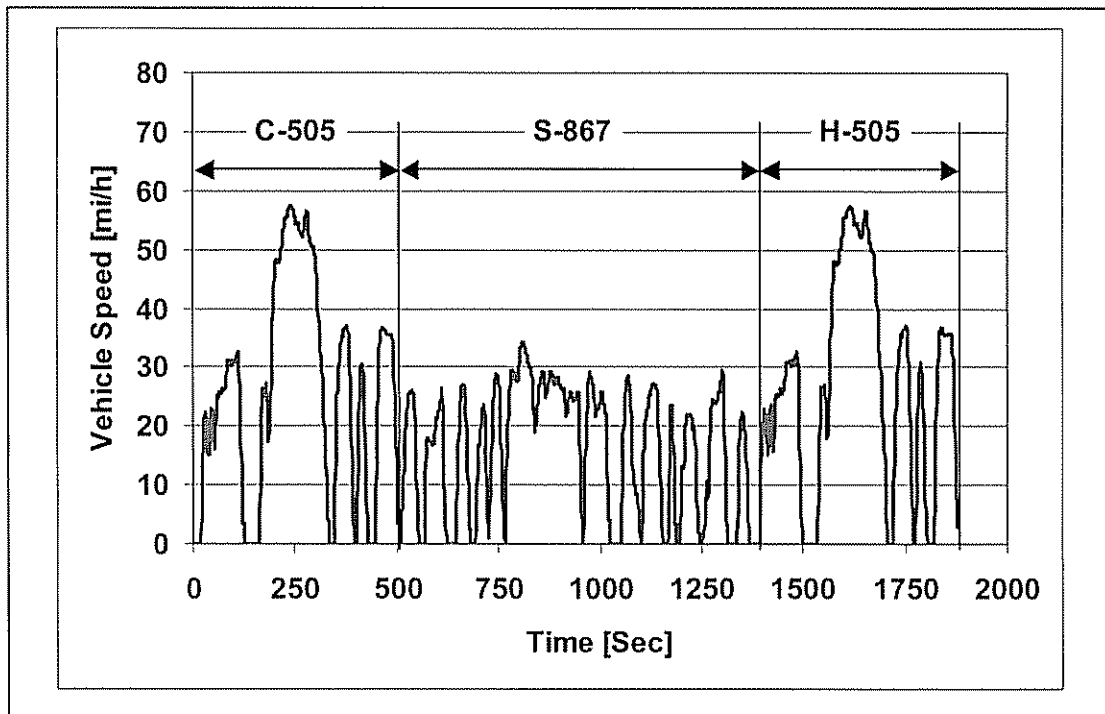


Figure A3 FTP75 Test Cycle

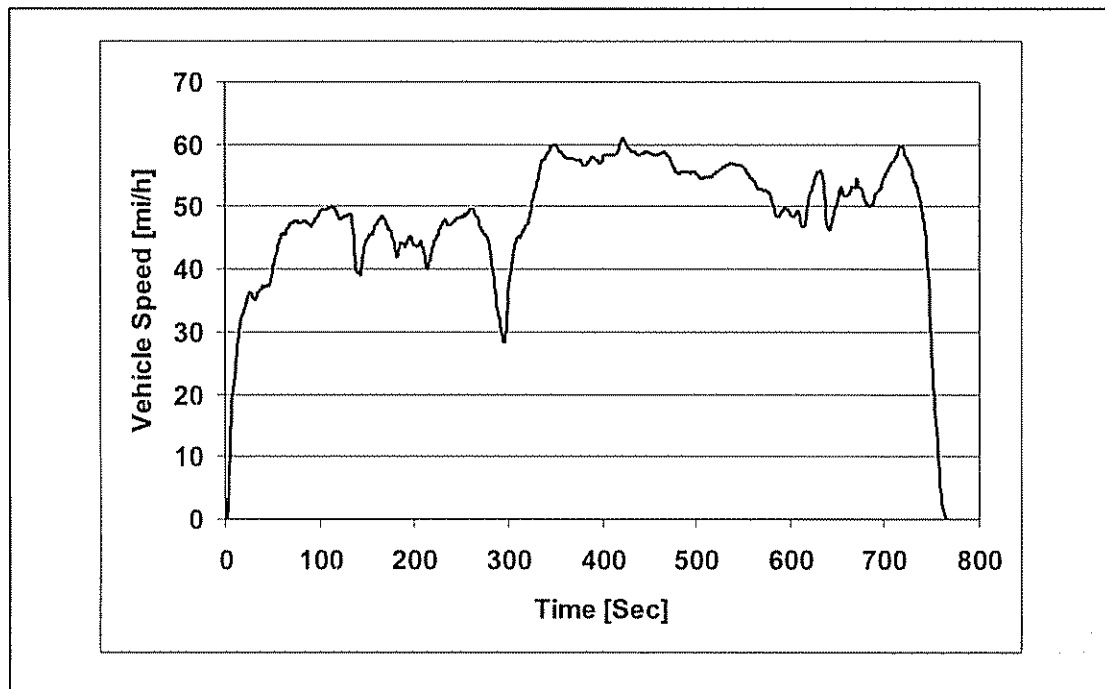


Figure A4 Highway Fuel Economy (HWYFE) Test Cycle

## APPENDIX 5: TEST SET-UP

### 1. Schematic of the Test Set-Up

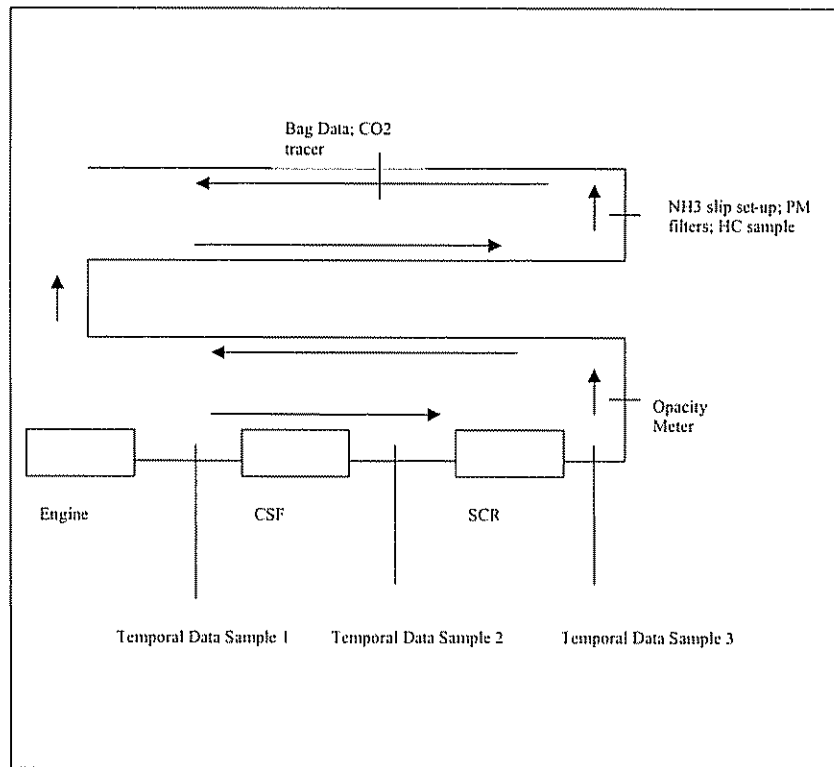


Figure A5 Schematic of the Vehicle Test Set-Up

### 2. Dynamometer Coefficients

A = 0.06 hp at 50 miles/hour

B = 0.34 hp at 50 miles/hour

C = 1.60 hp at 50 miles/hour

These coefficients were developed for a vehicle inertia weight of 2250 lbs and a drag loss of 2 hp-hr at a vehicle speed of 50 miles/hour.

### 3. Vehicle Instrumentation

Table A2 Vehicle Instrumentation

Channel	Name	Units	Range	Adapt Scaling	DMS Parameter
#1	Throttle (ECU_THR)	%	0-100	0-10 volts	ECU_THR
#2	Intake Manifold Pressure (ECU_IMP)	hPa	0-3000	0-10 volts	ECU_IMP
#3	Fuel Rail Pressure (ECU_Railp)	hPa	0-1.5e6	0-10 volts	ECU_RLP
#4	Air Mass Flow (ECU_AM)	mg/stroke	0-1600	0-10 volts	ECU_AM
#5	Actual Total Fuel Quantity (ECU_FVT)	mm^3	0-60	0-10 volts	ECU_FVT
#6	Engine Speed (ECU_rpm)	rpm	0-5000	0-10 volts	ECU_rpm
#7	Compressor Pressure In (CPI)	kPa	-10-0	0-5 volts	P_CPI
#8	Compressor Pressure Out (CPO)	kPa	0-150	0-5 volts	P_CPO
#9	Turbine Pressure In (TPI)	kPa	0-300	+/- 25mV	P_TPI
#10	Turbine Pressure Out (TPO)	kPa	0-150	+/- 25mV	P_TPO
#11	Intake Manifold Pressure (IMP)	kPa	0-150	0-5 volts	P_IMP
#12	Soot Filter Out Pressure (CSFPO)	kPa	0-10	+/- 25mV	P_CSFPO
#13	Catalyst Press Out (SCRPO)	kPa	0-10	+/- 25mV	P_SCRPO
#14	Soot Filter Out Temp. (CSFTO)	degC	0-1211	+/- 50mV	CSFTO
#15	Catalyst Temp Out (SCRTO)	degC	0-1211	+/- 50mV	SCRTO
#16	Ambient Temp (AMT)	degC	0-1211	+/- 50mV	AMT
#17	Compressor Temp In (CTI)	degC	0-1211	+/- 50mV	CTI
#18	Compressor Temp Out (CTO)	degC	0-1211	+/- 50mV	CTO
#19	Intercooler Temp Out (ICTO)	degC	0-1211	+/- 50mV	ICTO
#20	Intake Manifold Temp (IMT)	degC	0-1211	+/- 50mV	IMT
#21	Coolant Temp Out (CLTO)	degC	0-1211	+/- 50mV	CLTO
#22	EGR Temp In (EGRTI)	degC	0-1211	+/- 50mV	EGRTI
#23	EGR Temp Out (EGRTO)	degC	0-1211	+/- 50mV	EGRTO
#24	Turbine Temp In (TTI)	degC	0-1211	+/- 50mV	TTI
#25	Turbine Temp Out (TTO)	degC	0-1211	+/- 50mV	TTO
#26	Dyno Torque	N-m			
#27	Smoke Meter	%			N-Meter
#28	Dry Gas Meter (for ammonia slip device)	degF		+/- 50mV	TC#7

## APPENDIX 6: TIER 2 EMISSIONS REGULATIONS

Table A3 lists the Tier 2 emissions standards that apply to all vehicles, regardless of fuel type. Compliance by all light-duty vehicle classes, including heavy light-duty vehicles, is to be achieved by 2009. Tier 2 requirements have different levels of stringency, referred to as "EPA Bins" with an average standard of NOx. Automakers can certify vehicles to any one of the bins, but must meet fleet average NOx requirements of 0.07 g /mile.

**Table A3 Tier 2 Emissions Regulations, FTP75 at 120,000 km**

Bin #	NOx mi/g	PM mi/g	CO mi/g	HC mi/g
10	0.6	0.12	7.3	0.032
9	0.3	0.08	4.2	0.018
8	0.2	0.06	4.2	0.018
7	0.15	0.02	4.2	0.018
6	0.1	0.02	4.2	0.018
5	0.07	0.01	4.2	0.018
4	0.04	0.01	2.1	0.011
3	0.03	0.01	2.1	0.011
2	0.02	0.01	2.1	0.004
1	0	0	0	0

## **ACKNOWLEDGEMENTS**

DDC would like to express its gratitude to the program sponsor, DOE - Freedom Car and Vehicle Technologies, for making it possible to achieve the program objectives, both financially and technically.

DDC would also like to thank the multiple partners for their support throughout the program. We appreciate the support provided by Engelhard Corporation. Their state-of-the-art aftertreatment technologies and technical expertise played a major role in the success of the LEADER program.

Other partners that played instrumental roles in supporting this program include DaimlerChrysler Research and Technology Center, Michigan Tech University, Adapco, Gamma Technologies and Ricardo.